Master Thesis Integrated Product Design
Faculty of Industrial Design Engineering
Delft University of Technology

Living Textiles: Exploring Microalgae Growth on 3D Woven Structures in Design

Martina Mancini

20 March, 2025

Degree
MSc. Integrated Product Design
Faculty of Industrial Design Engineering
Delft University of Technology

Author:
Martina Mancini
5722381

Supervisory team:
Chair: Dr. Joana Martins Assistant Professor of Biodesign
Mentor: Dr. Holly McQuillan Assistant Professor of Multimorphic Textile Systems

Acknowledgments

Working on this graduation project has been an invaluable opportunity to expand my knowledge in biotechnology, engineered living materials, and their integration with industrial design. Throughout this journey, I have developed both technical expertise and soft skills, which have enabled me to successfully complete this thesis. I would like to express my deepest gratitude to my chair and mentor, Joana Martins and Holly McQuillan, for sharing their expertise and guiding me through this process. Thanks to their support, I was able to navigate the intersection of biotechnology, tissue engineering, and design, equipping myself with the right tools to pursue this research. Every meeting with them reaffirmed that I was on the right path, and together, we transformed innovative ideas into reality. Their trust, guidance, and willingness to help have been invaluable, and having them as mentors has been an absolute privilege.

I also wish to sincerely thank Joren Wierenga, the BioDesign lab technician, whose patience and expertise have been instrumental in my work. His guidance in lab techniques and his readiness to offer valuable advice have significantly contributed to my learning experience over the past months.

Finally, I am deeply grateful to my family, whose support not only allowed me to study in the Netherlands, at one of the world's most prestigious universities, but also gave me the opportunity to grow and become independent—one of the greatest gifts they could ever give me. I also extend my heartfelt thanks to my boyfriend and friends, who have stood by my side, constantly encouraging me to push my limits and give my very best. Their support and belief in me have been a source of strength throughout this journey.

Abstract

Microalgae cultivation systems face critical challenges in balancing efficiency, scalability, and sustainability. Existing methods, such as open ponds and photobioreactors (PBRs), present inherent limitations—open ponds are low-energy and cost-effective but lack environmental control, while PBRs offer higher efficiency but require significant infrastructure and energy input (Encarnação et al., 2023; Abdur Razzak et al., 2024). This research proposes a living textile system as an intermediate solution, combining the passive functionality of open ponds with the control and efficiency of PBRs, but at a lower cost and with reduced energy demands.

By integrating *Scenedesmus* sp. microalgae within a hydrogel-based woven structure, this study enhances gas exchange, promotes microalgal attachment, and optimizes photosynthetic efficiency—key challenges in previous systems. Findings reveal that fiber composition and weave structure play a fundamental role in microalgal viability, influencing hydration retention, and resilience against detachment. Additionally, origami-inspired folding mechanisms improve usability, allowing the textile to fold and unfold dynamically for controlled closure during adverse weather conditions and efficient rehydration.

To explore potential applications, this research conceptualized the Living Climate Panel, demonstrating how living textiles can function as an integrated cultivation system that not only supports microalgal growth but also enhances sustainability, improves air quality, and regulates microclimatic conditions in indoor environments. By merging biology, textile engineering, and design, this study redefines textiles as active, self-sustaining systems, rather than passive materials, offering a scalable and adaptable solution for sustainability-driven applications.

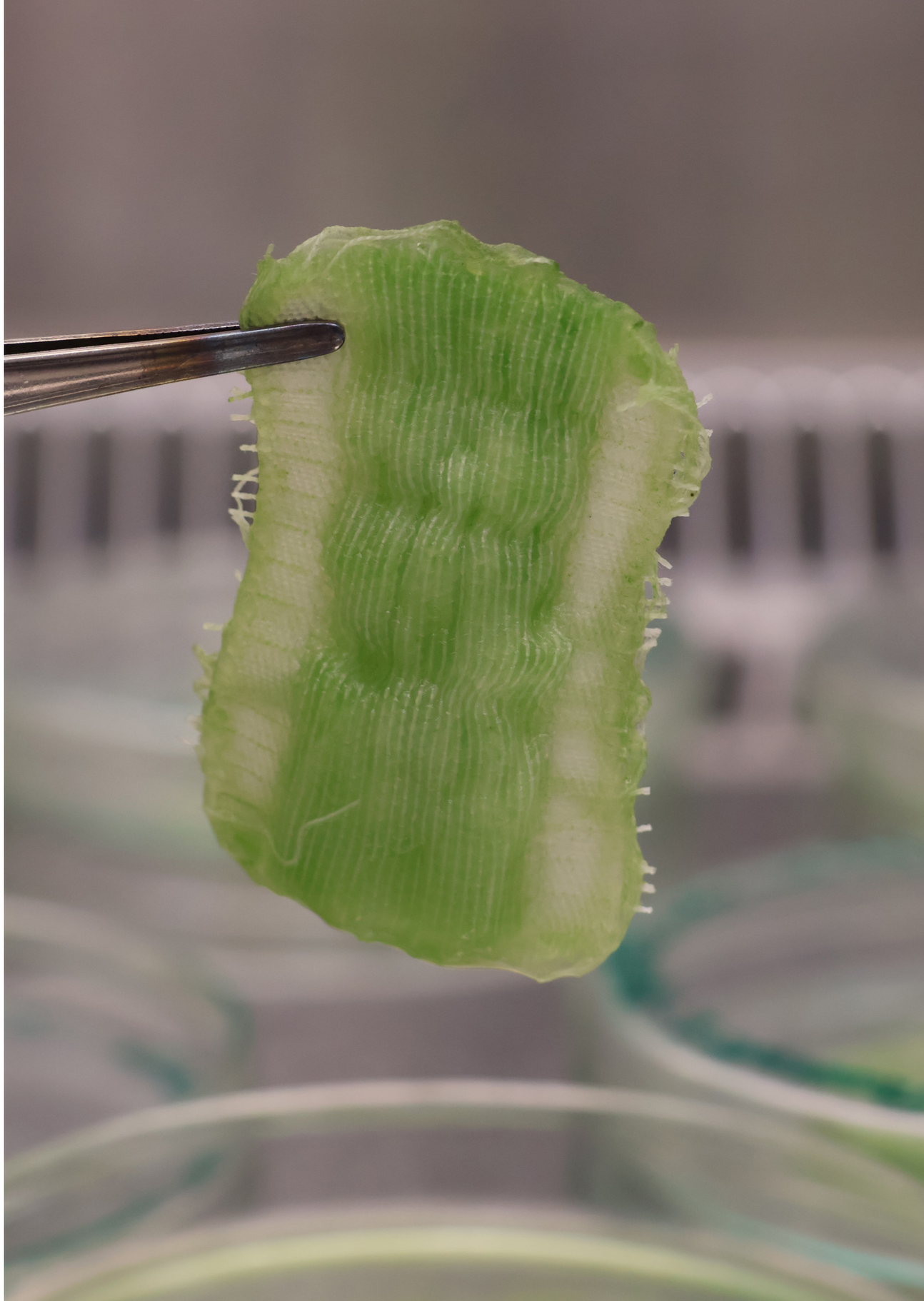

Glossary

Agar: a gelatinous colloidal extract of a red alga (as of the genera Gelidium, Gracilaria, and Eucheuma) used especially in culture media ("Agar," 2025)

ATP: it is a molecule found in the cells of all living organisms. ATP captures the energy obtained from the breakdown of food molecules and then it provide this energy to other cellular processes (The Editors of Encyclopaedia Britannica, 2025).

Biofilm: aggregate of bacteria held together by a matrix of carbohydrate that adheres to a surface (The Editors of Encyclopaedia Britannica, 2025).

Bitmap: it is a collection of binary data that encodes pixel values in an image or on a display.(The Editors of Encyclopaedia Britannica, 2009).

BG 11 medium: it provides all the essential nutrients required for the microalgae cultivation (Pandey et al., 2023).

Boat shuttle: a tool in weaving, used in looms, facilitates the passage of the weft yarn through the warp threads in a back-and-forth motion(Wikipedia contributors, 2025).

Brownian motion: is the movement of microscopic particles suspended in a liquid or gas, caused by collisions with surrounding molecules (Hugo Barbosa et al., 2018).

(CH2O): formed by plants from carbon dioxide and water during the photosynthesis. They serve as energy sources and as essential structural components in organisms (Davidson & A, 2025).

Crimp: is the reduction in yarn length within a textile structure (Sarkar, 2019)

*Drape:*the manner in which textile flows, folds, or hangs when placed on a surface or form (Drape, 2025).

EPS: Extracellular metabolites produced by microorganisms play a crucial role in microbial function, adaptation, and growth. The primary components of EPS include proteins, polysaccharides, nucleic acids, humic substances, and lipids

Float: is the length of yarn that passes over one or more adjacent warp without being interlaced with them(Shenton, 2014).

Freeze-thawing: is a method that involves alternating cycles of freezing (approximately -20°C) and thawing (around +20°C) to promote the formation of crystalline structures and hydrogen bonds within a polymer solution (Bernal-Chávez et al., 2023). With each cycle, the stability of the resulting gel-like network increases as additional crystalline structures are formed during the freezing phase (Waresindo et al., 2023). This technique has been used to develop hydrogels like LAPH3, which demonstrate antibacterial properties, water retention, and wound-healing capabilities (Fang et al., 2019).

Hydrodinamics: is a field of physics that focuses on the movement of fluids and the forces exerted on solid objects submerged in them ("Hydrodynamics," n.d.).

Hydroxyl groups: they are a functional group found in sugars and alcohols. Each group consists of one hydrogen and one oxygen atom (The Editors of Encyclopaedia Britannica, 2023).

Interlacement: the way in which warp and weft yarns cross over and under each other in a woven textile (Devendorf et al., 2022).

Ionic interactions: ionic bonds are formed between anionic polymers, such as alginate, and cations like calcium, enabling the creation of discrete structures like hydrogel microbeads, suitable for applications requiring small, discrete hydrogel structures (Lin et al., 2022).

Laminar Air Flow Cabinet:is a controlled, enclosed workspace designed to maintain a sterile environment by directing a continuous stream of filtered air, minimizing the risk of sample contamination (Wikipedia contributors, 2024).

Medium: a nutrient system for the artificial cultivation of cells or organisms ("Medium," 2025).

Microalgae encapsulation: is a process in which a substance (active agent) is enclosed by a carrier material to form a system (Vieira et al., 2020).

Microalgae entrapment: is defined as a living cell that is prevented from moving independently from its original location to all parts of an aqueous phase of a system (Kaparapu, 2017).

NADPH: Nicotinamide Adenine Dinucleotide Phosphate Hydrogen helps to fuel the reactions that occur in the photosynthesis to synthesize carbohydrates (What Is NADPH in Photosynthesis? - Full Form, Functioning, 2020).

Polymer Chains: It is a large, chain-like molecular structure composed of repeating smaller units known as monomers, which are chemically bonded together. This arrangement represents the structure for materials such as plastics (Structure and Form | School of Materials Science and Engineering - UNSW Sydney, n.d.).

Polysaccharide: is a complex carbohydrate composed of a chain of monosaccharide units linked by glycosidic groups (David F. Williams, 2019).

Thermal gelation: where polymer solutions are heated and then cooled, allowing polymer chains to form organized structures (Ambika et al., 2021). This process happens in the presence of salt, which helps the chains stick together at specific points, forming junction zones (Xiong et al., 2023).

Van der Waals force: are weak electrical interactions that attract neutral moleculestoward each other (The Editors of Encyclopaedia Britannica, 2025a).

Table of Contents

Introduction

The rapid growth in production and consumption, driven by capitalism's demand for continuous accumulation, has led to escalating pollution and resource depletion (McGowan, 2016). Overproduction significantly increases energy use, material extraction, and carbon emissions, contributing to critical environmental challenges such as greenhouse gas emissions and water contamination by organic and metallic pollutants (Sources of Greenhouse Gas Emissions | US EPA, 2025; Pauliuk et al., 2021; Encarnação et al., 2023).

While clean energy and environmental remediation strategies have emerged to combat these issues, economically viable and sustainable solutions remain unattainable (In-Na et al., 2022). In contrast, nature offers promising alternatives, such as photosynthesis, a process performed by plants and microorganisms (In-Na et al., 2022). Among these microorganisms, microalgae, including cyanobacteria, exhibit significant potential in carbon sequestration, wastewater treatment, and sustainable material development (Encarnação et al., 2023). This potential has inspired the development of engineered living materials (ELMs), where microorganisms are embedded within polymer matrices to perform biological functions such as self-repair and adaptation (Oh et al., 2023). By embedding microalgae into hydrogel systems, it is possible to create bioactive structures that contribute to environmental sustainability. Despite their promise, ELMs remain largely unexplored in the textile domain, where their flexibility, lightweight properties, and adaptability present unique opportunities for sustainable development.

Motivated by the need for cost-effective, sustainable materials, this thesis aims to design a living textile capable of sustaining and promoting microalgae growth within a 3D woven hydrogel. Textiles were chosen for their versatility, lightness, and adjustable properties like density and texture. These qualities have been ideal for exploring innovative techniques, such as origami-inspired designs, natural material behaviors, advanced weaving methods, and sustainable principles, addressing diverse design challenges.

To achieve this objective, the research investigates microalgae encapsulation techniques and develops tailored 3D woven microstructures to optimize microalgal habitats. Experimental results led to the formulation of three application concepts, demonstrating the scalability of the living textile in urban and architectural contexts. Furthermore, end-of-life strategies were explored and suggested for future research, ensuring alignment with circular material cycles and environmental responsibility.

To guide the iterative development process, this thesis employs the Parallel Prototyping Method, interlaced with the Material Driven Design (MDD) methodology, which facilitates systematic exploration and refinement of material properties through multiple cycles of testing and adaptation (Kesari, 2019; Karana et al., 2015). Through the implementation of the MDD and PPM methods, this research advances material innovation by introducing a novel approach to integrating living microorganisms within a textile-based hydrogel system, contributing to the emerging field of engineered living materials. By designing a textile capable of hosting microalgae, it enhances bioremediation applications, particularly in CO_2 capture and environmental remediation. The study further optimizes structural properties by developing and testing microstructured woven textiles that improve the viability and performance of embedded microalgae, while also enhancing macro-structural adaptability through self-folding mechanisms enabled by PVA's responsive properties. Inspired by origami principles, the textile incorporates embedded structural folding lines, allowing controlled shape transformations. This interdisciplinary work bridges material science, textile engineering, and biotechnology, fostering new approaches to sustainable design. By addressing these aspects, the thesis contributes to the development of bio-integrated material solutions that align with contemporary sustainability challenges, offering new possibilities for environmental applications.

Chapter 1
Context and Background

This chapter provides a literature review, exploring the context and background of the project. It examines the main problems, previous research efforts to address them, and the broader fields of microalgae, Engineered Living Materials (ELMs), and engineered textiles, establishing a comprehensive knowledge base for the study.

(Ciccolella, z.d.)

1.1. The environmental crisis

The environmental crisis, called the "Triple Planetary Crisis", encloses three main challenges: pollution, biodiversity loss, and climate change (UNFCCC, 2022). Pollution, particularly air pollution, causes over seven million premature deaths annually, resulting from sources like vehicle emissions, industrial processes, and household pollutants (Abbass et al., 2022; UNFCCC, 2022). Biodiversity loss, driven by habitat destruction, overfishing, deforestation, and desertification, threatens ecosystem resilience, food security, clean water, and global economic and human health (UNFCCC, 2022; Abbass et al., 2022). Climate change, perhaps the most urgent aspect of the crisis, is mainly driven by greenhouse gas emissions from human activities (Abbass et al., 2022). These emissions are causing global temperature increases and severe weather events (UNFCCC, 2022). The Paris Agreement, adopted in 2015, aims to limit global warming to below 2°C, with countries pledging emission reductions through renewable targets (Abbass et al., 2022; UNFCCC, 2022).

1.2. Carbon Capture

The link between CO_2 and climate warming, driven by the "greenhouse effect," has gained significant attention across scientific and public spheres (Anderson et al., 2016). While CO_2 naturally helps regulate Earth's temperature by trapping infrared radiation, excessive emissions since the Industrial Revolution have amplified global warming, necessitating urgent efforts to reduce atmospheric CO_2 (Fagorite et al., 2022).

Geological carbon capture and sequestration (GCS) is one approach to CO_2 reduction (Figure 1). This process involves injecting CO_2 into underground geological formations, where impermeable rock layers contain it permanently (Hua et al., 2023). However, GCS faces several limitations, including challenges in injecting CO_2 into low-permeability formations, the need for storage sites near CO_2 sources to minimize transport costs, and the risk of groundwater contamination from potential CO_2 leakage (Oldenburg, 2019) (Further details can be found in Appendix B - Carbon Capture).

Biological sequestration, on the other hand, uses living organisms like plants and algae to absorb CO_2 through photosynthesis, storing carbon naturally in the form of carbohydrates - in lignocellulosic plants - and polysaccharides - in algae - (Fagorite et al., 2022) (Figure 2). Algae, in particular, are highly efficient in utilizing CO_2 and have been widely adopted for biofuel production (Abdul Hai Alami et al., 2021). This process not only reduces atmospheric CO_2 but also provides a sustainable energy source, making algae-based carbon capture a promising strategy for addressing climate change while promoting energy production (Gayathri et al., 2021).

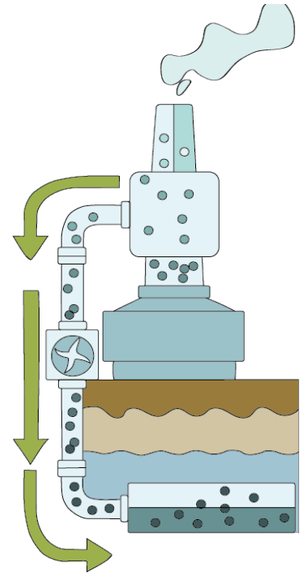

Figure 1: : Geological carbon sequestration method (Preventing Climate Change: The Power of Carbon Sequestration | Pro Enviro, n.d.).

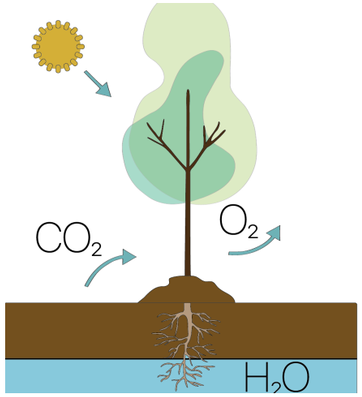

Figure 2: Biological carbon sequestration (Education, n.d.).

1.3. Microalgae

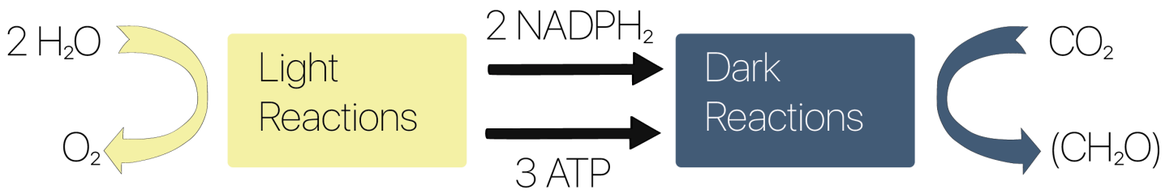

Figure 3: Photosynthetis (Masojídek et al., 2013).

Microalgae are photosynthetic microorganisms categorized into eukaryotic microalgae and prokaryotic cyanobacteria. Eukaryotic microalgae are classified in four main groups based on their pigments: Rhodophyta (red), Chrysophyceae (golden), Phaeophyceae (brown), and Chlorophyta (green)(Gigova & Marinova, 2016). These organisms perform photosynthesis within chloroplasts, specialized organelles that house pigments necessary for capturing light energy (Masojídek et al., 2013). Cyanobacteria, or blue-green algae, are predominantly unicellular but can form filaments and contribute around 50% of global primary oxygen production through photosynthesis (Kirchman, 2018).
Photosynthesis, a key biochemical process in plants and microalgae, converts light energy, carbon dioxide (CO_2), and water into carbohydrates and oxygen (O_2) (Jagannathan et al., 2009). This process occurs in two stages: light reactions, which generate $NADPH_2$ and ATP, and dark reactions, where these molecules reduce CO_2 into carbohydrates in the stroma (Masojídek et al., 2013) (Figure 3).

Under optimal conditions, microalgae achieve higher photosynthetic rates than terrestrial plants due to their fully photosynthetically active structure, enhancing their ability to sequester CO_2 and nutrients, making them valuable for mitigating greenhouse gas emissions and water pollution (Mateu Vera-Vives et al., 2024). However, photosynthetic efficiency declines with excessive light intensity as dark reactions, which utilize the energy produced, become rate-limiting (Masojídek et al., 2013). Therefore, microalgae require specific environmental conditions to thrive and maintain efficient photosynthetic activity (Figure 4). Light intensity plays a crucial role in regulating growth rate, lipid distribution, and pigment synthesis (Li et al., 2024). CO_2 availability is equally essential, with concentrated CO_2 streams commonly used to enhance growth (Li et al., 2024).
Additionally, nutrients are critical, including macronutrients such as carbon, nitrogen, and phosphorus, along with micronutrients like trace metals and vitamins (Li et al., 2024). pH levels influence CO_2 availability, enzyme function, and nutrient absorption, while temperature affects both nutrient solubility and enzymatic activity. Optimal growth typically occurs between 20 and 25°C (Li et al., 2024).

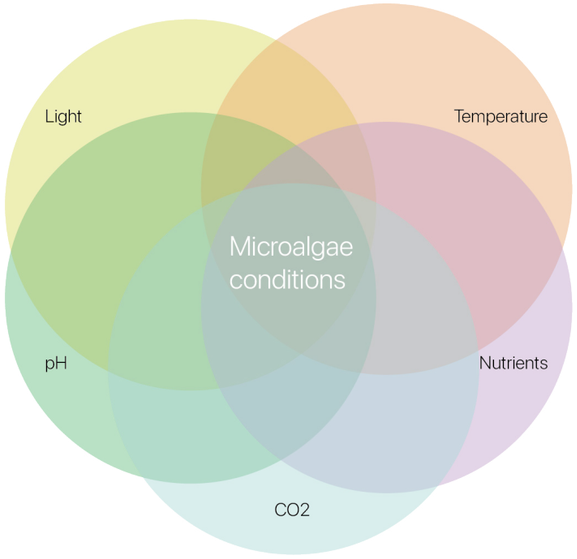

Figure 4: Good microalgae conditions given by the combinations of Light, Temperature, Nutrients, pH, and CO_2 (Li et al., 2024).

When these parameters are met, microalgae photosynthesize efficiently, enabling diverse applications. They can capture carbon, produce bioenergy, and assist in environmental remediation (Gayathri et al., 2021). . Beyond biofuels, certain microalgae produce biodegradable bioplastics like polyhydroxyalkanoates (PHAs) and polyhydroxybutyrate (PHB), which are used in packaging, medical devices, and other industries as sustainable alternatives to conventional plastics (Encarnação et al., 2023). Microalgae also play a vital role in wastewater treatment by absorbing nitrogen, phosphates, heavy metals, and other pollutants, reducing pollution while generating biomass for reuse (Abdur Razzak et al., 2024; Encarnação et al., 2023).

1.3.1. Microalgae cultivation systems

Microalgae can be cultivated in a variety of environments, including ponds, tanks, lakes, and open sea settings, without competing for arable land (Encarnação et al., 2023). Cultivation methods are primarily divided into open systems, such as ponds, and closed systems, like photobioreactors (PBRs).
Open ponds are cost-effective for large-scale production, relying on natural sunlight and atmospheric CO_2 to drive photosynthesis (Abdur Razzak et al., 2024) (Figure 5). Mechanical systems, such as paddle wheels, enhance CO_2 absorption and light distribution, making them ideal for high-volume biomass production at low costs, particularly for biofuel applications (Encarnação et al., 2023). They also offer scalability and low energy requirements, making them economically feasible (Abdur Razzak et al., 2024). However, open ponds are vulnerable to environmental fluctuations, contamination, and water loss from evaporation (Encarnação et al., 2023; Abdur Razzak et al., 2024). They also suffer from low CO_2 utilization efficiency due to the limited atmospheric concentration of CO_2, restricting the range of species that can be cultivated (Abdur Razzak et al., 2024).

Closed photobioreactors (PBRs), in contrast, provide controlled environments for optimal growth (Figure 6). These systems minimize contamination and allow precise regulation of temperature, light, and nutrients, enabling high-density cultures and uncontaminated biomass production (Abdur Razzak et al., 2024). PBRs are particularly suited for high-value applications

Figure 5: Microalgae open ponds (EuropaWire PR Editor, 2023).

requiring pure algal biomass (Abdur Razzak et al., 2024). However, their construction and operation are more costly than open ponds due to the materials required and the energy needed for artificial lighting and temperature control (Encarnação et al., 2023). Scaling up PBRs is challenging, as issues like biofouling, where organic material can reduced light penetration, and oxygen accumulation can hinder productivity over time (Abdur Razzak et al., 2024).
Recognizing the limitations of traditional microalgae cultivation methods, researchers have shifted their focus toward the innovative field of Engineering Living Materials (ELMs). ELMs explores a novel approach that try to overcome the existing limitations and unlock new applications.

Figure 6: PBR (Photobioreactor, 2011).

1.3.2. Microalgal ELMs

Engineering Living Materials (ELMs) are innovative systems composed of self-organized living cells encapsulated within a matrix to replicate biological functions (Zhao et al., 2019; Oh et al., 2023). These living cells utilize resources from their environment to produce essential components that create and preserve the material, representing a transformative approach to microalgae growth (An et al., 2022).

ELMs have shown significant promise in addressing key challenges in traditional microalgae systems. Encapsulation minimizes contamination risks, improves CO_2 uptake, and enhances operational efficiency, making ELMs more suitable than conventional methods (Zhao et al., 2019). For example, in wastewater treatment, encapsulated microalgae demonstrate superior performance over their free-living counterparts, providing an eco-friendly and cost-effective approach to resource management while supporting sustainability goals (Zhao et al., 2019; In-Na et al., 2021).

Beyond addressing the challenges of conventional cultivation, ELMs are engineered for a wide range of advanced functions. These include growth, reproduction, self-healing, self-organization, energy harvesting, and dynamic responsiveness to environmental changes. Such characteristics make ELMs highly promising for diverse applications, including green energy production, pollutant bioremediation, energy-efficient biobrick fabrication, space exploration, cell engineering, biosensors, and medical innovations like skin patches for wound healing and controlled drug release (An et al., 2022; Rodrigo-Navarro et al., 2021) (Figure7).

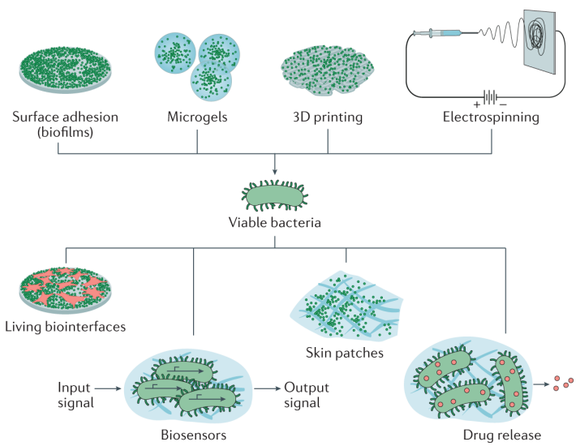

Figure 7: ELMs can be applied for cell engineering, as biosensors, as skin patches for wound healing and for controlled drug release (Rodrigo-Navarro et al., 2021).

1.3.3. Microalgae Immobilization

However, for microalgae to perform their functions effectively, they must exist in an environment that provides the optimal conditions for their growth and activity. To achieve this, microalgae require encapsulation, allowing them to remain in their ideal habitat while still delivering their beneficial effects.
Microalgae immobilization occurs both naturally and through biotechnological methods. In the following paragraphs these two immobilization methods have been explored more in depth.

1.3.3.1. Natural Microalgae Immobilization

Naturally, microalgae form aggregates such as granules, flakes, or biofilms by attaching to substrates, but this process often lacks the intensity and efficiency needed for large-scale use (Vasilieva et al., 2020). To overcome these limitations, controlled biotechnological approaches have been developed to enhance immobilization, ensuring higher productivity and preventing cell leakage (Moreno-Garrido, 2008). Passive immobilization, which leads to biofilm formation, occurs in four stages (Figure 8). First, suspended microalgae cells reach a carrier surface via motion mechanisms like flagellar movement, hydrodynamics, or Brownian motion (Li et al., 2024). Second, cells attach to the carrier using forces such as van der Waals interactions, supported by structures like flagella and outer membrane proteins (Li et al., 2024). In the third stage, cells produce extracellular polymeric substances (EPS), forming a lamellar colony that strengths their attachment (Li et al., 2024). Finally, cells grow and reproduce, forming a mature biofilm with complex structures (Li et al., 2024).

1.3.3.1.1. Carrier Properties

The properties of the carrier play a critical role in immobilization efficiency. Factors such as surface roughness, wettability, surface energy, and biotoxicity influence cell attachment (Li et al., 2024). Rough surfaces, in particular, enhance immobilization by providing more contact points and trapping cells effectively, leading to increased biomass production (Li et al., 2024). An ideal carrier for microalgae immobilization should be low-cost, phototransparent, hydrophilic, and nontoxic, with high cell affinity and no interference with cellular functions (Vasilieva et al., 2020). It must also possess mechanical, chemical, and thermal stability for durability, have low affinity for contaminants, and be environmentally friendly, preferably biodegradable or recyclable (Vasilieva et al., 2020).
Compared to free-floating cells, immobilized microalgae offer significant benefits, including better substrate utilization, higher volumetric productivity, and greater resilience to environmental stresses such as pH fluctuations, high temperatures, and toxic compounds (Vasilieva et al., 2020).

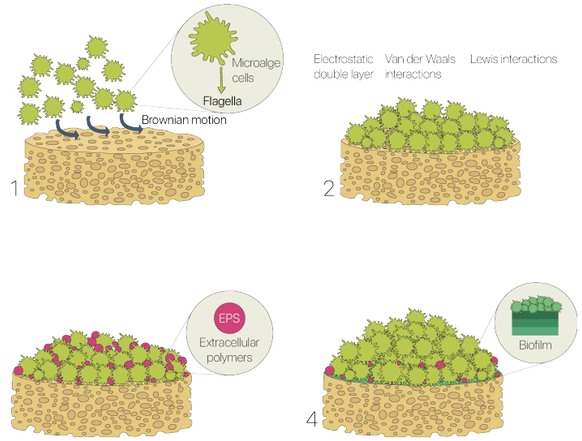

Figure 8: Four necessary steps for microalgae attachment on biofilms (Li et al., 2024).

1.3.3.2. Microalgae Immobilization techniques (biotechnological methods)

As already seen, passive immobilization relies on the

natural ability of microalgae to adhere to a carrier surface without chemical or mechanical intervention (Vasilieva et al., 2020). While adhesion is energy-efficient and eco-friendly, its tendency to cause cell leaching limits its use in high-stability applications.

Active immobilization provides a more controlled and stable environment by embedding microalgae within a matrix, typically through gel-like structures (Vasilieva etal., 2020) (Figure 9). This method protects cells from environmental stress and contamination while maintaining high cell concentrations (Vasilieva et al., 2020). Materials like synthetic polymers (e.g., polypropylene phthalamide, polyurethane) and natural gels (e.g., agar, sodium alginate, carrageenan, chitosan) are commonly used due to their biocompatibility and ability to allow diffusion of small molecules like oxygen and nutrients (Li et al., 2024). Therefore, active immobilization is mainly used when it is necessary to provide a stable and protective environment for microalgae.

It can be performed using two main approaches: covalent bonding and entrapment (Xiong et al., 2023). Covalent bonding involves forming irreversible chemical bonds between cells and the support matrix, ensuring strong stability but often reducing cell viability and activity due to cytotoxic binding agents and structural changes (Xiong et al., 2023). In contrast, entrapment gently incorporates cells into a porous, hydrated material, supporting the exchange of nutrients and gases while preserving cell viability (Han et al., 2023). The latter method uses biocompatible precursors to create matrices with adjustable porosity and mechanical robustness (Xiong et al., 2023). While it is simple and effective for enhancing stability, its limitations include restricted cell proliferation and scalability (Xiong et al., 2023). Despite these challenges, entrapment remains one of the most reliable techniques for improving the stability of microalgae (Xiong et al., 2023). Among the various materials used for this purpose, hydrogels stand out as highly effective carriers.

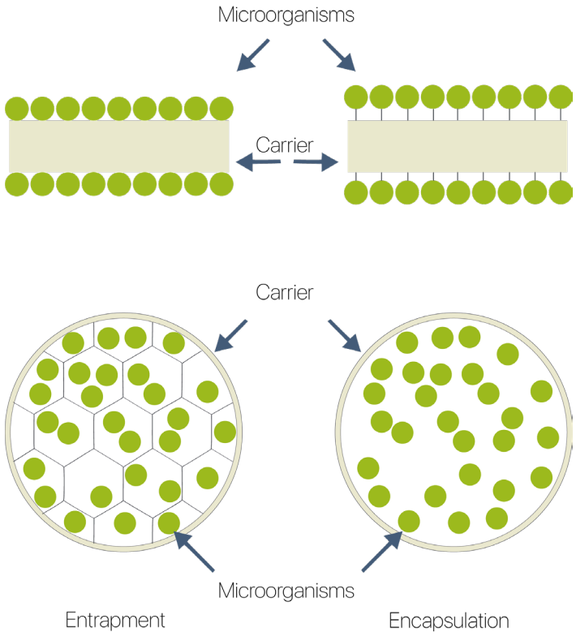

Figure 9: Immobilization methods (Valdivia-Rivera et al., 2021).

1.4. Hydrogel

Hydrogels are three-dimensional polymeric networks capable of absorbing large quantities of fluids, typically ranging from 70% to 99% of their weight (Ambika et al., 2021; An et al., 2022). The nutrients embedded within the gel matrix can support the long-term survival of living organisms encapsulated within the hydrogel (An et al., 2022). Their porous and permeable structure enables efficient molecular exchange with the external environment, while their chemical composition offers protection against harsh conditions such as low pH, extreme temperatures, and phage exposure (An et al., 2022). Furthermore, hydrogels act as a physical barrier, preventing bacterial intrusion and enhancing system stability (Tong et al., 2023).
Initially developed from petroleum-based polymers, hydrogels are now being increasingly researched for their bio-based alternatives due to growing environmental concerns (Ambika et al., 2021). These alternatives offer promising advantages such as biocompatibility, biodegradability, nontoxicity, and renewability, making them more environmentally friendly and versatile for various applications (Ambika et al., 2021).

1.4.1. Microalgae Immobilization

Hydrogels can be categorized based on their preparation method into chemically or physically cross-linked types (Waresindo et al., 2023). Chemically cross-linked networks are formed by using cross-linking agents that create covalent bonds between polymer chains, resulting in a stable and permanent network. However, the use of chemical cross-linkers can increase toxicity, limiting their suitability for certain bioengineering applications (Ambika et al., 2021). In contrast, physically cross-linked hydrogels, rely on temporary junctions of the polymer chains formed through physical interactions like entanglements, electrostatic forces, and hydrogen bonds (Waresindo et al., 2023). These methods avoid the need for toxic cross-linking agents, making them more biocompatible (Waresindo et al., 2023). Common physical cross-linking techniques include: thermal gelation, freeze-thawing and ionic interactions (Ambika et al., 2021).

1.4.2. Hydrogels exploration

Until now, researchers have primarily explored the combination of hydrogels and microalgae through two main techniques: bio 3D printing and bio–coating. In the following paragraphs these two techniques have been explored in depth.

1.4.2.1. 3D Printed Hydrogels

Digital fabrication, or 3D printing, involves creating physical objects by depositing materials layer-by-layer based on computer-aided design (CAD) models, enabling the production of complex and precise structures (Shahrubudin et al., 2019). Recently, algae-based materials have emerged as sustainable bio-inks, offering an eco-friendly alternative to traditional printing materials (Grira et al., 2023).
Bio 3D printing with microalgae-based inks provides unique advantages for biomedical and environmental applications such as tissue regeneration scaffolds, drug delivery systems, and customized nanofilters for water purification (Grira et al., 2023). While promising for wastewater treatment and carbon capture, maintaining the viability of microalgae within 3D-printed scaffolds remains a key challenge.

Zhao et al. (2019) demonstrated the use of silk-based hydrogels reinforced with hydroxypropyl methylcellulose (HPMC) to immobilize marine microalgae (*Platymonas* sp.) for long-term photosynthetic activity (Figure 10). The hydrogel successfully supported microalgae growth and sustained photosynthesis for up to 90 days without releasing cells into the environment. However, limited gas exchange and reduced light penetration, attributed to the gel's thickness, impeded growth after the first 10 days, underscoring the need for further optimization (Zhao et al., 2019).

Similarly, Oh et al. (2023) explored 3D printing engineered living materials (ELMs) with *Chlamydomonas reinhardtii* in a bio-ink made from κ-carrageenan, sodium, alginate, agar and cellulose -based thickener, cross-linked with Ca^{2+} ions (Figure 11). Although the microalgae remained

active for 42 days, growth decreased due to limited light penetration caused by the gel's thickness (Oh et al., 2023).. Additionally, CO_2 capture diminished after three days as colony growth did not enhance carbon capture efficiency (Oh et al., 2023).. The study highlighted that designs with larger surface areas captured more CO_2, suggesting that optimizing scaffold geometry could improve performance (Oh et al., 2023).

Balasubramanian et al. (2021) combined *Chlamydomonas reinhardtii* with alginate applied onto a bacterial cellulose substrate to create durable living materials (Figure 12). The cellulose provided mechanical strength, flexibility and nutrient absorption, supporting photosynthetic activity for 28 days (Balasubramanian et al., 2021). However, reduced nutrient availability and reduced tensile strength after prolonged water exposure revealed limitations (Balasubramanian et al., 2021). Additionally, further research is needed to evaluate its scalability and ensure environmental safety for widespread real-world applications (Balasubramanian et al., 2021).

These studies highlight the potential of microalgae-based living materials for carbon capture and wastewater treatment, emphasizing the need to optimize light penetration, gas exchange, and structural stability during prolonged contact with water. Further exploration of alternative encapsulation methods, such as coating techniques, may address these challenges and expand practical applications.

1.4.2.2. Bio-Coating

Coatings are layers applied to surfaces, such as substrates, to protect materials from environmental factors like radiation, moisture, and chemical or mechanical damage (Tajarudin & Ng, 2022; Noreen et al., 2016). Among these, biocoatings—porous polymer films designed to attach and retain microorganisms on surfaces—have gained significant attention (Tajarudin & Ng, 2022). Separately, biocoatings have also been employed in the development of hydrogels for encapsulating microalgae and cyanobacteria.

In-na et al. (2020) tested a 3D biocomposite system for biological carbon capture by immobilizing microalgae and cyanobacteria onto loofah sponge scaffolds coated with latex binders. This approach showed improved CO_2 fixation rates and long-term functionality, demonstrating potential for carbon capture and utilization (CCU) systems. However, challenges arose, including limited light penetration through the loofah sponge, restricted gas exchange due to the latex coating, and inconsistent microorganism adhesion, which led to cell escape. Furthermore, balancing cell density to prevent light and nutrient blockages remained a challenge.

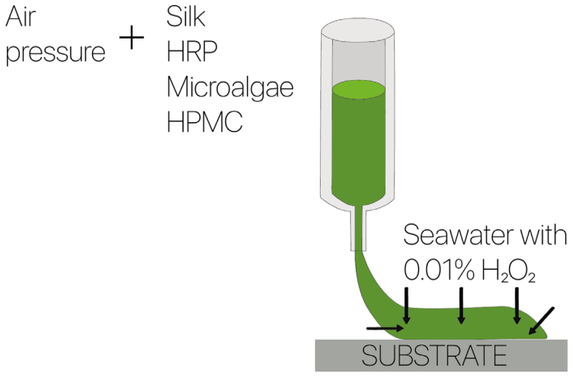

Figure 10: A schematic illustrating the printing process of silk/HPMC ink mixture containing microalgae (Zhao et al., 2019).

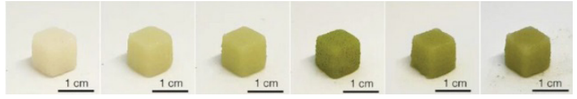

Figure 11: Time-series of ELM-maturation during 28 days under auto-trophic conditions (Oh et al., 2023).

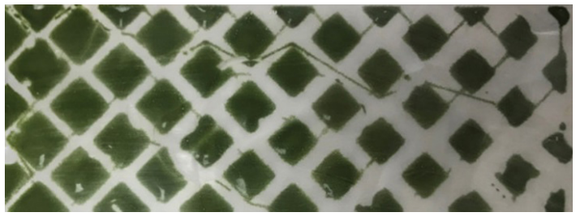

Figure 12: up-scaled bioprinted living materials (Balasubramanian et al., 2021).

In-na et al. (2021) revised their approach by replacing the loofah sponge scaffold with polyester and cotton blends in varying ratios and substituting the latex coating with kappa-carrageenan as a gel topcoat to enhance microalgae retention (Figure 13). While these changes improved light penetration and gas exchange, new challenges emerged, such as reduced microalgae adhesion on polyester, cotton degradation in moist conditions, and partial detachment of algae despite the topcoat (In-na et al., 2021). These findings underscore the need for more durable materials and advanced coating solutions to enhance operational stability.

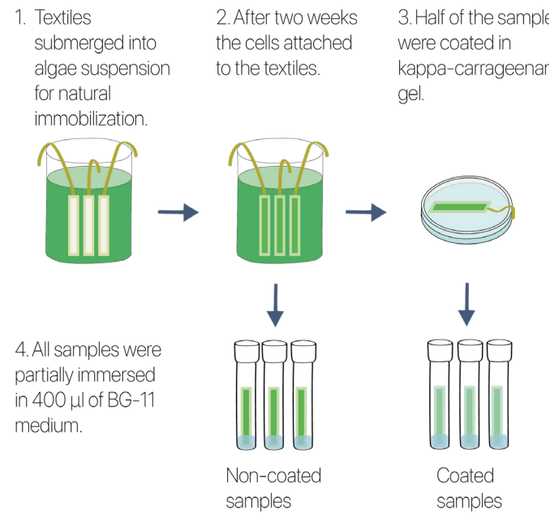

Figure 13: A schematic of textile biocomposite production and testing process under batch CO2 exposure for a period of 28 days (In-na et al., 2021).

Innovative scaffolds and coatings offer significant potential for sustainable applications but require further refinement to overcome challenges like material stability, gas exchange, and microorganism retention. Rethinking material design and fabrication is crucial for improving the functionality and durability of these systems. Textiles, with their structural versatility and absorptive properties, present a promising avenue for creating durable and adaptable solutions capable of addressing challenges such as material stability, gas exchange, and microorganism retention. To fully harness their potential, optimizing textile design at the fiber and yarn level is essential. In this context, weaving emerges as a fundamental fabrication technique, able to enhance functionality and performance.

1.5. Weaving

Weaving stands out as a foundational method for textile construction, involving the interplay of two sets of yarn: the warp, which runs vertically through the loom, and the weft, which interlaces horizontally between the warp threads (Shenton, 2014) (Figure 14). The particular way the weft travels over and under the warp yarns determines the pattern and structure of the textile (Devendorf et al., 2019). For additional information about weaving structures, see Appendix C.

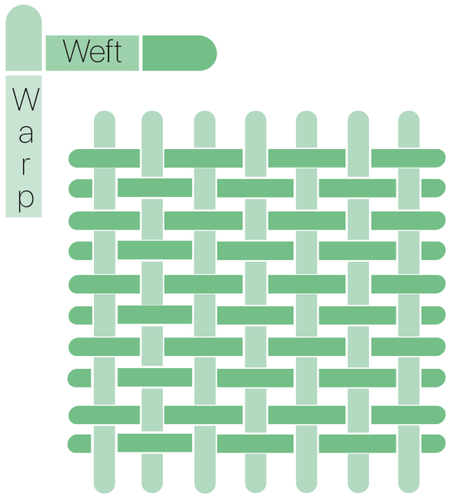

Figure 14: Woven textile.

However, the production of woven textiles structures requires detailed planning, documented in specifications or worksheets (Shenton, 2014). Therefore, utilizing instruments like drafts, patterns and cross-section structures is crucial to guide the designer during the production of the final textile structure.
A draft is a binary map or plan indicating which warps or heddles should be lifted for each pick (Figure 15). In the draft, black cells represent raised warps, while white cells indicate lowered warps (Devendorf et al., 2022). The draft provides a comprehensive overview of the entire cloth, often containing regions of varying repeating structures (Devendorf et al., 2022). The pattern, on the other hand, focuses on the visual qualities of the woven textile and is typically accompanied by material information (Devendorf et al., 2022) (Figure 16). Additionally, the cross-section structure of the cloth describes its smallest repeating unit, visible when the textile is examined in cross-section (Devendorf et al., 2022) (Figure 17).

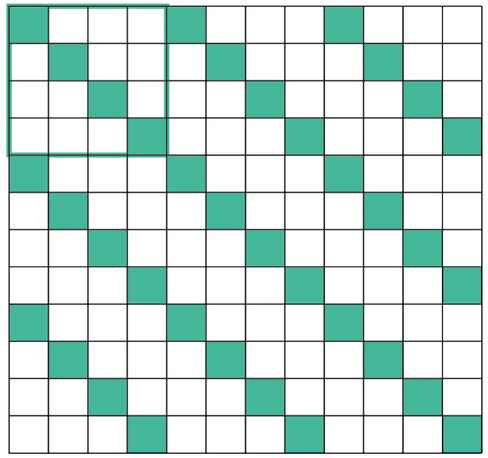

Figure 15: Draft (Devendorf et al., 2022).

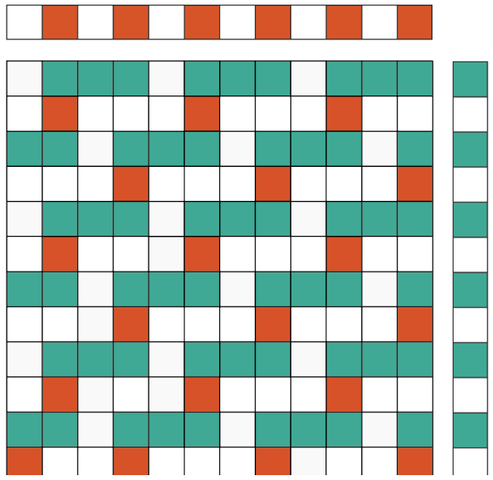

Figure 16: Pattern (Devendorf et al., 2022).

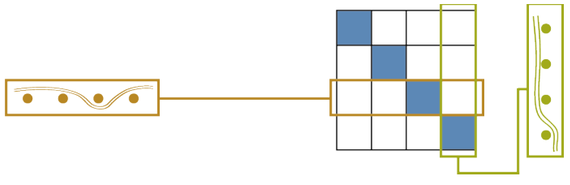

Figure 17: Cross-section (Devendorf et al., 2022).

Weaving remains a fundamental aspect of textile production, combining its historical roots with practicality and design adaptability. Through meticulous planning and innovative techniques, it continues to evolve to meet the needs of contemporary applications (Devendorf et al., 2022).

1.5.1. Loom

The loom serves as the fundamental tool for weaving textiles, designed to maintain warp threads under tension while facilitating the interlacing of weft threads to form textile (Perera et al., 2021). This process relies on precise coordination, where warp yarns are unwound from the warp beam during the let-off mechanism and guided through heddle eyes, which are attached to heddle frames (Bulathsinghala, 2022). The complexity of the woven structure directly influences the number of heddle frames required, as more intricate patterns demand greater control over warp thread movement, necessitating additional frames (Bulathsinghala, 2022).
Looms serve the consistent purpose of maintaining warp thread alignment and facilitating weft insertion, a principle that has evolved into a foundation for modern weaving technologies (Salolainen, 2022). The binary coding system inherent in weaving has inspired advancements such as the Jacquard loom, which uses indipendent

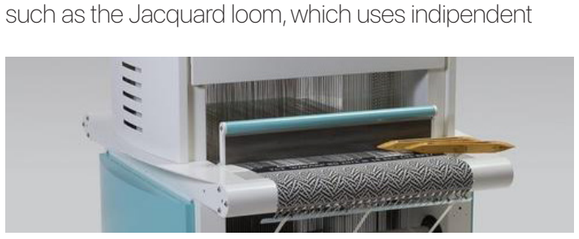

Figure 18: Jacquard loom TC2 (2012) (Engineering, n.d.-b).

warp thread control to produce intricate patterns and complex 3D woven textiles with digital precision (Salolainen, 2022; Liu et al., 2021).

1.5.2. Textiles Structures and Dimensions

Early fiber development focused primarily on improving the tactile comfort of textiles, as fibers, Early fiber development prioritized enhancing the tactile comfort, as textiles were primarily used for apparel (Perera et al., 2021). These textiles were traditionally two-dimensional (2D) woven structures, with warp and weft yarns interlaced at 0° and 90° angles, respectively (Koncar, 2019). With advancements in technical textiles, the focus shifted toward performance-driven applications, leading to the development of three-dimensional (3D) woven structures. Unlike conventional 2D and 3D textiles incorporate yarns aligned in three orthogonal directions (x, y, and z), with z-yarns providing through-thickness reinforcement (Perera et al., 2021). This structural evolution has expanded textile applications to fields such as textile architecture, smart electronics, reinforcement materials, and medical devices (Gries et al., 2022; Perera et al., 2021).
However, textile classification extends beyond 2D and 3D structures. Weave patterns can also vary from double-layered to multi-layered constructions, allowing the integration of multiple materials with distinct properties. By associating different materials with specific weave structures, woven textiles can achieve complex functional variations (Pouta et al., 2024). Double weaving allows to weave twolayers at once. It works by splitting the warp yarns into two groups and weaving those yarn groupings separately from each other to create two layers that sit atop of each other (Devendorf et al., 2019) (Figure 19). This technique enables semi-complex structures that introduce additional functionalities. For instance, layer orientation in a double weave can be reversed, allowing the back face of the textile to switch to the front and vice versa (Devendorf et al., 2019). This mechanism can be used to create pockets, potentially serving as enclosures for objects or even living microorganisms, a structure known as double cloth (Pouta et al., 2024).

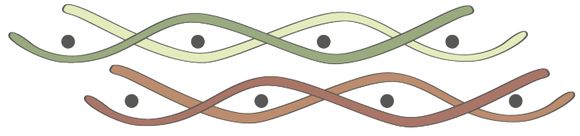

Figure 19: Double layer structure.

However, the layer count does not need to be limited to two. Multi-layer textiles allow for various linked or independent layers, expanding the possibilities for durability, protection, and structural enhancement (Pouta et al., 2024). A practical example is the study by Pouta et al. (2024), which explored multi-layered e-textiles, enhancing their inner-layer protection and mechanical durability (Figure 20).

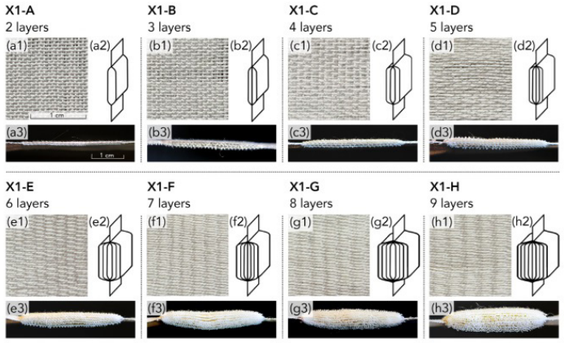

Figure 20: layer count increasing from 2 (top left) all the way to 9 (bottom right) (Pouta et al., 2024).

Another example is provided by McQuillan (2020), who demonstrated that multilayer textiles can be utilized to create three-dimensional forms by simply weaving multiple two-dimensional textile layers. As illustrated in Figure 21, this approach leverages the structural properties of layered textiles to achieve complex 3D shapes without the need for additional cutting or stitching (McQuillan, 2020). This technique underscores the potential of layering in textile engineering, further expanding the possibilities for innovative textile design and functionality (McQuillan, 2020).

Figure 21: Multilayer structures used to design pants (McQuillan, 2020).

The final category, compound textiles, consists of two or more interconnected layers, linked through an additional warp system or specialized warp arrangements (Witczak et al., 2021). This structure is widely used in drive belts, conveyor belts, and composite reinforcements, offering superior compactness and strength (Witczak et al., 2021). In compound weaves, warp yarns are divided into two or more groups, and the weft crosses through multiple groups, forming a dense, reinforced textile structure (Figure 22).

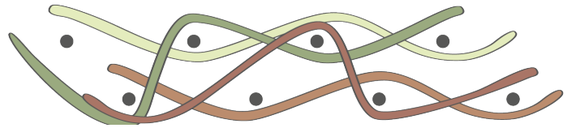

Figure 22: compound structure.

1.5.3. Materials influences

Chapter 3.3. highlighted the diverse structures that textiles can adopt. In this chapter, it is essential to recognize that as the structure changes, so do the textile's properties (Begum & Milašius, 2022). A key factor influencing these variations is the balance between floats and interlacements, which directly affects textile density, softness, and rigidity (Devendorf et al., 2022). Longer floats create denser and softer textiles, while a greater number of interlacements result in thinner, more rigid structures (Devendorf et al., 2022).

However, textile properties are not solely dictated by structure but also by material composition. For instance, Buso et al. (2024) studied PVA's response to water exposure and observed that PVA fibers swell, absorb H_2O molecules, and gradually dissolve, leading to thicker and shorter yarns (Figure 23) (Buso et al., 2024). Based on these findings, they explored how PVA's dissolution properties could be leveraged for origami folding, utilizing weaving techniques to manipulate textile transformation (Buso et al., 2024).

Similarly, Scott (2018) examined the influence of water on material properties in the Responsive Knit project, which utilized wool's natural shrinkage and shape transformation when wet (Figure 24). By combining specific yarn twists and knit structures, the project developed textiles that. respond dynamically to environmental changes (Scott, 2018).

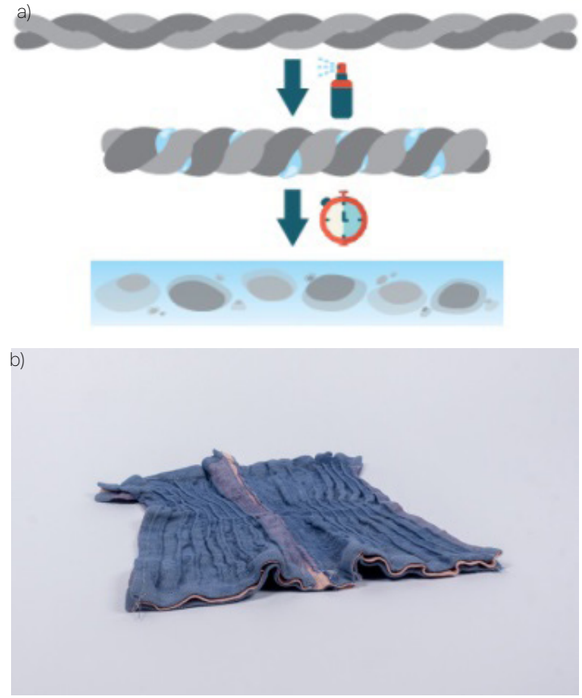

Figure 23: a) stages of PVA dissolution when in contact with water (Buso et al., 2024); b) final product obtained by origami techniques used to exploit PVA natural properties (Buso et al., 2024).

Figure 24: On the left, the textile is shown before being sprayed with cold water, and on the right, after being sprayed with cold water (Scott, 2018).

Beyond structural and mechanical performance, material composition also affects biological interactions. In-na et al. (2021) investigated how textile composition influences microalgae attachment by immersing four textile variations (100% PET, 100% Co, 80% PET / 20% Co, and 65% PET / 35% Co) in *Chlorella vulgaris* medium (In-na et al., 2021). After 14 days, they found that 100% PET retained the least chlorophyll, while cotton-containing textiles enhanced microalgae attachment due to their hydrophilic properties (In-na et al., 2021). The experiment continued with 100% PET and 100% Co textiles, which were further immersed in kappa-carrageenan to assess long-term attachment. The results confirmed that microalgae adhered better to cotton, as its surface charge (zeta potential) ranged from –15 to –20 mV, closely matching *Chlorella vulgaris* (–17 to –18 mV). In contrast, polyester exhibited a zeta potential of –60 to –65 mV, explaining its poor microalgal attachment (In-na et al., 2021). Based on these findings, In-na et al. (2021) recommended using textiles that enhance microalgae adhesion, ensuring better attachment and long-term stability. Additionally, they emphasized the importance of selecting textiles with good light penetration, as adequate illumination is crucial for sustaining microalgal growth and photosynthetic activity.

Finally, it has been studied that the ratio of yarn blends plays a crucial role in determining the properties of the resulting textile. According to MR et al. (2024), a higher IPI (Imperfections Index) value in yarn increases the areal density of the textile, meaning that as the number of thick, thin places, and neps in the yarn rises, the fabric's GSM (Grams per Square Meter) also increases. This relationship is particularly evident in blended yarns with varying cotton-to-jute ratios. The study demonstrates that 100% jute yarn exhibits the highest IPI value, leading to the greatest textile GSM and air permeability. Conversely, as the cotton content increases in blends (e.g., 40C:60J, 60C:40J, 80C:20J, and 100C), the IPI value systematically decreases, resulting in lower textile GSM and reduced air permeability. The findings indicate a strong correlation between the properties of the yarn input and the characteristics of the final textile output. This highlights the importance of carefully selecting yarn blend ratios to achieve desired textile properties in terms of density, breathability, and overall performance (MR et al., 2024).

1.5.4. Textiles Opportunities

Textiles provide a versatile platform for creative exploration, offering lightweight flexibility and adaptable properties such as variable density and texture. Their customizability makes them an ideal foundation for developing tailored, application-specific materials.
One approach to textile transformation is origami, the Japanese art of paper folding, which enables flat surfaces to become intricate three-dimensional structures (Origami for Beginners: Easy Guide to Origami | Discount Art N Craft Warehouse, n.d.). Emilie Palle Holm's ORIORI project exemplifies this principle by incorporating origami-inspired jacquard-woven structures to create self-supporting textile forms (Emilie-palle-holm, n.d.).
However, textiles offer a dynamic platform for creative exploration, combining lightweight flexibility with adaptable properties such as density and texture variations. Their customizable nature makes them an ideal foundation for developing tailored, application-specific materials.

One approach is origami, a traditional Japanese art of paper folding, which involves transforming flat surfaces into complex three-dimensional structures (Origami for Beginners: Easy Guide to Origami | Discount Art N Craft Warehouse, n.d.). For instance, Emilie Palle Holm's ORIORI project utilizes origami structures as a foundational construction principle to create jacquard-woven, three-dimensional surface structures and self-supporting textile forms (Figure 25) (Emilie-palle-holm, n.d.).

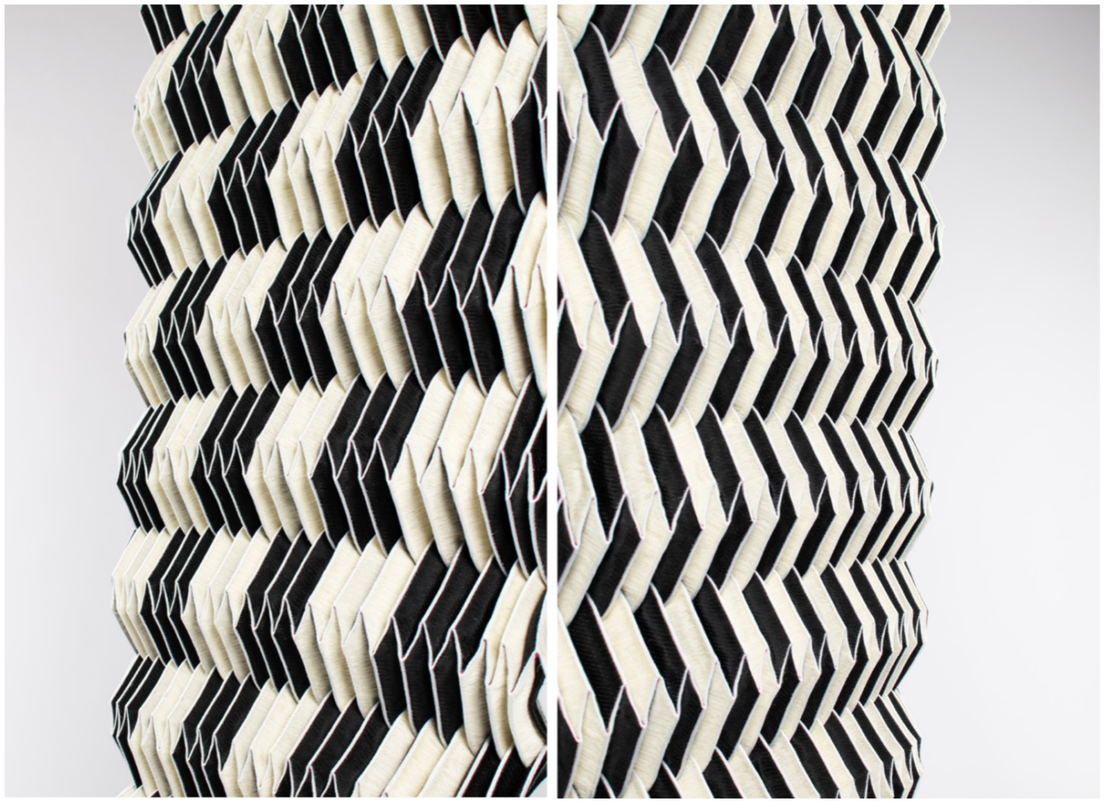

Figure 25: Emilie Palle Holm's ORIORI project (Emilie-palle-holm, n.d.).

Beyond folding techniques, weaving methods also shape textile behavior. Buso et al. (2022) explored the role of weave structure, density, and heat application in programming shape-changing textiles (Figure 26). By adjusting interlacements—such as reducing them in a 3x1 twill weave compared to a 1x1 plain weave—they engineered textiles capable of transforming into predefined 3D shapes (Buso et al., 2022).

Sustainability is another key area of focus in textile innovation. McQuillan and Karana's Multimorphic Textile-Forms (MMTF) highlight the integration of principles like zero waste and extended life cycles. These textile-based objects are designed to evolve over time, minimizing waste and promoting local, on-demand production. The approach considers the relationship between material, form, and production, creating multifunctional and eco-friendly solutions (McQuillan & Karana, 2023).
These examples highlight textiles as a medium for innovation, whether through origami-based folding, programmed weaving techniques, or sustainable material strategies. Their dynamic nature enables solutions that bridge functionality, aesthetics, and environmental responsibility.

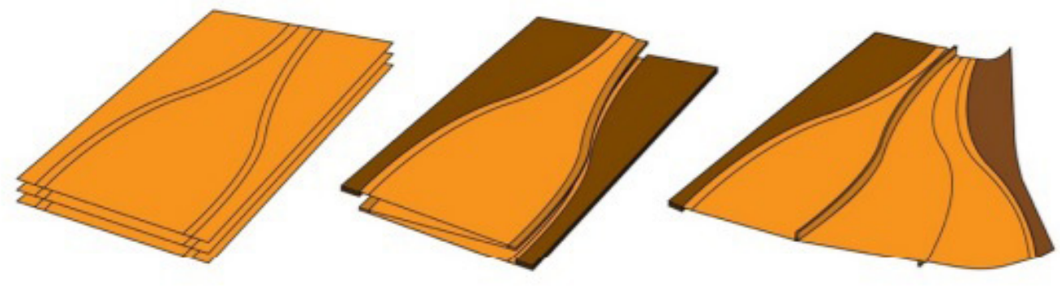

Figure 26:The diagram illustrates how variations in heat-reactive yarn density and weave structures influence shape-changing behavior, with brown areas representing high density and orange areas indicating low density (Buso et al., 2022).

Chapter 2
Project Definition

This chapter defines the research direction and explores how the Material Driven Design Method serves as the foundation for the applied approach. It presents the problem definition, methodology, and project scope, along with the research questions that guide the project.

2.1. Problem Definition

As previously reported, Microalgae offer immense potential for carbon capture, biofuel production, and environmental remediation. However, existing cultivation and encapsulation techniques face significant challenges. Suspension cultures, while commonly used, are resource-intensive and vulnerable to contamination, reducing scalability (Razzak et al., 2017). Immobilization methods, such as loofah sponges with latex binders, face issues like obstructed light and gas exchange, restricted oxygen release, poor microalgae adhesion, and scaffold degradation, limiting productivity and long-term stability (In-na et al., 2020; In-na et al., 2021).

Meanwhile, textile-based scaffolds, like polyester and cotton blends coated with kappa-carrageenan, show promise in optimizing light exposure, gas diffusion, and nutrient availability. Yet, challenges such as reduced CO_2 absorption and microbial detachment indicate the need for more robust materials and coatings (In-na et al., 2021).

Is fundamental to highlight that these existing structures are not inherently designed to support microalgal growth and viability. Thus, the challenge lies in exploring new 3D woven textile structures and novel encapsulation methods to develop living textiles capable of sustaining and enhancing microalgal viability.

2.2. Approach and Methodology

To design the new 3D woven textile scaffold, it is essential to study textile structures and test their compatibility with microalgae. Unlike traditional engineering approaches that begin with a predefined goal, this project adopts a combination of the *Material-Driven Design (MDD) Method* and the *Parallel Prototyping Method (PPM)* to enable exploratory and iterative development (Karana et al., 2015; Kesari, 2019) .

The MDD method is mainly divided into four phases (Figure 27). The first phase, "Understanding the Materials" focuses on understanding the material's technical properties. The second phase, "Creating Materials Experience Vision" is where the desired interaction and behavior of the material are envisioned. The third phase, "Manifesting Materials Experience Patterns" focuses on experimenting with forms and prototypes to realize the envisioned experience. Finally, the fourth phase, "Creating Material/Product Concepts" focuses on translating the material and its qualities into tangible product concepts (Karana et al., 2015).

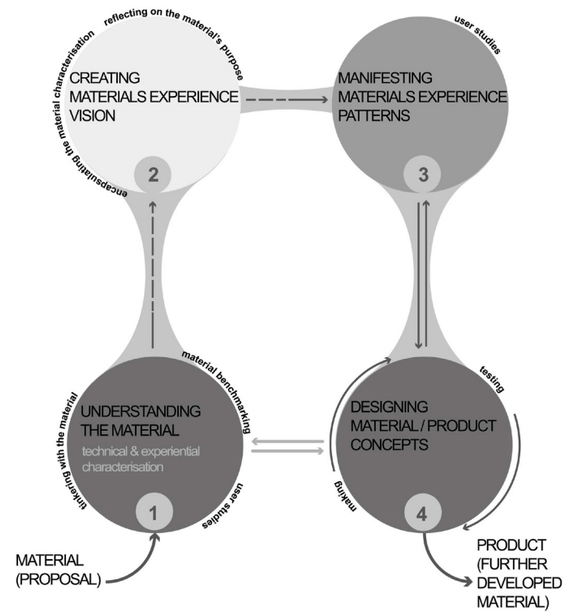

Figure 27: Material Driven Design Method (Karana et al., 2015).

In this project, the traditional sequence of the Material-Driven Design (MDD) method has been adapted (Figure 28). The process begins with *Understanding the Materials*, phase will focus on analyzing and testing various materials to ensure they meet the biological requirements of microalgae. To enhance efficiency, the *Parallel Prototyping Method* is employed, enabling simultaneous experiments to explore different material configurations within a shorter timeframe (Kesari, 2019). The next phase, *Manifesting (Organism-Centered) Materials Experience Patterns,* positions microalgae as the primary "users" of the textile, assessing how well the environment supports their growth, activity, and survival. These two phases will be iteratively applied throughout the project. Following this, the *Creating Materials Experience Vision* phase involves reflecting

on these results to outline the next steps needed and to envision potential outcomes of this research. Finally, the *Creating Material/Product Concepts* consolidates the most effective solutions into a cohesive final product design.

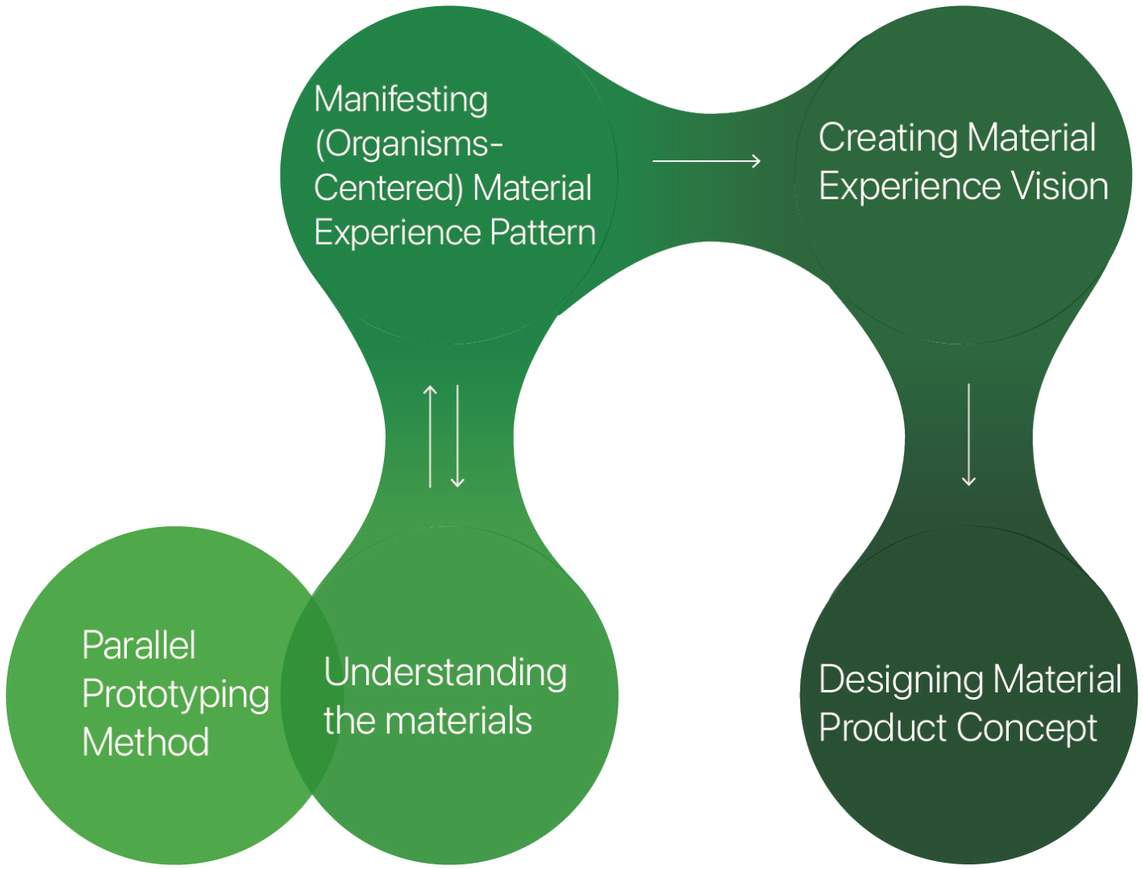

Image 28: MMD and Parallel Prototyping Method (Karana et al., 2015; Kesari, 2019)

2.3. Project Scope and Research Questions

The primary objective of this project is to determine the optimal method for encapsulating microalgae in textiles effectively.

The second focus is to identify the most suitable types of yarns for the creation of the textile.

The third, and perhaps the most critical aim, is to explore how various weaving techniques can be employed to construct a textile structure with enhanced mechanical properties.

The last one focus on studying origami techniques that could be applied to living textiles.

By combining these four key insights, the project aims to develop a 3D woven textile capable of hosting microalgae while promoting their growth. This endeavor addresses two fundamental questions:

1. Can we design a 3D woven textile that supports the survival and growth of microalgae?

2. What opportunities can this innovation unlock to deliver value for the stakeholders involved?

Chapter 3
Understanding the Materials / Manifesting (Organism-Centered) Materials Experience

This chapter explores the three main objectives from the previous chapter through experiments assessing microalgae responses to different environmental conditions. As part of the cyclical methodology steps—"Understanding the Materials" and "Manifesting (Organism-Centered) Materials Experience Patterns"—these tests aim to develop a new cultivation environment for microalgae, integrating material properties with biological functionality.

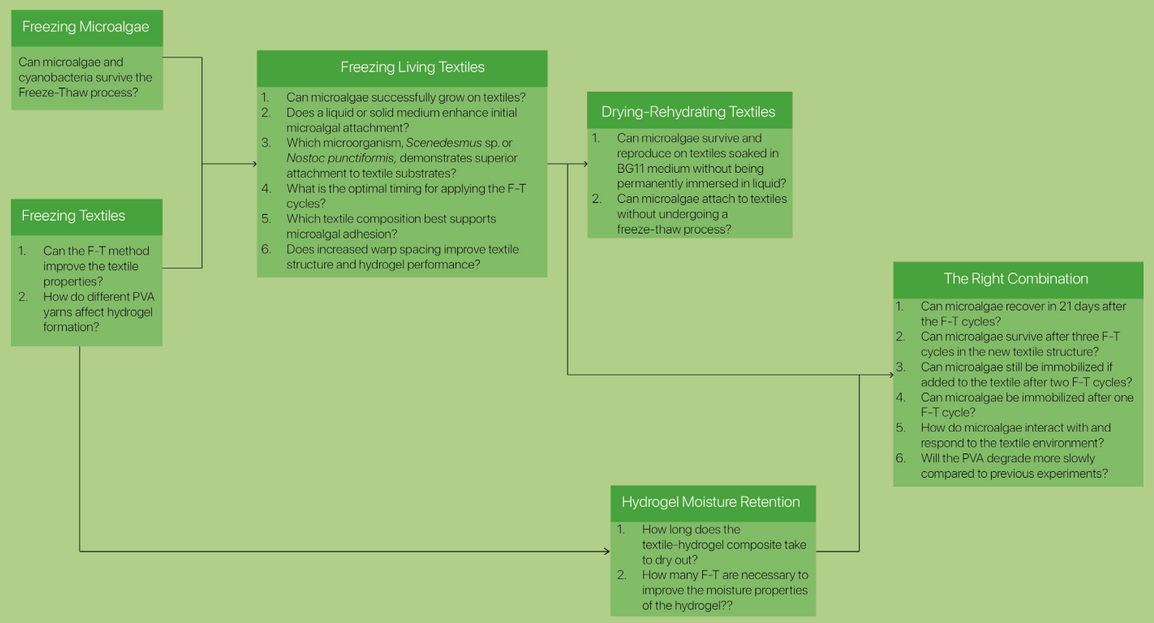

3.1. Freezing Microalgae and Cyanobacteria

The first method explored for microalgal and cyanobacterial encapsulation into textiles is the Freeze-Thaw (F-T) process. This method creates crosslinks between polymer chains in PVA, forming a three-dimensional network that traps the solvent and transitions the material into a gel phase (Ayoub El Idrissi et al., 2024). Although it is primarily used to enhance the mechanical properties of hydrogels through crystal formation, this process could potentially encapsulate microalgae/cyanobacteria by physically entrapping them within the textile network. Unlike chemical crosslinking agents such as glutaraldehyde, this approach avoids the use of toxic substances, making it a safer alternative (Ambika et al., 2021).
To determine the feasibility of the Freeze-Thaw (F-T) approach, the microalga *Scenedesmus* sp. and the cyanobacterium *Nostoc punctiformis* were subjected to the F-T process in their liquid medium at -20°C. This step aimed to evaluate their viability under temperature cycles, comparing the resilience of microalgae and cyanobacteria to freezing conditions. By addressing these factors, this experimental session seeks to answer two key questions:

1. Can microalgae and cyanobacteria survive the Freeze-Thaw process?
2. Which organism demonstrates greater resilience to this process: *Scenedesmus* sp. or *Nostoc punctiformis*?

By answering these questions, this experiment establishes the foundation for using the F-T method in microalgal/cyanobacterial encapsulation and informs the direction of future investigations.

3.1.1. Materials

- 1 culture flask of *Scenedesmus* sp. (200 ml);
- 1 culture flask of *Nostoc punctiformis* (200 ml);
- 4 pipettes (25 ml);
- BG 11 medium;
- 4 culture flasks (40 ml);
- Incubator;
- Laminar Air Flow (LAF) Cabinet.

3.1.2. Method

The experiment began in the BioLab, where a sterilized Laminar Air Flow (LAF) Cabinet was used to maintain a controlled and sterile environment. To initiate the procedure, two 200 ml culture flasks containing *Scenedesmus* sp. with BG-11 medium and *Nostoc punctiformis* with BG-11 medium were placed at the center of the Biosafety Cabinet. Using sterile pipettes, 20 ml of *Scenedesmus* sp. culture was transferred into two separate sterile 40 ml flasks, ensuring proper separation for subsequent testing. The same process was repeated for *Nostoc punctiformis*, with 20 ml of its culture transferred into two additional 40 ml sterile flasks (Figure 30).
To dilute the cultures, 20 ml of BG-11 medium was added to each flask. This preparation ensured equal initial conditions for both species. Once prepared, one flask containing *Scenedesmus* sp. and one containing *Nostoc punctiformis* were placed in a 20°C incubator set to provide a daily cycle of 16 hours of light and 8 hours of darkness, simulating optimal growth conditions. The incubation period lasted four days, covering the entire duration of the experiment (Figure 31).

The remaining flasks were transferred to a freezer set at -20°C to initiate the Freeze-Thaw (F-T) process (Figure 32). After 24 hours of freezing, the flasks were moved from the freezer to the incubator at 20°C for a thawing phase lasting four hours. Following this phase, the cultures were carefully monitored macroscopically, and detailed observations were recorded to assess the microorganisms' response to the temperature shifts. This Freeze-Thaw cycle was repeated three times to evaluate the resilience of *Scenedesmus* sp. and *N. punctiformis* under freezing conditions and to explore their viability and potential for encapsulation within a hydrogel matrix.

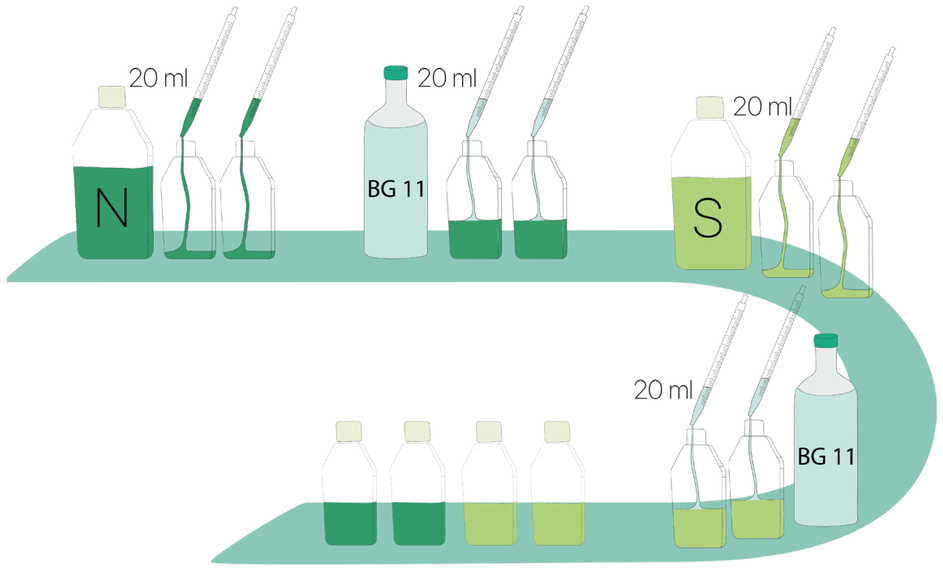

Figure 30: Steps to prepare *Nostoc Punctiformis* and *Scenedesmus* solutions.

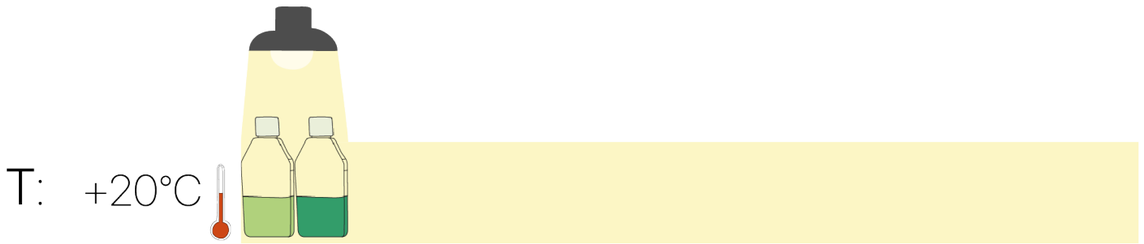

Figure 31: Two flasks of *Nostoc Punctiformis* and *Scenedesmus* left under controlled light conditions and at room temperature.

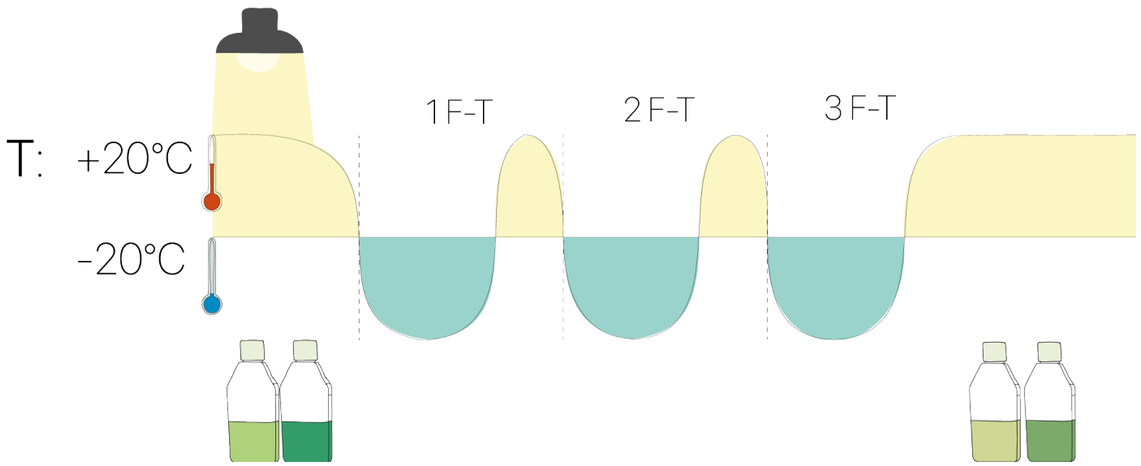

Figure 32: Description of the Freeze-Thaw process using two culture-flasks of *Nostoc punctiformis* and *Scenedesmus* sp. each.

3.1.3. Conclusion

Through microscopic observation was possible to visualize the resilience of both species to sub-zero temperatures (Figure 33a and 33b). While some cell death was observed in both strains, at least half of the cells remained viable after each Freeze-Thaw (F-T) cycle. However, a noticeable deterioration in the color of both *Scenedesmus* sp. and *Nostoc punctiformis* was observed after the second cycle, suggesting potential stress or reduced photosynthetic activity in response to repeated freezing (Figure 33d and 33e). Due to limitations in available resources, it was not possible to objectively quantify cell death, making it challenging to determine which species exhibited greater resistance to the freezing process. Despite these limitations, the success of these trials supports the hypothesis that microalgae/cyanobacteria resist the F-T process and may potentially be immobilized within a matrix using this method. This outcome paves the way for further exploration of F-T as a viable encapsulation technique for microalgae/cyanobacteria, with potential applications in creating stable, embedded hydrogels to support the long-term viability of these microorganisms.

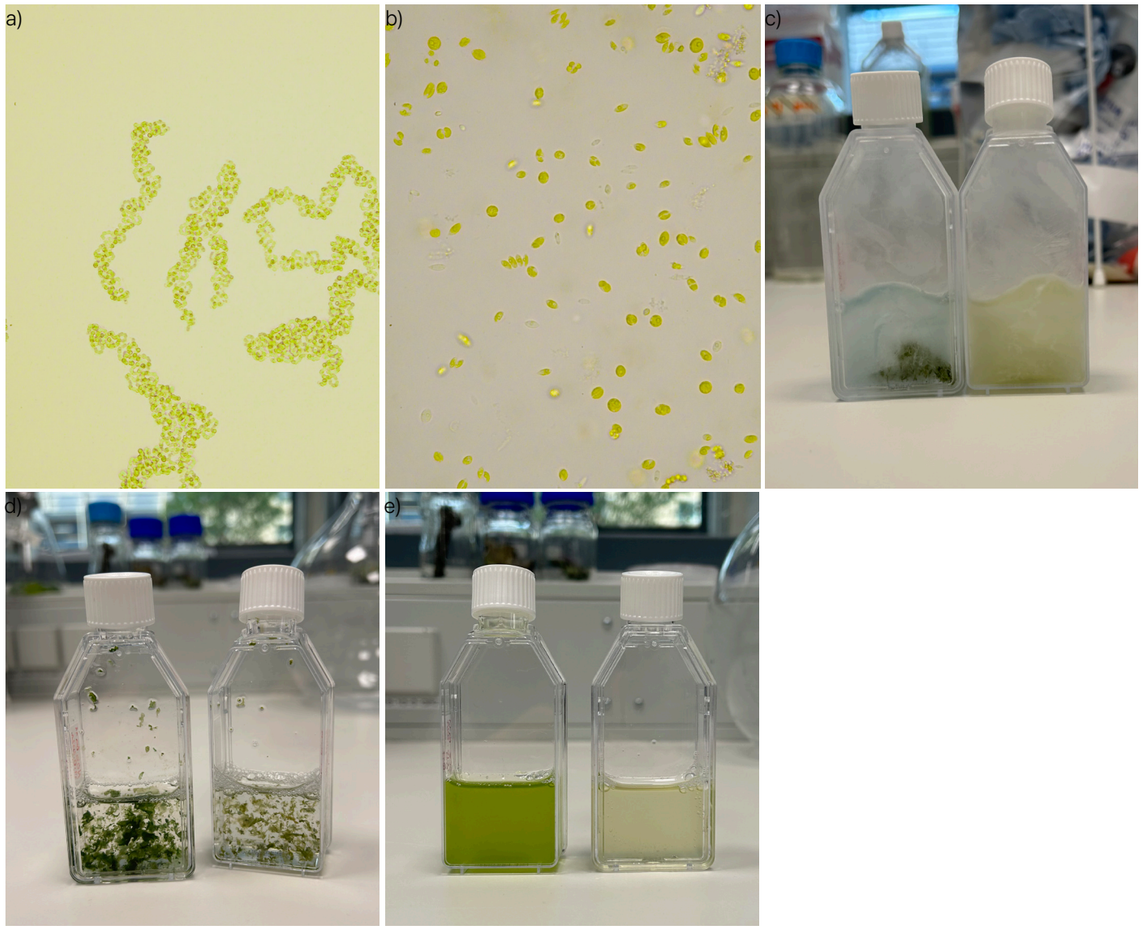

Figure 33: a) Microscopic image of *N. punctiformis* cells after three freeze-thaw cycles (100×); b) Microscopic image of *Scenedesmus* sp. cells after three freeze-thaw cycles (100×); c) *Nostoc punctiformis* (left) and *Scenedesmus* sp. (right) cultures immediately after the 3rd freezing process. ; d) *N. punctiformis* cultures after the 3rd thaw process; e) *Scenedesmus* sp. cultures after the 3rd thaw process;.

3.2. Freezing Textiles

After exploring the effects of the F-T method on microalgae, now it is necessary to discover its effect on textiles. Therefore, the Freezing Textiles Experimental Session investigates the stability of a PVA-Cotton (Co) textile blend under repeated Freeze-Thaw (F-T) cycles, aiming to assess its potential as a robust hydrogel matrix for possible microalgae encapsulation.

The selection of cotton and polyvinyl alcohol (PVA) for this experiment is based on their complementary properties.
Cotton, with its porous structure and surface roughness, promotes microalgal adhesion and retention while facilitating nutrient diffusion and gas exchange—both essential for microalgal viability and growth (Vasilieva et al., 2020). Additionally, high cotton content increases the textile's alkalinity, maintaining an optimal pH range for photosynthesis (In-Na et al., 2021). These characteristics make cotton a valuable component for supporting microalgal encapsulation within the textile matrix. PVA, on the other hand, enhances the mechanical strength and durability of the textile. Known for its transparency in its gel state when in contact with water, PVA forms physically cross-linked hydrogels through polymer chain crystallization during the Freeze-Thaw (F-T) method, significantly enhancing tensile strength and material stability (Waresindo et al., 2023; Ayoub El Idrissi et al., 2024). During this process, previous immersion in an aqueous solution is fundamental, as it allows hydroxyl groups in the polymer chains to form hydrogen bonds with water molecules, further stabilizing the hydrogel structure (Koc et al., 2020). By leveraging these properties, PVA contributes to the creation of a durable, water-diffusive matrix capable of supporting encapsulated microalgae.

Building on these complementary properties, this experiment focuses on three key factors: 1.) the effectiveness of the F-T method in creating a stable hydrogel within the textile; 2.) a comparison of two types of PVA (Solvron SF.330 and Solvron MH.750)—one characterized by its dissolution property and the other by its tendency to shrink—to determine which performs best for this application, and 3.) the impact of the liquid medium, with textiles immersed in either BG11 or dH_2O, on the mechanical properties of the textile. To efficiently evaluate these variables, the Parallel Prototyping Method (Kesari, 2019) was employed, enabling simultaneous testing of multiple configurations. By leveraging this approach, the experiment aims to identify the optimal formulation and F-T conditions needed to create a stable hydrogel capable of facilitating water diffusion—an essential requirement for supporting microalgal viability. To achieve this, the session focuses on addressing three key questions:

1. Can the F-T method improve the textile properties?
2. How do different PVA yarns effect hydrogel formation?
3. In what way does BG11 effect the textile?

3.2.1. Textile Materials

- Warp:Cotton yarn NE 38/2;
- Weft: Solvron MH.750 (H Shrink Monofilament) 3x 750 dtex - Count: 1/4.5 Nm;
- Weft: Solvron SF.330 (Dissolvable 55c+ Yarn) 330x3 d tex - Count: 1/10 Nm;
- Jacquard loom TC2;
- Boat shuttle;
- Bobbin;
- Scissors;

3.2.2. Textile Method

The textile samples were fabricated in the Material Lab using the Jacquard loom TC2. The 50% PVA and 50% Co textile has been realized twice to verify two different types of polyvinyl alcohol (PVA) yarns. The preparation began with activating the TC2 weaving program on the lab computer and configuring the tabby weave structure.
The bobbin winder was then set up, and the first type of PVA yarn (Solvron MH.750) was wound onto the bobbin from its cone. Once fully loaded, the bobbin was transferred to the boat shuttle. With the loom and shuttle ready, the weaving process commenced. The selected tabby plan was transmitted to the Jacquard loom, and the weaving sequence began. By pressing the loom pedal, the cotton warp yarns alternated positions - based on the draft uploaded on the TC2 weaving program -, allowing the shuttle carrying the PVA yarn to pass through. This cyclical process was executed until the textile reached a length of 70 cm and a height of 5 cm. An additional 2 cm of textile was woven to separate the current sample from the next.
The same process was followed to create the second textile using the second type of PVA yarn (Solvron SF.330). Once both textiles were complete, they were carefully removed from the loom and cut into samples. As illustrated in Figure 35, each textile was divided into four samples measuring 7 cm x 5 cm: two from the cotton-PVA (Solvron MH.750) textile, known for its higher shrinkage, and two from the cotton-PVA (Solvron SF.330) textile, characterized by higher dissolution.

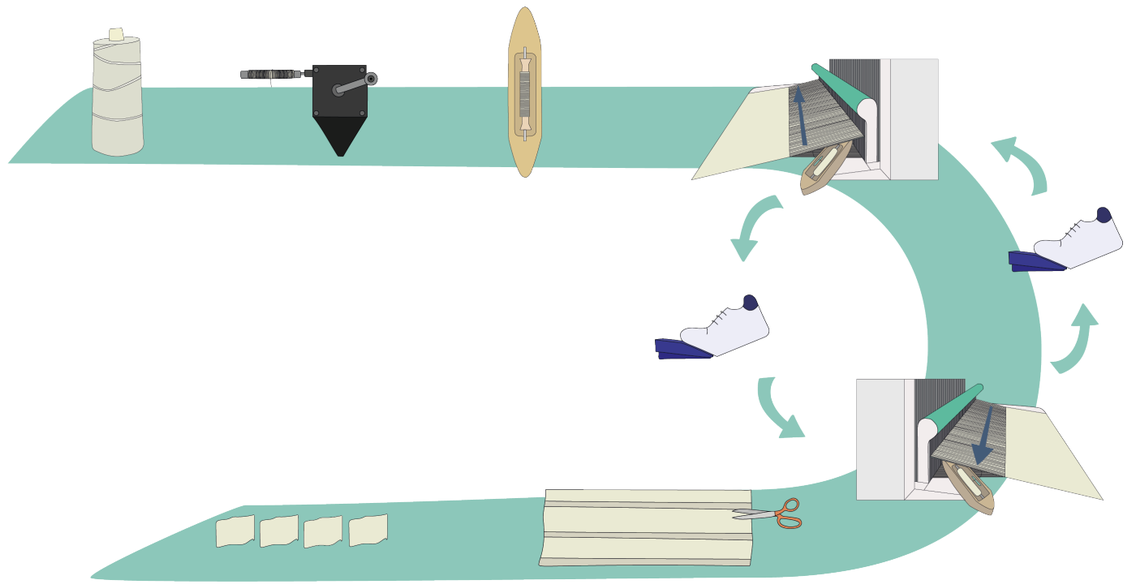

Figure 34: Steps to prepare the 50% PVA 50% Co textiles.

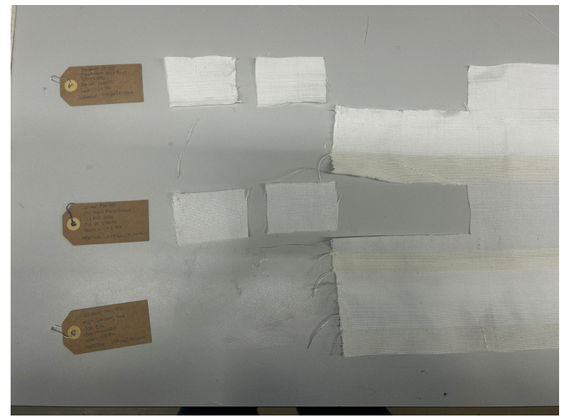

Figure 35: Textiles cut into 7 x 5 cm samples.

3.2.3. Experiment Materials

- 2 tabby textile (50% PVA - 50% Cotton; 7x5 cm) realized with PVA Solvron SF. 330 (Dissolvable 55c+ Yarn) 330x3 dtex, and Cotton NE 38/2;
- 2 tabby textile (50% PVA - 50% Cotton; 7x5 cm) realized with PVA Solvron MH. 750 (H Shrink Monofilament) 3x750 dtex and Cotton NE 38/2;

- dH_2O;
- BG11 medium;

- 4 Petri dish;

- Freezer;

- Tweezers;
- Parafilm.

3.2.4. Method

The experiment was carried out in the Material Lab, as no microorganisms were involved. Two cotton-PVA Solvron SF.330 textiles and two cotton-PVA Solvron MH.750 textiles were used, each assigned to specific conditions for testing (Figure 36). The two Solvron SF.330 textiles were placed into separate Petri dishes containing deionized water (dH_2O) and BG11 medium. Similarly, the Solvron MH.750 textiles were placed into separate dishes containing dH_2O and BG11 medium. The Petri dishes were securely sealed to ensure stable conditions and stored in a freezer at -20°C for 24 hours, after which they were thawed at room temperature for 4 hours under specific light conditions (16 h light - 8h dark). This Freeze-Thaw (F-T) cycle was repeated three times to determine the number of cycles required for hydrogel formation (Figure 37).

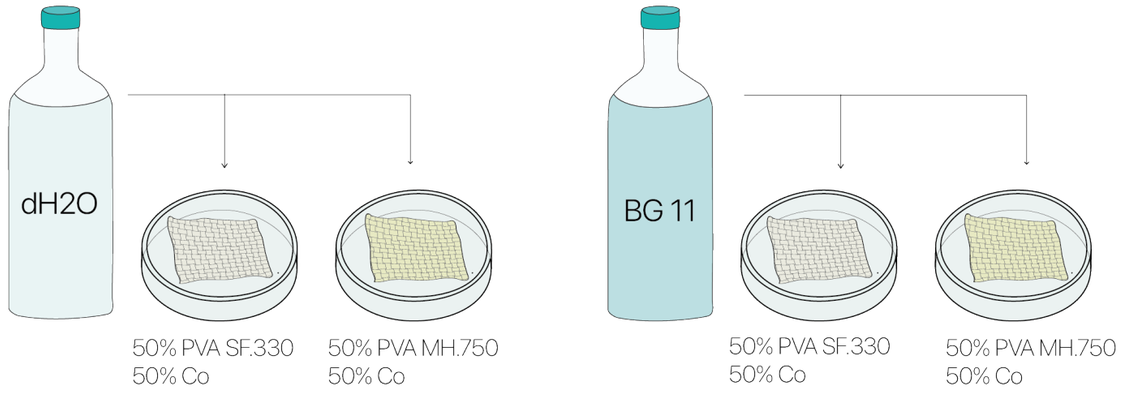

Figure 36: Textiles immersion in dH_2O and BG11.

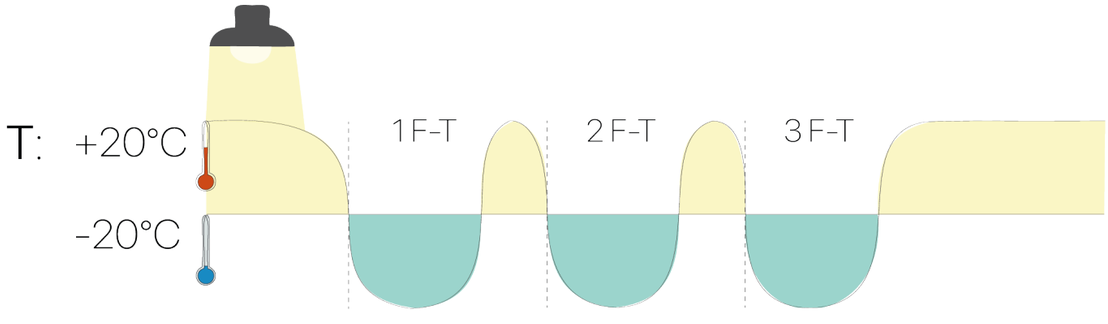

Figure 37: Textiles through the F-T cycles (24h -20°C; 4h 20°C under light conditions).

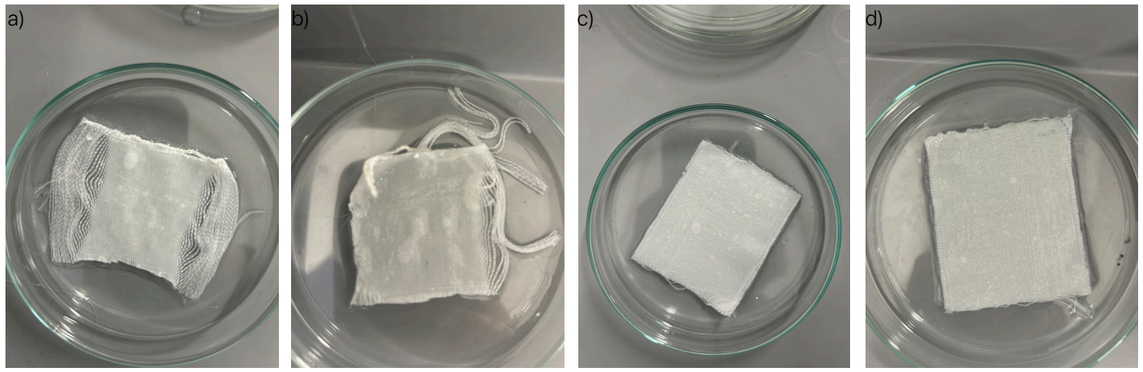

Figure 38: Textile samples after the 1st cycle of Freezing. a) PVA Solvron SF. 330 and BG 11; b) PVA Solvron SF. 330 and dH_2O; c) Solvron MH.750 and BG 11; d) Solvron MH.750 and dH_2O.

3.2.5. Conclusion

The three freeze-thaw cycles did not yield sufficient insights into improvements in gel formation, mechanical properties, or moisturization. However, the experiment identified the most suitable PVA for hydrogel development. Determining this was challenging due to the tight attachment of yarns, which obscured the gel network and made it difficult to assess hydrogel formation. Increasing the spacing between warp yarns could improve visibility, allowing for a more defined gel structure and enhanced transparency. However, the gel-like texture of PVA was noticeable by touch, indicating its viscous properties.

Among the tested variants, Solvron MH.750 formed a flexible but overly compact textile, limiting light penetration (see Fig 39 c and 39 d)—an essential factor for microalgal viability. In contrast, Solvron SF.330, despite initial challenges in creating a bonding hydrogel with cotton (Co) yarns, demonstrated promising dissolution properties, particularly at the textile edges, where a transparent PVA structure was observed (Figures 39a and 39b). This transparency is crucial for facilitating light penetration and maintaining microalgae growth, and therefore PVA Solvron SF.330 was selected for future experiments. Finally, the results confirmed that BG11 medium does not compromise textile integrity, as no structural degradation was observed.

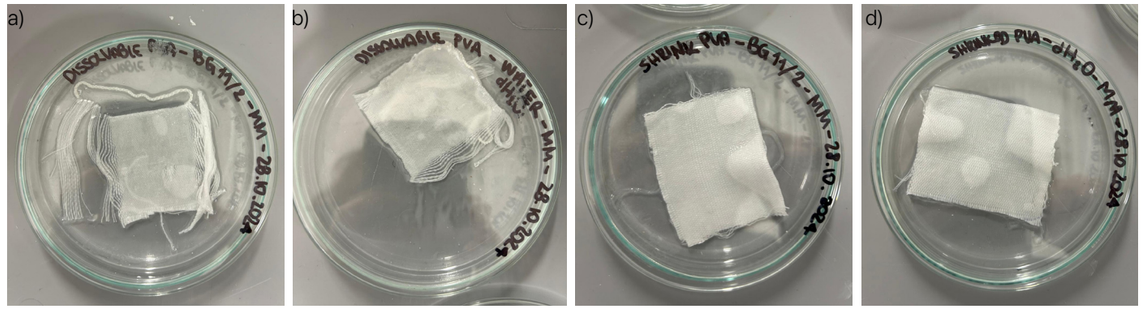

Figure 39:Textile samples after the 3rd cycle of Freezing a) PVA Solvron SF. 330 and BG 11; b) PVA Solvron SF. 330 and dH_2O; c) Solvron MH.750 and BG 11; d) Solvron MH.750 and dH_2O.

3.3. Freezing Living Textiles

This 21-day experiment builds on the findings of 3.1. *Freezing Microalgae and Cyanobacteria* and 3.2. *Freezing Textiles experiments*, further investigating microalgal growth and encapsulation within a textile matrix. *Freezing Microalgae and Cyanobacteria* demonstrated that both microalgal strains can withstand subzero temperatures, confirming their resilience to freeze-thaw (F-T) cycles. *Freezing Textiles* established that BG-11 medium does not compromise textile integrity, it suggested that Solvron SF. 330 PVA was the best, and that increasing the spacing between cotton yarns could enhance hydrogel structure. Building on these insights and and applying the Parallel Prototyping Method (Kesari, 2019), this experiment aims to realize a living textile able to maintain microalgae/cyanobacteria viability by addressing four key variables: textile composition, growth medium, microorganism strain and the optimal timing for applying the F-T method.

To improve textile functionality, three textile compositions—50% PVA-50% cotton (Co), 25% PVA-75% Co, and 75% PVA-25% Co—were tested. Yarn spacing was adjusted through different weaving techniques, employing a double-layer plain weave for the first two compositions and a compound twill-reverse twill weave for the latter. These structural modifications aimed to enhance PVA gel formation, improve textile transparency, and optimize conditions for microalgal adhesion. In addition to textile properties, the experiment examined the effect of liquid (BG-11) and solid (BG-11 with agar) medium on microalgal growth and attachment, drawing inspiration from In-Na et al. (2021) but focusing solely on adhesion rather than additional coatings. Furthermore, the experiment compared the attachment behaviors of *Scenedesmus* sp. and *Nostoc punctiformis*, investigating how the different microorganisms respond to adhesion effectiveness. Finally, two experimental timelines were introduced to determine the ideal balance between microalgal growth and recovery time after applying the F-T method. This approach evaluates whether extending the growth phase while shortening the recovery period yields better results, or if a shorter growth phase with a longer recovery period is more effective.
Building on these findings, *Freezing Living Textiles* seeks to answer six key questions:

1. Can microalgae/cyanobacteria successfully grow on these textiles composition?
2. Does a liquid or solid medium enhance initial microalgal attachment?
3. Which microorganism, *Scenedesmus* sp. or *Nostoc punctiformis*, demonstrates superior attachment to textile substrates?
4. What is the optimal timing for applying the F-T cycles?
5. Which textile composition best supports microalgal/cyanobacterial adhesion?
6. Does increased warp spacing improve textile structure and hydrogel performance?

By answering these questions, this experiment seeks to optimize conditions for integrating microalgae/cyanobacteria into living textiles, ensuring their viability while enhancing the functionality and durability of the textile matrix.

3.3.1. Textile Materials

- Warp: Cotton yarn NE 38/2;
- Weft: Solvron SF.330 (Dissolvable 55c+ Yarn) 330x3 d tex - Count: 1/10 Nm;
- ADACAD software;
- Jacquard loom TC2;
- Boat shuttle;
- Bobbin;
- Scissors.

3.3.2. Textile Method

The textile samples were fabricated in the Material Lab, utilizing the Jacquard loom TC2. Three textile variations composed of different ratios of Cotton (CO) and polyvinyl alcohol (PVA) yarns have been prepared in different ratios(Figure 40). Lift plans for these textiles were designed using ADACAD software to create precise patterns tailored to the loom. Two primary designs were designed: a double-layer plain weave for the 50% PVA-50% Co and 25% PVA-75% Co textiles, and a compound weave combining twill and reversed twill for the 75% PVA-25% Co textile. The decision to use two double layer textiles and a compound was taken because these structures increase the distance between warps. As in Freezing Textiles, the draft was uploaded to the TC2 loom, and the weaving process followed the same setup. To improve structural variations, the double-layer textiles (50% PVA-50% Co and 25% PVA-75% Co) were cut into four 7 cm × 5 cm samples each, with each cut yielding two samples due to the double-layer construction (Figures 41a and 41b). For the compound weave, incorporating twill and reverse twill patterns, the same method was applied, producing eight samples of the same dimensions.

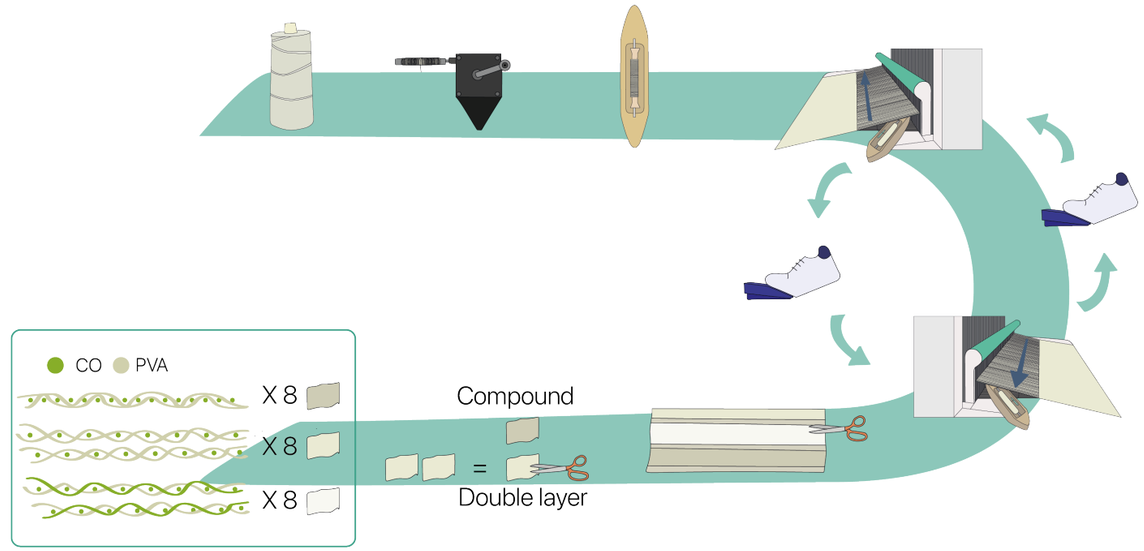

Figure 40: Steps to prepare the 24 samples (25% PVA - 75% Co; 50% PVA - 50% Co; 75% PVA - 25%Co).

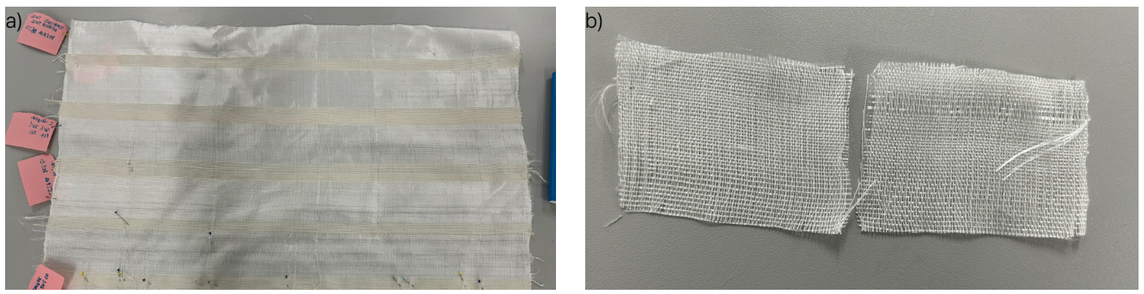

Figure 41: a)Textile containing the three different wave structures; b) Double-layer textile. How the textile has been divided to obtain a structure with more distance between the cotton yarns.

3.3.3. Experiment Materials

- 8 tabby textiles 50% PVA 50% Co (7 x 5 cm);
- 8 tabby textiles 25% PV 75% Co (7 x 5 cm);
- 8 compounds 75% PVA 25% Co (7 x 5 cm);
- 200 ml of *Scenedesmus* sp. cultured in BG 11;
- 200 ml of *Nostoc punctiformis* cultured in BG 11;
- 12 empty Petri dishes;
- 12 Petri dishes containing solid medium - agar and BG 11;
- 2 pipettes (5 ml);
- 1 pipette (60 ml)
- 3 pipettes (25 ml);
- Tweezers;
- Parafilm;
- Microscope;
- Laminar Air Flow (LAF) Cabinet.

3.3.4. Method

The experiment was conducted in the BioLab to safely work with microorganisms. First, twelve empty Petri dishes were placed inside the Laminar Air Flow (LAF) Cabinet.

Fifteen ml of a *Scenedesmus* sp. cultivated in BG 11 medium was added to six of Petri dished using a 25 ml pipette. Another pipette was used to add 15 ml of a *N. punctiformis* cultivated in BG 11 medium to the remaining six dishes. After filling, the twelve Petri dishes were covered with the lid, wrapped in aluminum foil, and set aside. To prepare the textile samples, the 24 textile pieces were placed in the Laminar Air Flow (LAF) Cabinet, where they were sterilized under UV light for 30 minutes. Following sterilization,three textile compositions (24 textiles in total) were tested: 50% PVA / 50% Co 25% PVA / 75% Co, and 75% PVA / 25% Co. Each composition was evaluated in combination with the microalgal strains *Scenedesmus* sp. and *N. punctiformis* under controlled conditions and in combination with liquid medium and solid medium.

For the liquid-based setup, each textile composition was immersed in 30 ml BG11 medium, inoculated with either *Scenedesmus* sp. or *N. punctiformis*. For instance, the 50% PVA / 50% Co textile was placed in one Petri dish containing BG11 and *Scenedesmus* sp., while another identical textile was placed in a separate dish with BG11 and *N. punctiformis*. The same process was followed for the 25% PVA / 75% Co and 75% PVA / 25% Co textiles, ensuring that each composition was tested with both microorganisms. This setup resulted in six combinations (plus their copies) for the liquid-based environment, providing a thorough evaluation of microalgal attachment. Once the textiles were positioned, the Petri dishes were sealed with parafilm and then placed under controlled lighting conditions (16 hours of light and 8 hours of darkness) (Figures 43a-f).

For the agar-based setup, textiles were placed individually on BG11 solid medium and inoculated with 3 ml of BG11 liquid medium containing either *Scenedesmus* sp. or *N. punctiformis*. The same three textile compositions—50% PVA / 50% Co, 25% PVA / 75%Co, and 75% PVA / 25% Co—were tested under identical conditions. As in the liquid setup, each textile type was assigned to a Petri dish containing one of the two microorganisms, ensuring a comprehensive evaluation of microalgal behavior on solid medium. After preparation, the Petri dishes were sealed with parafilm and incubated under identical lighting conditions (16 hours of light, 8 hours of darkness), allowing for a systematic comparison of microalgal growth and attachment across both liquid and agar environments (Figure 43g).

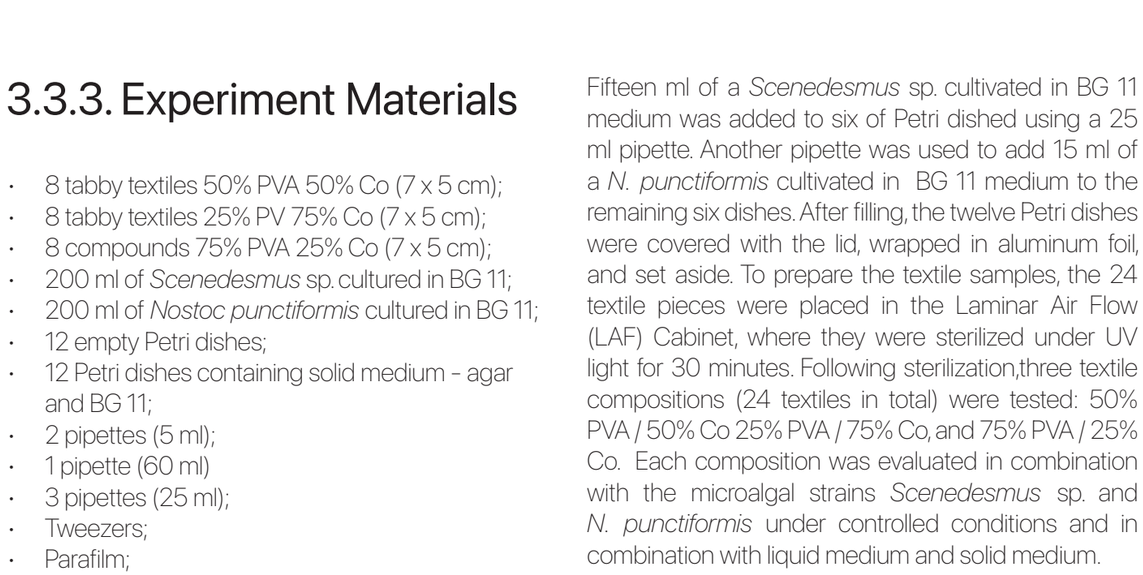

Figure 42: Two methods of including microalgae/cyanobacteria cultures to textiles and two media were explored.

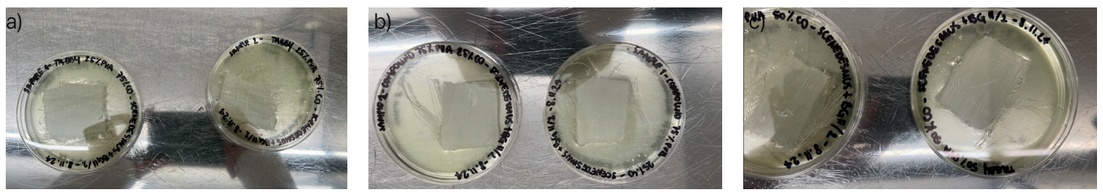

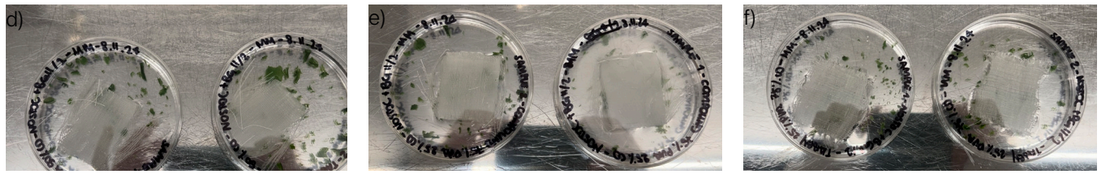

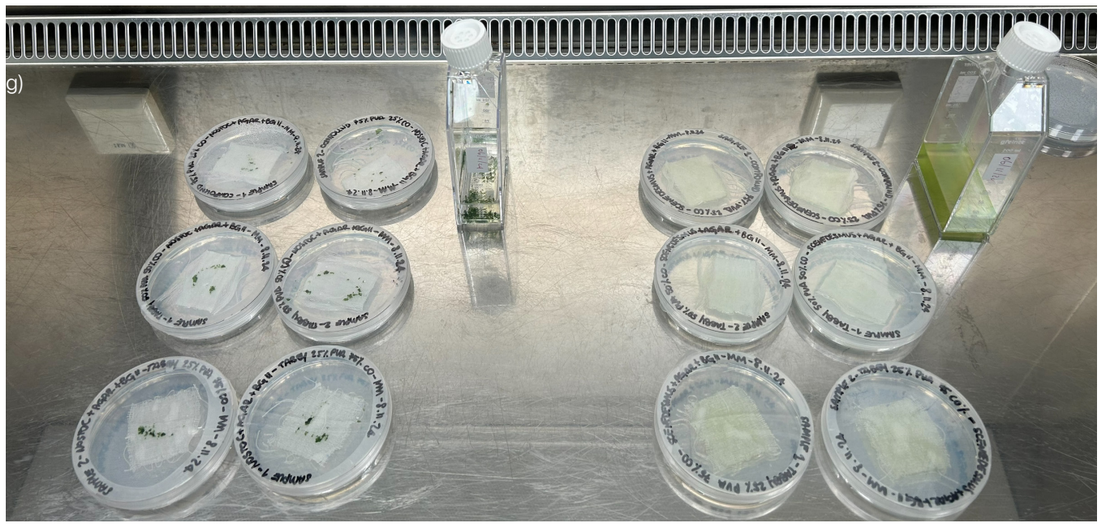

Figure 43: a,b,c,d,e,f) Living textiles in liquid medium; g) Living textile in solid medium.

Following initial growth, the 24 samples were divided into two groups to determine the optimal growth period before subjecting them to F-T cycles (Figure 44). The goal was to assess whether microalgae/cyanobacteria benefited from a longer growth phase and shorter recovery time or vice versa.

Timeline 1 - 3 days of growth

As shown in figure 45, twelve Petri dishes were incubated under light conditions for three days. After this period, they were transferred to the Laminar Air Flow (LAF) Cabinet, where the Petri dishes were unsealed. Using sterilized tweezers, each textile was carefully moved into a new plastic Petri dish without medium. The samples then underwent three Freeze-Thaw (F-T) cycles (23 hours at -20°C, followed by 3 hours at +20°C).

Following the three F-T cycles treatment, the textiles were transferred to sterilized glass Petri dishes containing only liquid or solid BG11 medium, without introducing new microalgae or cyanobacteria. This step allowed for the assessment of microbial viability and growth potential post-F-T cycles. The glass petri dishes were sealed with parafilm and incubated under controlled light conditions (16 hours light, 8 hours dark) at room temperature for 14 days.

Timeline 2 - 10 days of growth

As shown in figure 46, the second set of twelve Petri dishes followed the same procedure as Timeline 1, but the samples were incubated under light conditions for ten days before undergoing three F-T cycles (24 hours at -20°C, followed by 4 hours at +20°C). However, these samples were incubate only for seven days.

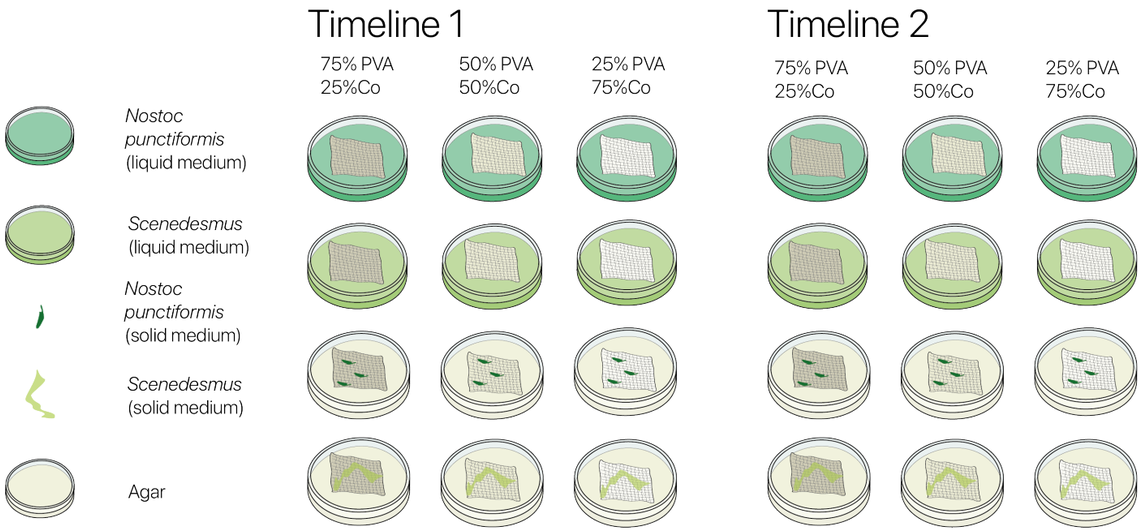

Figure 44: Living textiles combinations.

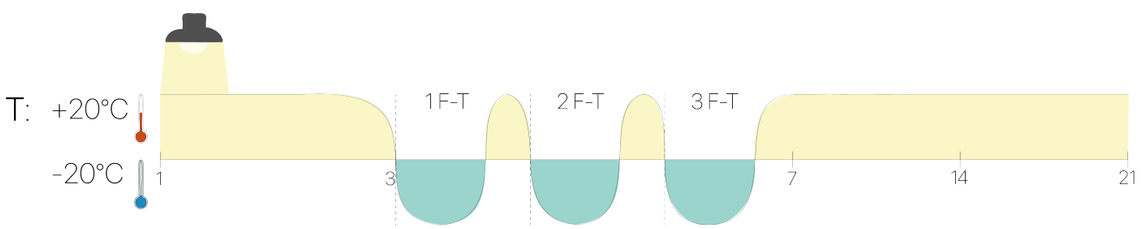

Figure 45: Description of the Freeze-Thaw process. The samples were grown for 3 days before the starting of the F-T process and incubated for an additional 14 days to assess recovery and growth.

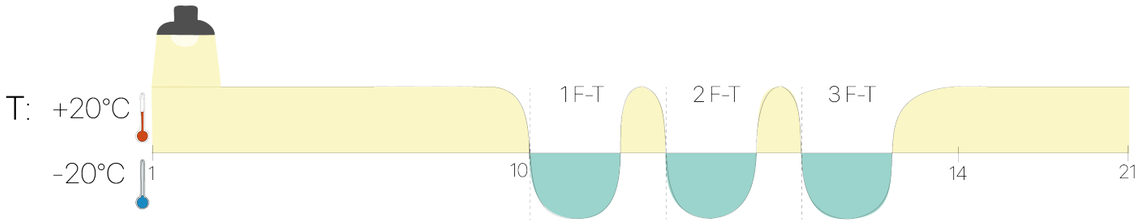

Figure 46: Description of the Freeze-Thaw process. The samples were cultivated for 10 days before the starting of the F-T process. Following the treatment, they were incubated for an additional 7 days to assess recovery and growth.

3.3.5. Microscopic observation

Timeline 1 - 3 days of growth

Three days after the Freeze-Thaw process, samples were examined under a microscope, leading to several observations. *N. punctiformis* visibly failed to attach to the textiles, as observed when textiles with 50% PVA and 50% Co in a liquid medium were gently shaken, causing the *N.punctiformis* to move freely (Figure 47a). Microscope analysis confirmed that *N.punctiformis* cells were merely resting on the textile surface without integration as illustrated in Figure 47b.

The living textile composed of 50% PVA and 50% Co with *N. punctiformis* grown in a solid medium also produced poor results, with *N.punctiformis* failing to attach after three days. Microscopic analysis confirmed that the cells remained loosely on the textile surface (Figure 48b). Observing the cells through the agar was challenging, and even inverting the Petri dish reveal reveal any visible *N.punctiformis* cells (Figure 48c).

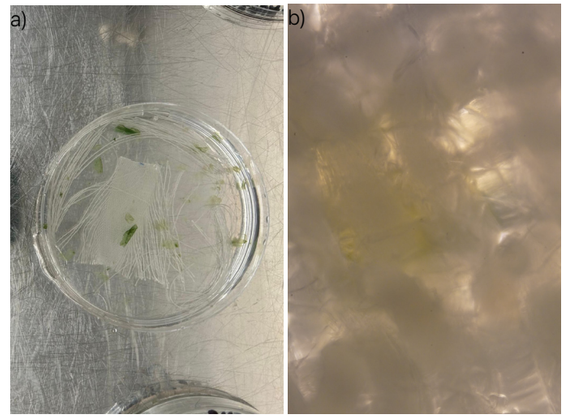

Figure 47: *N.punctiformis* on 50% PVA and 50% Co in liquid medium. a) Naked eye; c) Microscope image (50x).

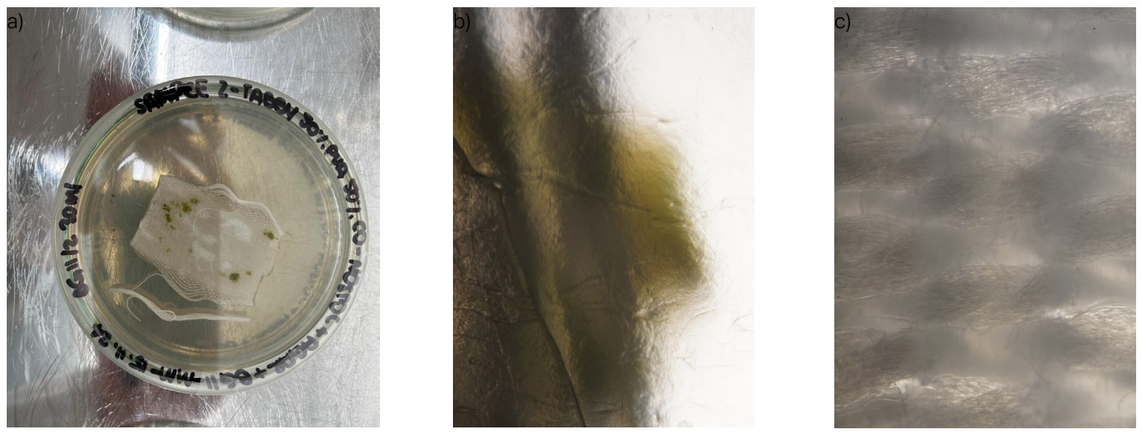

Figure 48 *N.punctiformis* on 50% PVA and 50% Co in solid medium. a) Naked eye; b,c) Microscope image (50x).

In the living textiles composed of 25% PVA and 75% Co with *Scenedesmus* sp. grown in liquid medium, the microalgae adhered to the cotton fibers, likely due to their rough structure, but did not attach to the PVA component. This highlights the significance of the yarn ratio in influencing attachment. However, the *Scenedesmus* sp. colonies were only partially secured, loosely resembling fruit hanging from a tree branch, as shown in Figure 49.

A third observation was made regarding the living textiles composed of 50% PVA and 50% Co, as well as 75% PVA and 25% Co, with *Scenedesmus* sp. grown in a liquid medium. The microalgae were found to be immobilized within the PVA gel, as shown in Figure 50. These findings confirm that *Scenedesmus* sp. can be successfully immobilized within PVA. The next question to address is whether the immobilized microalgae can survive and grow under these conditions.

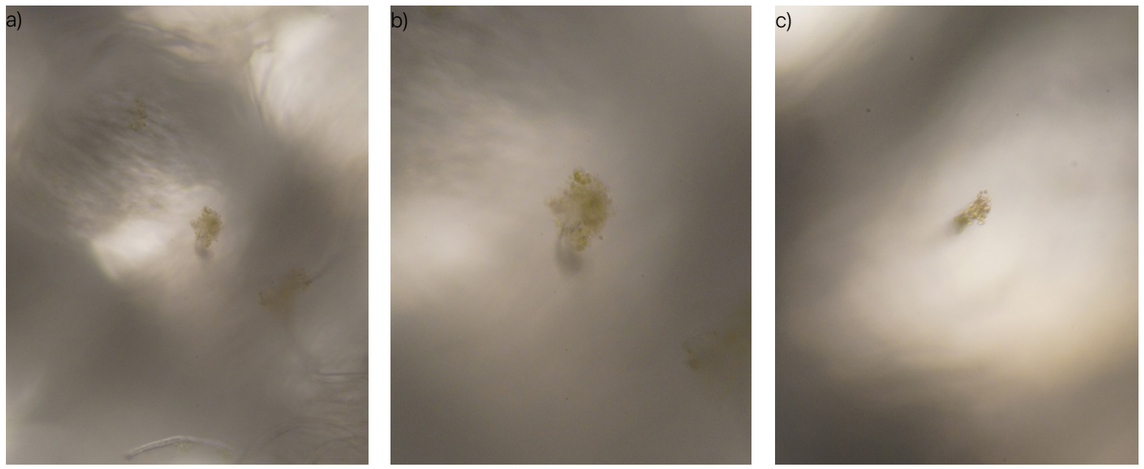

Figure 49: *Scenedesmus* sp. on 25% PVA and 75% Co in liquid medium. a) Microscope image (50x); c)Microscopic image (100x); c) Microscopic image (150x).

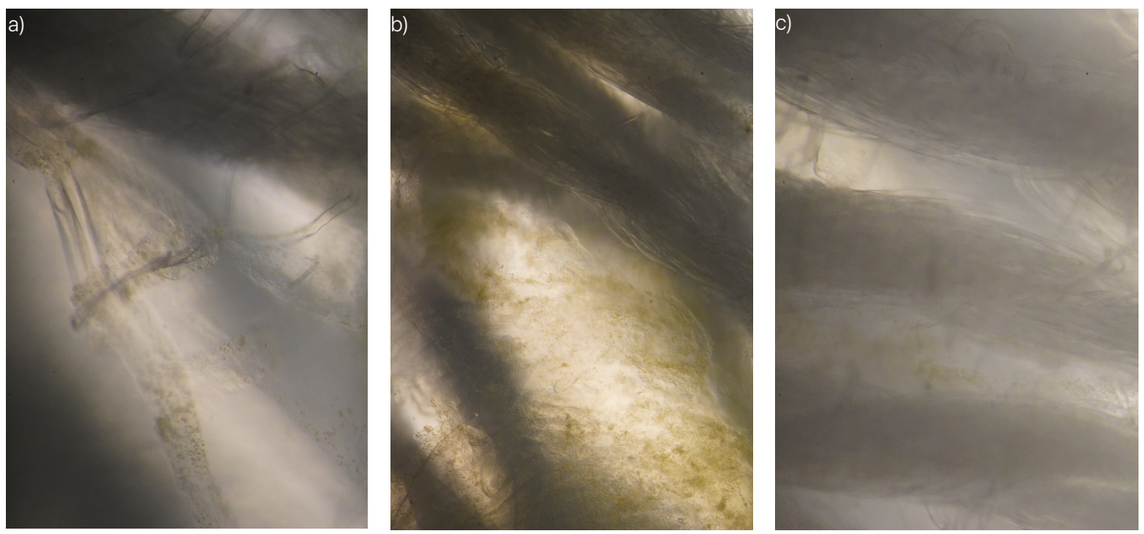

Figure 50: a) *Scenedesmus* sp. on 50% PVA and 50% Co in liquid medium. Microscope image (100x). b) *Scenedesmus* sp. on 75% PVA and 25% Co in liquid medium. Microscopic image (100x). c) *Scenedesmus* sp. on 75% PVA and 25% Co in liquid medium. Microscopic image (50x).

Timeline 2 - 10 days of growth

Three days after the Freeze-Thaw process, samples were examined under a microscope, revealing key observations about the behavior of microalgae and cyanobacteria under different conditions.
After 10 days and three freeze-thaw cycles, *Nostoc punctiformis* grown in the liquid medium failed to attach to the textile, regardless of the yarn composition. This was consistent across samples with varying percentages of PVA and cotton (Figure 51).

More promising results were observed with *Scenedesmus* sp. grown in the liquid medium (Figure 52). The textile composed of 75% PVA and 25% cotton exhibited a uniform attachment of microalgae across its surface (Figure 52a). In contrast, the 50% PVA textile showed larger but unevenly distributed colonies (Figure 52b). Partial detachment of *Scenedesmus* sp. was observed in all samples, with detachment being most pronounced in the 25% PVA textile, followed by the 50% and 75% PVA samples.

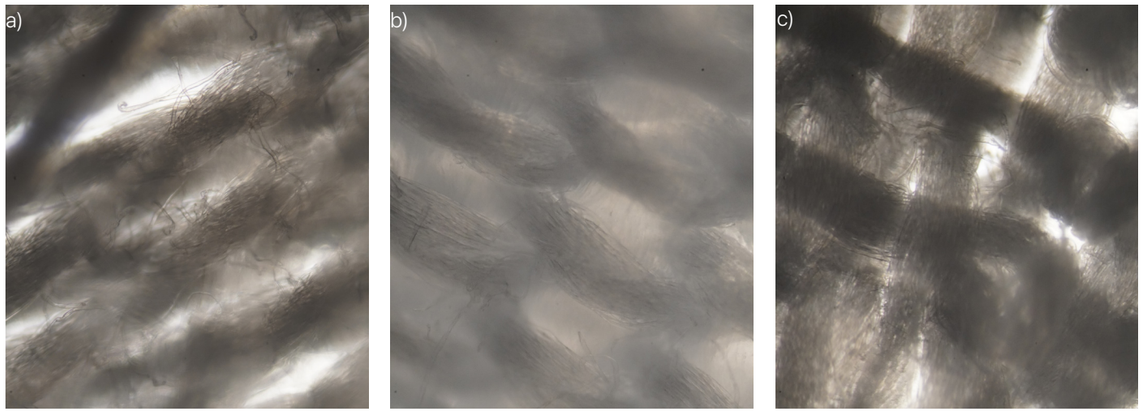

Figure 51: a) *N. punctiformis* on 50% PVA and 50% Co in liquid medium. Microscopic image (50x). b) *N.punctiformis* on 25% PVA and 75% Co in liquid medium. Microscopic image (50x); c) N.*punctiformis* on 75% PVA and 25% Co in liquid medium. Microscopic image (50x).

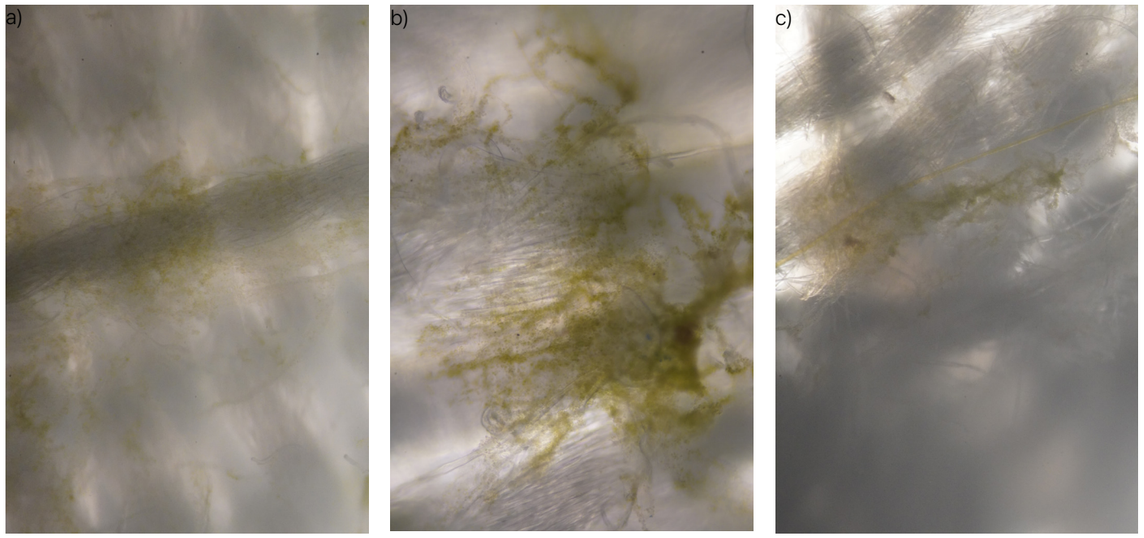

Figure 52: a) *Scenedesmus* sp. on 75% PVA and 25% Co in liquid medium. Microscopic image (50x); b) *Scenedesmus* sp. on 50% PVA and 50% Co in liquid medium. Microscopic image (50x); c) *Scenedesmus* sp. on 25% PVA and 75% Co in liquid medium. Microscopic image (50x).

In contrast, the samples grown on the solid medium exhibited higher levels of fungal contamination,, and cell death. That was particularlly evident on on the 50% PVA textile (Figure 53a). The 75% PVA textile was almost entirely lacking in cells, while the 25% PVA textile retained some living microalgae, though they appeared to be in poor condition (Figure 53b and 53c respectively). These outcomes may be attributed to inadequate sealing or insufficient sterilization of both sides of the textiles.

For *N. punctiformis* grown on the solid medium, the results were varied (Figure 54). While the samples on the 25% and 50% PVA textiles remained viable, they displayed signs of stress (brown color) and were more prone to fungal contamination, especially on the 25% PVA textile (Figure 54 a and b). In contrast, the 75% PVA textile supported healthier-looking cyanobacteria, as indicated by their vibrant coloration. However, this textile exhibited sparse colonization, with large portions of the surface remaining unpopulated.

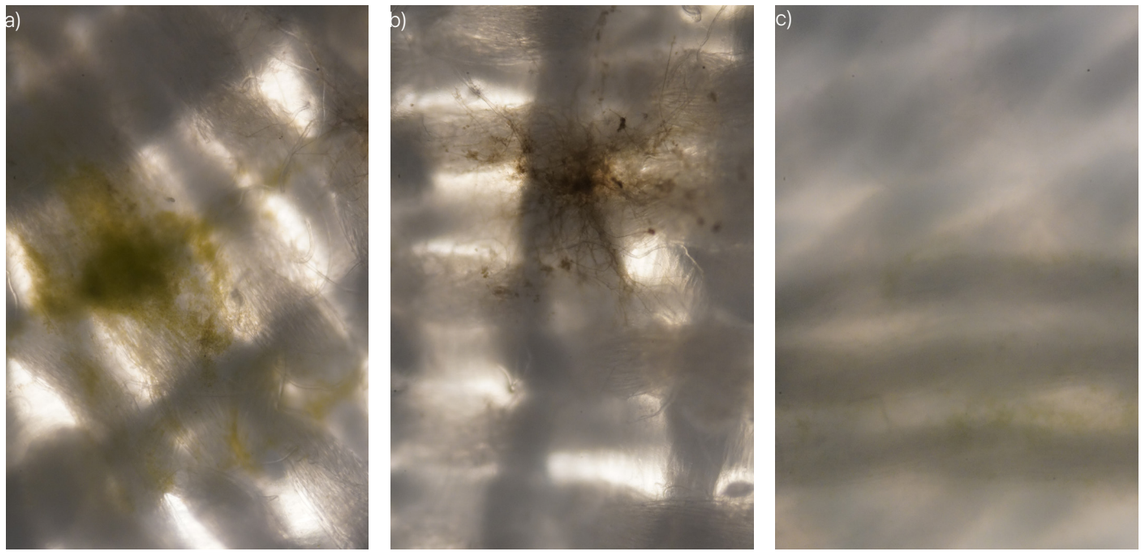

Figure 53: a) *Scenedesmus* sp. on 25% PVA and 75% Co in solid medium. Microscopic image (50x); b) *Scenedesmus* sp. on 50% PVA and 50% Co in solid medium. Microscopic image (50x); c) *Scenedesmus* sp. on 75% PVA and 25% Co in solid medium. Microscopic image (50x).

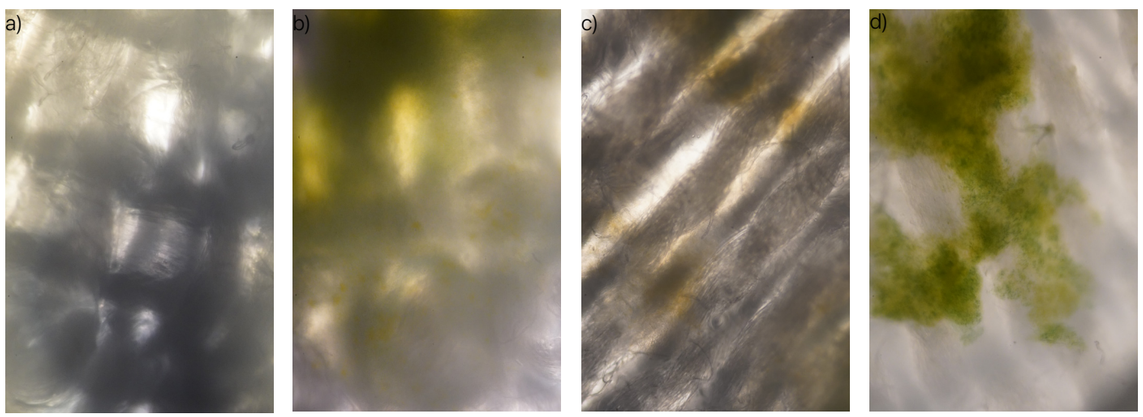

Figure 54: a) and b) *N.punctiformis* on 25% PVA and 75% Co in solid medium. Microscopic image (50x); c) *N.punctiformis* on 50% PVA 50% Co in solid medium. Microscopicimage (50x); d) *N.punctiformis* on 75% PVA and 25% Co in solid medium. Microscopic image (50x).

Microalgae and cyanobacteria have faced significant challenges in surviving the current conditions. Many cells had perished, others were in poor condition, and only a few remain healthy. Additionally, some contamination has been observed.
To address these problems, it is crucial to revise the freeze-thaw (F-T) protocol to reduce the stress on the microalgae and cyanobacteria. The current three F-T cycles may be too intense, making recovery challenging. One potential solution is to maintain the three cycles but introduce the microalgae/cyanobacteria only before the final cycle, reducing their exposure to extreme conditions. Alternatively, the microalgae and cyanobacteria could be added after completing all three F-T cycles.

3.3.6. Conclusion after 21 days

Nostoc punctiformis exhibited poor attachment overall.

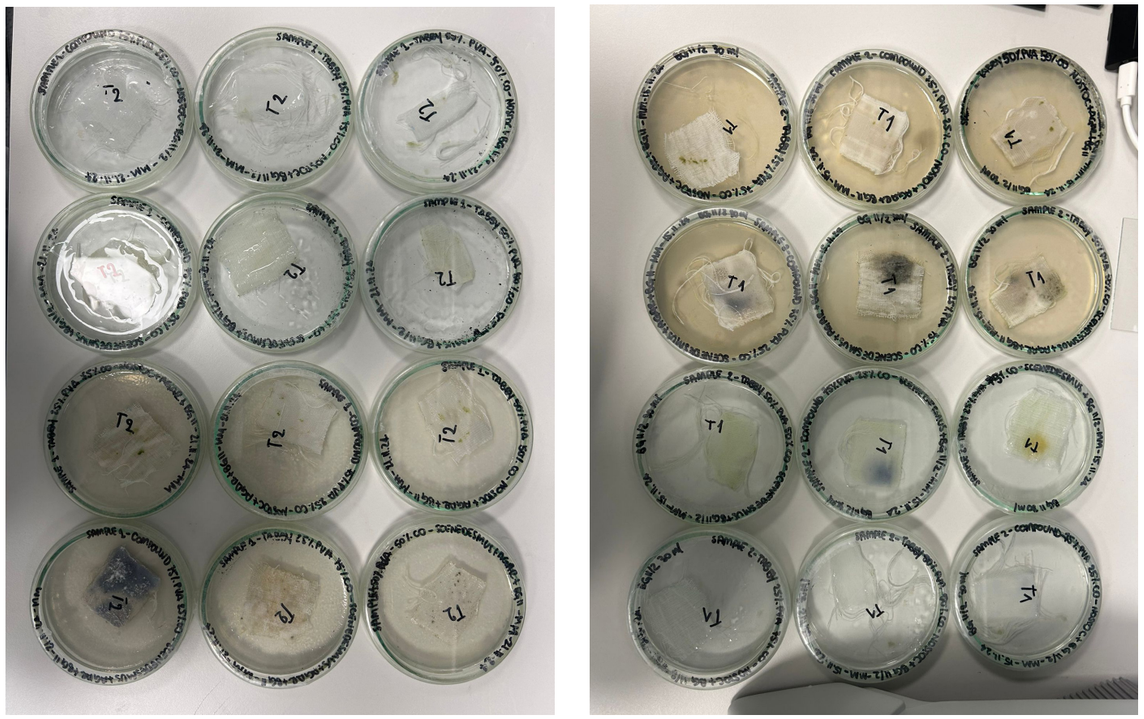

Figure 55: The 24 samples at the end of the experiment.

A notable challenge was *Nostoc punctiformis* resting on the textile surface without forming stable attachments, raising concerns about its survival and attachment efficiency when not fully submerged or in direct contact with the medium. Other samples were plagued by fungal contamination, minimal growth, or cell death and were excluded from further consideration. However, the 75% PVA textile in the solid medium showed healthier-looking cells with vibrant coloration, indicating a possible pathway for improving *N. punctiformis* viability. Lastly, the experiment revealed the rapid degradation of PVA, likely due to prolonged immersion in the liquid medium. This degradation highlights the need for strategies to enhance the durability of PVA-based textiles in aqueous environments. Overall, the 75% PVA 25% Co textile emerges as the most promising substrate for *Scenedesmus* sp. in the liquid medium.

3.3.7. Conclusion after 30 days

After 30 days, clearer trends emerged, confirming the feasibility of microalgal growth and attachment on textiles. Freezing Living Textiles demonstrated that *Scenedesmus* sp. exhibited the strongest attachment, particularly when cultivated in a liquid medium. The findings also suggest that microalgae require approximately 21 days to fully recover after F-T method and that three days of initial growth before undergoing three Freeze-Thaw (F-T) cycles is sufficient for the living textiles development. (Timeline 1 -3 days of growth).

The most promising results for microalgal attachment and growth were observed in textiles composed of 50% PVA / 50% Co and 75% PVA / 25% Co. Additionally, increasing the spacing between cotton yarns slightly improved the hydrogel structure. However, after 30 days, PVA degradation varied across samples. As shown in Figures 56a and 56b, PVA had completely degraded, whereas Figures 56c, 56d, 56e, and 54f indicate its partial retention. This suggests that a higher PVA content may contribute to a more durable hydrogel, though further experiments are needed to confirm this relationship and better understand the interaction between microalgae and the PVA matrix.

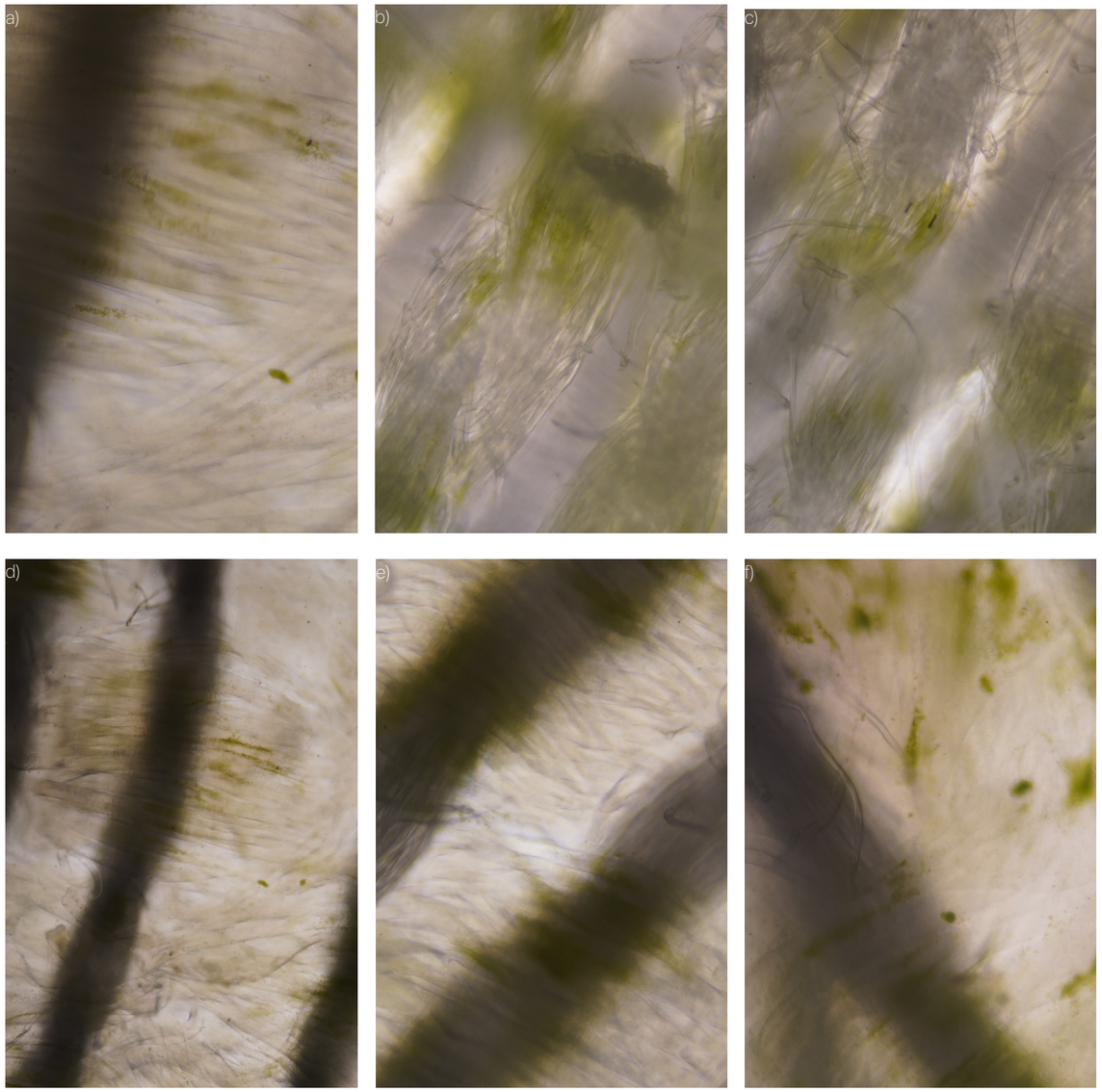

Figure 56: a) Timeline 1, *Scenedesmus* sp. on 50% PVA and 50% Co in liquid medium. Microscopic image (100x); b,c) Timeline 1, *Scenedesmus* sp. on 50% PVA and 50% Co in liquid medium. Microscopicimage (50x). d,e,f) Timeline 1, *Scenedesmus* sp. on 75% PVA and 25% Co in liquid medium. Microscopic image (50x).

3.4. Drying-Rehydrating Textiles

Building on the findings of Section 3.3, this phase aimed to refine the conditions for microalgal attachment and viability on textile substrates. The *Freezing Living Textiles* experiment identified 75% PVA–25% Co and 50% PVA–50% Co yarn ratios as the most effective compositions for *Scenedesmus* sp. attachment in liquid medium. Additionally, the results suggested that *Scenedesmus* sp. requires a specific recovery period to regain growth following freeze-thaw (F-T) cycles. In contrast, *N. punctiformis* failed to attach reliably to hydrogels, making it unsuitable for further testing in this context. As a result, the *Drying-Rehydrating Textiles* experiment focused exclusively on *Scenedesmus* sp. and explored ways to optimize its attachment.
To achieve this, an alternative approach was explored to determine whether *Scenedesmus* sp. could adhere to textiles without undergoing F-T cycles and whether it could survive on pre-soaked textiles outside a liquid medium. This led to the introduction of a drying phase, inspired by In-Na et al. (2021), who used textile drying to measure microalgae biomass as an indicator of CO_2 uptake rates. However, in this experiment, drying served a different purpose. Following three F-T cycles, the hydrogel became fully saturated with BG11 medium, potentially hindering microalgae attachment. It was hypothesized that drying the textile post-F-T and subsequently rehydrating it with *Scenedesmus* sp. and liquid medium would improve hydrogel receptivity, thereby enhancing microalgal adhesion. To validate this hypothesis, a targeted experiment was conducted. To address these objectives, the experiment sought to answer three primary questions:

1. Can microalgae attach to textiles without undergoing a freeze-thaw process?
2. Can microalgae survive and reproduce on textiles soaked in BG11 medium without being permanently immersed in liquid?

To explore these questions, three variables were investigated: textile composition, environmental conditions, and time. The textile composition focused on the two blends with the most potential—50% PVA-50% Co and 75% PVA-25% Co. Environmental conditions examined the attachment of *Scenedesmus* sp. in liquid medium versus textiles removed from the medium. The time variable tested three distinct timelines, evaluating the textiles after 10 minutes, 3 days, and 7 days in liquid medium, followed by extended periods of 25, 23, and 18 days outside the medium, respectively. This setup aimed to determine the time required for *Scenedesmus* sp. to attach to the textile and assess its ability to survive on the hydrogel by deriving nutrients solely from the pre-soaked textile. By addressing these variables and utilizing the Parallel Prototyping Method (Kesari, 2019), *Drying-Rehydrating Textiles* sought to identify the ideal parameters for maximizing *Scenedesmus* sp. attachment and viability with a completely different attachment method.

3.4.1. Textile Materials

- Warp: Cotton yarn NE 38/2;
- Weft: Solvron SF.330 (Dissolvable 55c+ Yarn) 330x3 d tex - Count: 1/10 Nm;
- ADACAD software;
- Jacquard loom TC2;
- Boat shuttle;
- Bobbin;
- Scissors.

3.4.2. Textile Method

The textile samples were fabricated in the Material Lab using the Jacquard loom TC2. While the fundamental weaving process remained consistent with *Freezing Living Textiles*, a key structural modification was introduced to enhance textile compactness. Cotton yarn was incorporated at three strategic points— the start, middle, and end of each textile— to reinforce stability. Therefore, the weaving process followed a structured sequence to ensure proper integration: 10 passes of PVA, 5 passes of Co, 60 passes of PVA, 5 passes of Co, 60 passes of PVA, 5 passes of Co, and a final 10 passes of PVA. Each textile was woven to a length of 70 cm and a width of 5 cm, with a 2 cm gap separating successive samples. After completing the weaving process, the textiles were cut from the loom. The compound weave textile was sectioned into eight samples, each measuring 7 cm x 5 cm. Similarly, the double-layer textiles were each cut into four samples of the same dimensions, with each cut yielding two layers due to the double-layer construction.

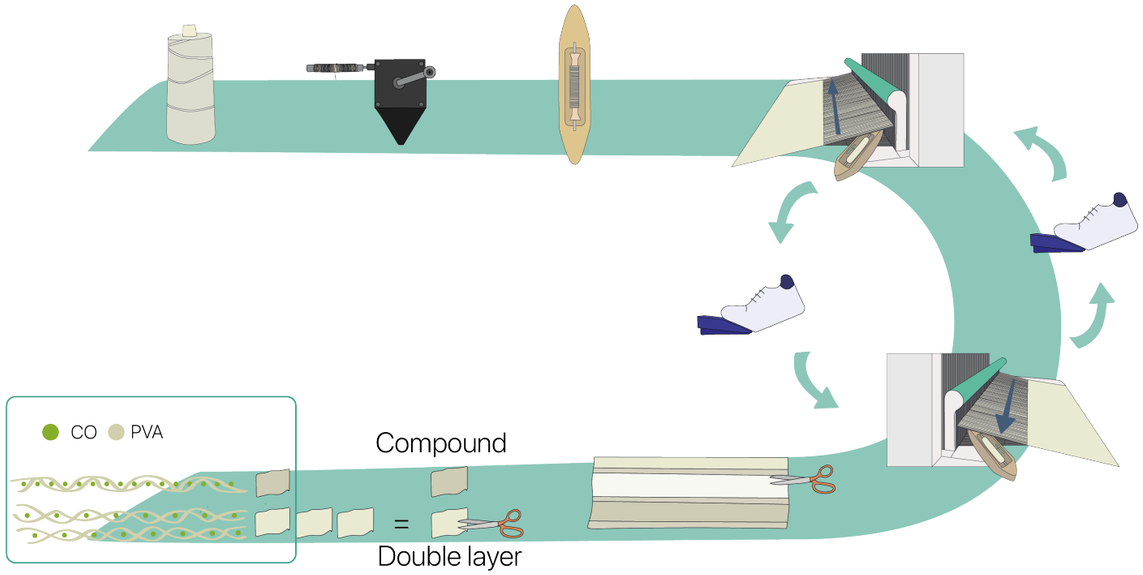

Figure 57: Steps to prepare the 6 samples (50% PVA - 50% Co; 75% PVA - 25%Co).

3.4.3. Experiment Materials

- BG11 medium;
- 3 textiles 50% PVA 50% Co (7 x 5 cm);
- 3 textiles 75% PVA 25% Co (7 x 5 cm);
- Freezer;
- 4 metal yarns;
- 4 squared tube of metal;
- Sterile Chamber (Figures 59 and 60);
- UV box;
- tweezers;
- 8 petri dishes;
- 10 flasks;
- *Scenedesmus* sp. culture;
- Microscope;
- Laminar Air Flow (LAF) Cabinet.

3.4.4. Method

The experiment was conducted in the BioLab under sterile conditions to safely handle microorganisms. The process began by placing the UV light cube inside the Laminar Air Flow (LAF) Cabinet. Six textile samples (three composed of 50% PVA and 50% Co, and three composed of 75% PVA and 25% Co) were sterilized in the UV light box for 20 minutes on one side, then flipped and sterilized on the other side for further 20 minutes. Following sterilization, each textile was immersed in BG11 medium for 5 minutes, transferred to empty petri dishes, and sealed with parafilm. The sealed petri dishes were subjected to three freeze-thaw cycles (23 hours freezing at -20°C and 3 hours thawing at room temperature) to allow the hydrogel formation.
After the final thawing cycle, a sterilized metallic structure was assembled in a sterilized chamber to air-dry the textiles.t consisted of four perforated metal plates arranged in pairs, with metal wires threaded through the holes to form a framework for suspending the textiles (Figure 59) . The samples were carefully removed from their petri dishes, hung on the metal wires within the chamber, and left to air-dry for 20 hours, allowing residual medium to evaporate while preserving the hydrogel's structural integrity (Figure 60).

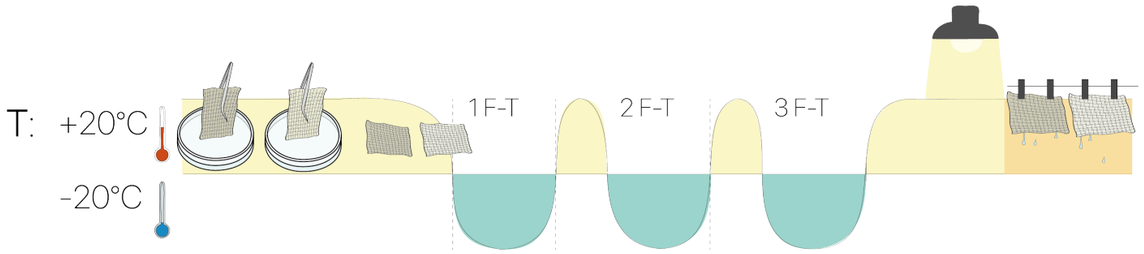

Figure 58: The six textile samples have been immersed in BG 11 medium and went through 3 F-T cycles. After that, they have been dried for 20 h.

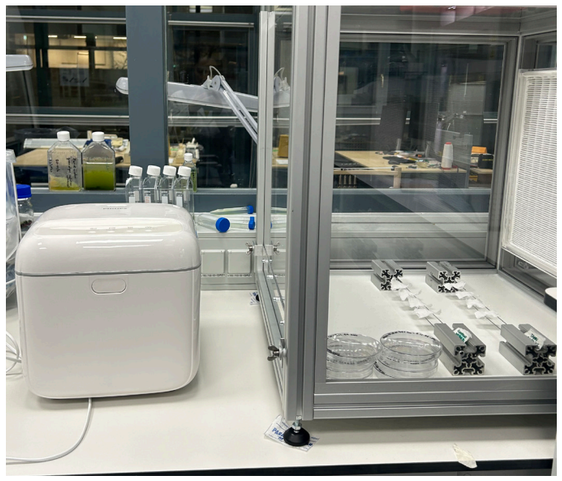

Figure 59: The 6 textiles have been placed into a sterilized chamber.

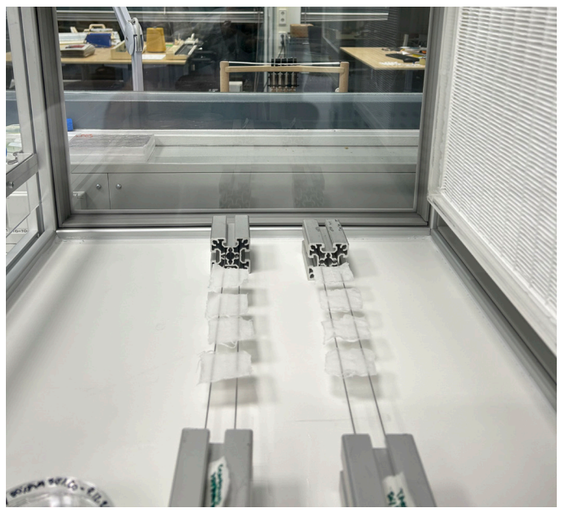

Figure 60: The 6 textiles have been disposed over two sterilized stainless steel yarns.

After the drying process, as shown in figure 61, textiles were subjected to three different conditions.

Timeline 1 - 10 minutes in *Scenedesmus* sp. medium: One dry textile from each composition (50% PVA/50% Co and 75% PVA/25% Co) was immersed in the petri dishes containing the *Scenedesmus* sp. liquid medium for 10 minutes. After immersion, the textiles were carefully transferred using tweezers into separate empty flasks. These samples were monitored for 27 days to evaluate whether *Scenedesmus* sp. could survive on hydrogels saturated with medium but not submerged in it.

Timeline 2 - 3 days in *Scenedesmus* sp. medium: A second pair of dry textiles (one from each composition) was immersed in the *Scenedesmus* sp. and liquid medium until they absorbed the microalgae and regained flexibility. The textiles were then transferred into flasks containing 30 mL of *Scenedesmus* sp. and liquid medium and incubated for three days. After incubation, the textiles were moved to empty flasks to observe *Scenedesmus* viability on the hydrogels for an additional 24 days.

Timeline 3 - 7 days in *Scenedesmus* sp. and liquid medium: The final two textiles were treated similarly to Timeline 2, first immersed in the *Scenedesmus* sp. and liquid medium until flexible and then transferred to flasks containing 30 mL of the *Scenedesmus* sp. and liquid medium. These textiles were incubated for seven days before being moved to empty flasks, where they were monitored for 20 days to assess the microalgae's ability to persist on hydrogels in the absence of surrounding medium.

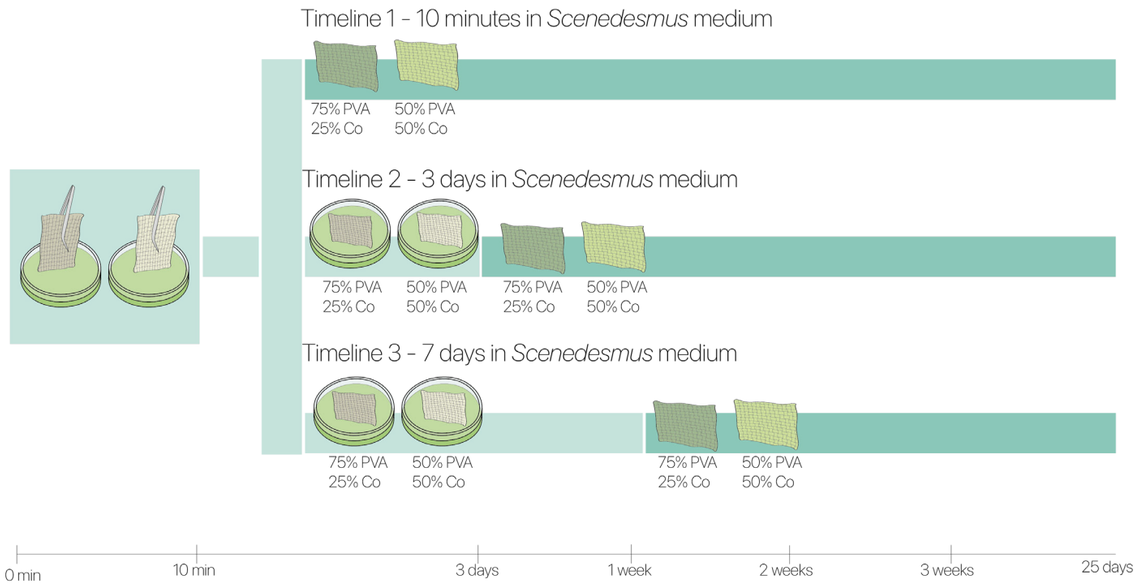

Figure 61: Three different time of textile immersion in *Scenedesum* sp. and liquid medium.

3.4.5. Conclusion

Drying-Rehydrating Textiles revealed that drying the textile after three freeze-thaw (F-T) cycles, followed by rehydration with *Scenedesmus* sp. and liquid medium, facilitated microalgae attachment but severely compromised hydrogel integrity. The gel-like PVA became brittle upon drying, and rehydration failed to restore its original structure, reducing its ability to encapsulate and protect the microalgae. These findings indicate that the drying-rehydration method is not a viable approach for microalgal attachment and encapsulation. To better understand this outcome, the results of *Drying-Rehydrating Textiles* were compared with those of *Freezing Living Textiles* (Figure 63).

In *Freezing Living Textiles,* where textiles underwent three F-T cycles. and remained submerged in medium, a stable PVA hydrogel formed, effectively immobilizing microalgae for 10–15 days before degradation began (Figure 64a). In contrast, in *Drying-Rehydrating Textiles,* drying prevented hydrogel reformation, leading to brittleness and structural failure, even after rehydration (Figure 64b). Additionally, the prolonged absence of medium in *Drying-Rehydrating Textiles* caused complete drying within 25 days, resulting in microalgal death due to nutrient deprivation, as confirmed by photosynthesis testing.

Even though the Drying-Rehydrating method was already deemed unsuitable for future applications, *Timeline 3* yielded the best results, with the textile submerged in *Scenedesmus* sp. and liquid medium for seven days (Figure 65). Moreover, findings from *Drying-Rehydrating Textiles*, along with the re-evaluation of *Freezing Living Textiles,* highlight the challenge of achieving a permanent living textile due to PVA's degradability. Therefore, the living textile has a limited lifespan, emphasizing the need for future efforts to enhance PVA durability and develop a cyclical system that repurposes materials, minimizing waste.

Figure 62: The six dried textiles after 25 days.

Figure 63: a) Microscopic picture of 75%PVA 25% Co - Freezing Living Textiles Microscopic image (100x); b) Microscopic picture of 75%PVA 25% Co - Drying-Rehydrating Textiles. Microscopic image (50x).

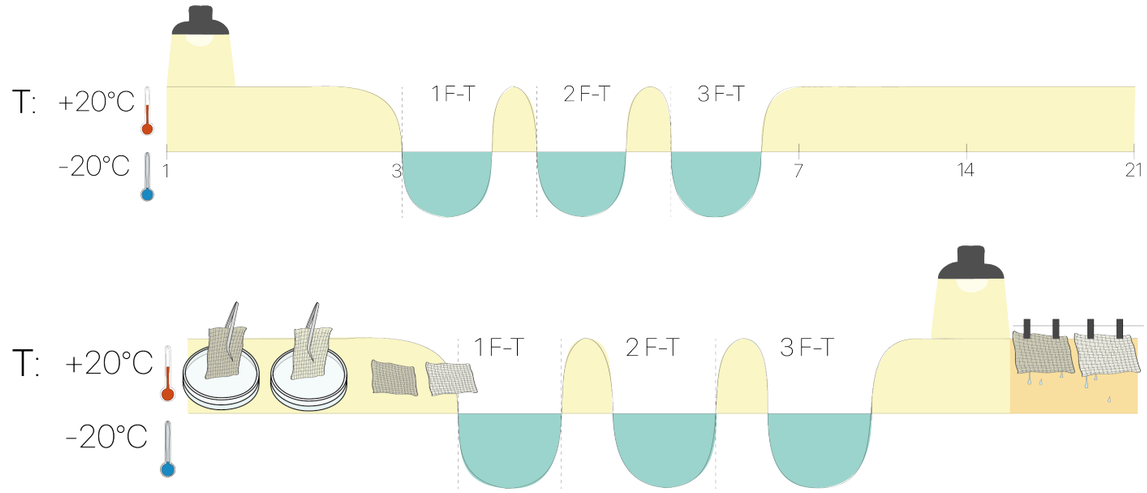

Figure 64: a) Living textiles process of *Freezing Living Textiles*. The numbers represent the days; b) textiles process of *Drying-Rehydrating Textiles*.

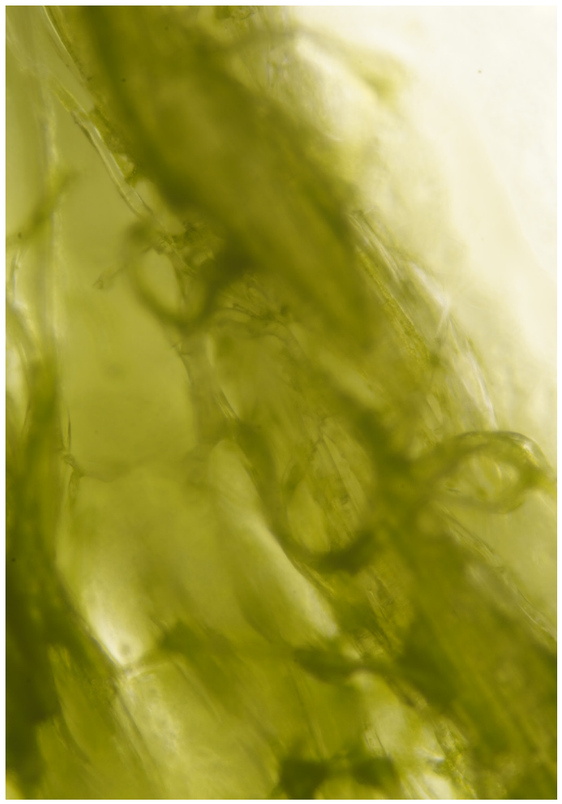

Figure 65: 75%PVA 25% Co after 27 days. Microscopic image (100x).

3.5. Hydrogel Moisture Retention

Since the *Freezing Textiles* experiment did not yield the expected improvements in hydrogel properties through the F-T process, a new experiment was designed to specifically investigate the hydrogel's moisture dynamics. This study focused on assessing the effects of freeze-thaw (F-T) cycles on the hydrogel's structural integrity and moisture retention, providing deeper insights into its stability and functionality.

As previously mentioned, a hydrogel is a three-dimensional polymeric network capable of absorbing significant amounts of fluid, typically ranging from 70% to 99% of its weight (Ambika et al., 2021; An et al., 2022). Previous studies have demonstrated that subjecting hydrogels to the F-T process can enhance their mechanical properties, increasing their durability and stability (Waresindo et al., 2023). The primary objective of this experiment was to evaluate the influence of repeated F-T cycles on hydrogel performance by subjecting four samples to distinct conditions. The first textile sample served as a control, initially immersed in BG11 medium but not subjected to any F-T cycles. Instead, it was placed under standard light conditions and monitored throughout the experiment to assess its moisture retention and structural integrity over time. The second sample was subjected to a single F-T cycle, while the third and fourth samples experienced two and three F-T cycles, respectively. The hypothesis was that the hydrogel with superior mechanical properties - given by the F-T cycles- would be able to retained moisture for the longest duration. Therefore, this experiment aimed to answer three main questions:

1. How long does the textile-hydrogel composite take to dry out?
2. How many F-T are necessary to improve the moisture properties of the hydrogel??

3.5.1. Textile Materials

- Warp: Cotton yarn NE 38/2;
- Weft: Solvron SF.330 (Dissolvable 55c+ Yarn) 330x3 d tex - Count: 1/10 Nm;
- ADACAD software;
- Jacquard loom TC2;
- Boat shuttle;
- Bobbin;
- Scissors.

3.5.2. Textile Method

The textile samples for *Hydrogel Moisture Retention* were fabricated in the Material Lab using the Jacquard loom TC2, with the intent of also using them in *The Right Combination* (section 3.6.), which involves microalgae attachment and viability testing. A single triple-layer textile was designed, consisting of plain-weave layers for the primary structure, while the edges were reinforced with a compound weave (twill and reverse twill) to ensure secure bonding of the layers. The outer layers comprised 90% PVA and 10% cotton, while the central layer was made entirely of cotton. Each sample measured 7 cm × 5 cm, with an additional 1 cm along the edges featuring the twill-reinforced compound structure for added durability. This structure was woven using the same method as the previous experiments, with the only difference being the alternation of weft yarns in a 4:1 ratio—four passes of PVA followed by one pass of Co.

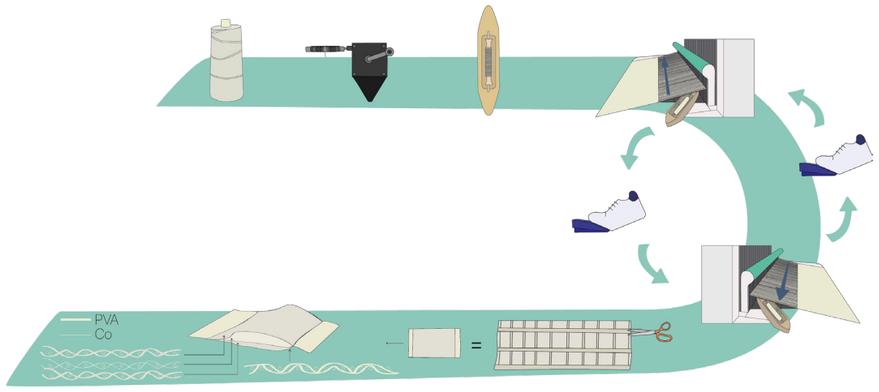

Figure 66: Steps to prepare the triple layer textiles.

3.5.3. Experiment Materials

- 4 textiles;
- 4 glass Petri dishes;
- 3 plastic Petri dishes;
- 120 ml of BG 11;
- Tweezers.
- Freezer;
- UV box;
- Laminar Air Flow (LAF) Cabinet;
- Microscope.

3.5.4. Method

The experiment was conducted in the BioLab under sterile conditions to prevent contamination. A UV light box was placed inside the Laminar Air Flow (LAF) Cabinet, where the four textile samples underwent sterilization, with each side exposed to UV light for 20 minutes. Following sterilization, the samples were immersed in BG11 medium and each was placed in empty petri dishes under controlled conditions.

The first sample was immediately placed under standard light conditions and monitored throughout the experiment. The remaining three samples underwent the first F-T cycle, consisting of 23 hours of freezing at -20°C followed by 3 hours of thawing under a controlled light-dark cycle (16 hours of light and 8 hours of darkness). After this initial cycle, one of the three samples was removed from the process placed in a new petri dish and maintained under standard light conditions for monitoring, while the other two proceeded through a second F-T cycle. Upon completion of the second cycle, another sample was removed and placed in a new petri dihs for observation under light conditions, leaving only one textile to undergo a third and final F-T cycle. Once this last cycle was completed, the remaining sample was also placed in a new petri dish under standard light conditions and monitored.

3.5.5. Observations Method

The textiles were observed and analyzed through two complementary approaches. A macroscopic evaluation was performed by direct visual inspection to assess moisture retention, determining whether the samples remained hydrated over time. Additionally, microscopic analysis was conducted to examine the microstructural changes in the hydrogel matrix, particularly focusing on the dissolution of the PVA component. This dual assessment provided insights into the mechanical resilience of the hydrogel and the potential influence of freeze-thaw cycling on its structural stability and moisture abilities.

3.5.5. Conclusion

The *Hydrogel Moisture Retention* experiment demonstrated the significant role of the Freeze-Thaw process in enhancing the hydrogel ability to retain moisture over time (Figure 67). The findings revealed that the sample not subjected to any Freeze-Thaw cycles developed an adhesive surface just five days after immersion in BG11 medium. In contrast, the sample that underwent a single Freeze-Thaw cycle maintained its structural integrity for 11 days before exhibiting a similar adhesive behavior. The samples subjected to two and three Freeze-Thaw cycles exhibited similar behavior, maintaining their structural integrity for 12 days before developing adhesive characteristics. These findings indicate that while increasing the number of Freeze-Thaw cycles has only a marginal effect, the presence of the process itself plays a critical role in improving hydrogel performance. By reinforcing crosslink formation within the polymeric network, the Freeze-Thaw process enhances moisture retention, reducing the need for frequent supplementation with additional BG11 medium and contributing to a more stable and self-sustaining system.

Although these results were obtained under controlled laboratory conditions, it is essential to consider the hydrogel's behavior in real-world environments, where factors such as temperature fluctuations, wind, and rainfall could impact its stability. While the specific outcomes may vary under such conditions, the formation of a well cross-linked hydrogel remains advantageous, as it helps to mitigate moisture loss and decreases the need for frequent rehydration. This ability to retain hydration despite environmental challenges underscores the importance of optimizing the Freeze-

Thaw process to improve the long-term durability and resilience of living hydrogels in practical applications.

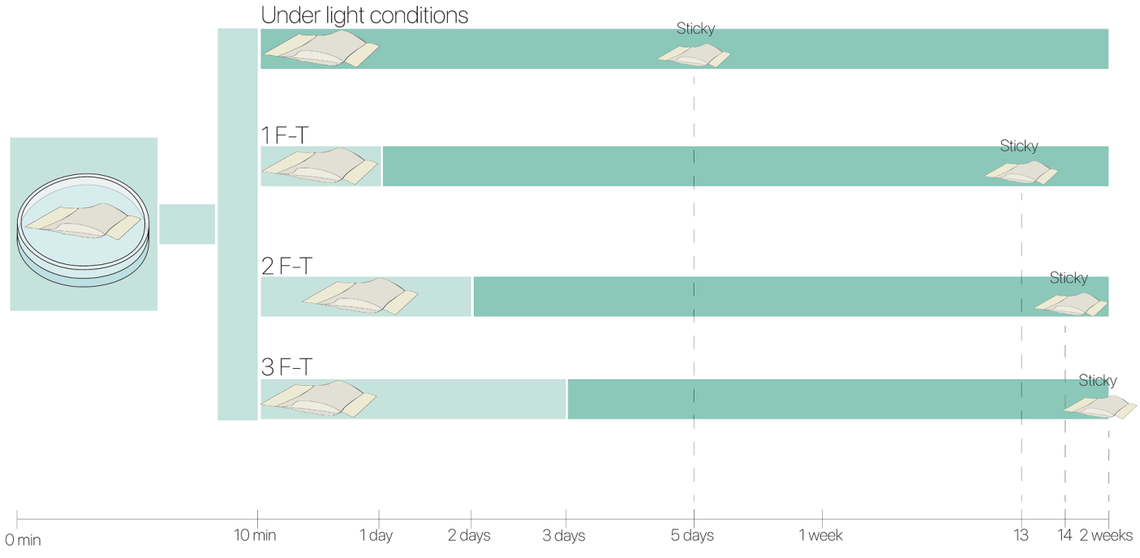

Figure 67: The graph shows the importance of Freezing the textile to improve its moisture properties.

3.6. The Right Combination

The results and considerations from all the experiments have been analyzed to guide the design and objectives of *The Right Combination*. This experiment focuses on exploring key variables to optimize the immobilization and viability of microalgae while addressing the limitations observed in previous experiments. The primary variables investigated include textile structure, methods of microalgae deposition, and processing timelines.

To enhance textile performance, the arrangement of polyvinyl alcohol (PVA) and cotton (Co) was restructured. The textile design incorporates a triple-layer structure, combining the microalgae-attracting properties of cotton with the protective and structural role of PVA. Second, two methods of microalgae deposition were tested. The first involves immersing the textile in a microalgae suspension, as previously done in *Freezing Living Textiles* esperiment. The second involves pipetting microalgae directly onto the cotton layer, ensuring localized deposition along both edges. Additionally, three distinct timelines were examined to assess the impact of freeze-thaw (F-T) cycles and the timing of microalgae addition on their attachment and viability.

A modified hydration protocol was also introduced to address challenges identified in previous experiments, including rapid PVA degradation during immersion (*Freezing Living Textiles* experiment) and desiccation when left without any medium sources for long period of time (*Drying-Rehydrating Textiles* experiment). The controlled hydration approach aimed to achieve a balance between maintaining microalgae viability and reducing PVA degradation. To efficiently explore these variables and configurations, the Parallel Prototyping Method was employed (Kesari, 2019).

The primary goals of this experiment are to extend the lifespan of the PVA layer, ensuring it can effectively moisture the environment. Additionally, the experiment aims to facilitate the rapid recovery of microalgae following the freeze-thaw cycles. Finally, it seeks to determine the most efficient method for depositing microalgae onto the textile, optimizing both their attachment and viability.
This experiment aimed to answer five key questions:

1. Can microalgae recover in 21 days after the F-T cycles in the new textile structure?
2. Can microalgae survive after three F-T cycles in the new textile structure?
3. Can microalgae still be immobilized if added to the textile after two F-T cycles?
4. Can microalgae be immobilized after one F-T cycle?
5. How do microalgae interact with and respond to the textile environment?
6. Will the PVA degrade more slowly compared to previous experiments?

Ultimately, this experiment sought to identify the ideal parameters for maximizing microalgae immobilization and viability on textile substrates.

3.6.1. Textile Materials

- Warp: Cotton yarn NE 38/2;
- Weft: Solvron SF.330 (Dissolvable 55c+ Yarn) 330x3 d tex - Count: 1/10 Nm;
- ADACAD software;
- Jacquard loom TC2;
- Boat shuttle;
- Bobbin;
- Scissors.

3.6.2. Textile Methods

The textile samples for *The Right Combination* experiment were fabricated in the Material Lab using the Jacquard loom TC2. For this experiment, a single triple-layer textile was designed to optimize both mechanical stability and microalgae attachment (Figure 68). The textile consisted of plain-weave layers for the primary structure, while the edges were reinforced with a compound weave (twill and reverse twill) to ensure the layers remained securely bonded. The outer layers were composed of 90% PVA and 10% cotton, with the PVA serving to immobilize and protect *Scenedesmus* sp. from external agents. The central layer was made entirely of cotton, which served as the main substrate for microalgae immobilization. This structure have been woven with the same method used for the previous

experiments, the only difference was in the fact that weft yarns were alternated in the following way: 4 times PVA 1 time Co.

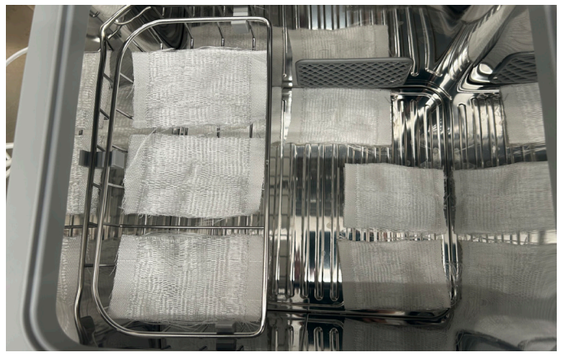

Figure 68: Triple layer textiles.

3.6.3. Experiment Materials

- 12 textiles;
- 12 plastic Petri dishes;
- 400 ml of BG 11 medium;
- 400 ml of *Scenedesmus* sp. and liquid medium;
- 16 glass Petri dishes;
- 4 Pipette;
- Tweezers;
- Freezer; UV box;
- Laminar Air Flow (LAF) Cabinet;
- Monitoring Pam;
- Microscope.

3.6.4. Methods

The experiment was conducted in the BioLab under sterile conditions to ensure the safe handling of microorganisms. A UV light cube was placed inside the Laminar Air Flow (LAF) Cabinet, and twelve textile samples underwent sterilization, with each side exposed to UV light for 20 minutes. Following sterilization, the samples were divided into three groups of four textiles each, designated as Timeline 1 - 3 F-T cycles, Timeline 2 - F-T Cycles Pre- and Post-Microalgae Addition, and Timeline 3 - 1 F-T cycle, each following distinct experimental protocols (Figure 69).

In Timeline 1 - 3 F-T Cycles, the textiles were divided into two subgroups (Figure 70). The first subgroup was immersed in a 30 mL culture of *Scenedesmus* sp. and BG11 medium for four days, while the second subgroup received 3 mL of the same culture pipetted between the textile layers daily for four days. On the fourth day, all textiles were transferred to empty Petri dishes and kept under light/dark conditions for three days before undergoing three freeze-thaw cycles (23 hours freezing at -20°C, followed by 3 hours thawing at room temperature). Afterward, the textiles were transferred to glass Petri dishes and exposed to controlled light/dark conditions for 20 days where 3 mL of BG11 medium was added every three weeks.

Figure 69: Combinations of F-T cycles and Microalgae disposition methods applied for the experiment.

Timeline 2 - F-T Cycles Pre- and Post-Microalgae Addition followed a slightly modified approach (Figure 71). The four textiles were first immersed in BG11 medium until noticeable shrinkage occurred. They were then transferred to empty Petri dishes and subjected to two freeze-thaw cycles, maintaining the same freezing and thawing durations as in the previous timeline (3 F-T Cycles). After this treatment, the textiles were placed in glass Petri dishes and divided into two subgroups. The first subgroup was immersed in a 30 mL solution of *Scenedesmus* sp. and BG11 medium for five days. The second subgroup received 3 mL of the same culture pipetted between the textile layers daily for five consecutive days, followed by a two-day rest period in empty Petri dishes. After this phase, all textiles underwent an additional freeze-thaw cycle before being transferred to new glass Petri dishes. To support microalgae recovery, 3 mL of BG11 medium was added to each sample every three weeks—the time required before the hydrogel exhibited adhesive behavior.

In Timeline 3 - 1 F-T Cycle, the textiles followed the same subgroup division (Figure 72). One subgroup was immersed in a 30 mL *Scenedesmus* sp. and BG11 medium for four days, while the other received 3 mL of the same culture pipetted daily over the same period. On the fourth day, all textiles were transferred to empty Petri dishes and kept under controlled conditions for three days before undergoing a single freeze-thaw cycle. The following day, they were moved to individual glass Petri dishes and under controlled light conditions, with 3 mL of BG11 medium added every three weeks to sustain microalgae recovery.

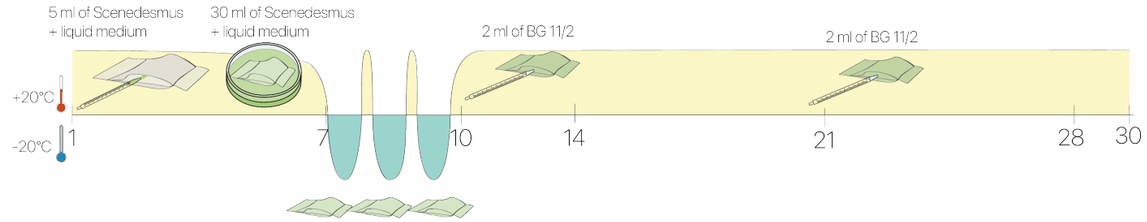

Figure 70: Timeline 1- 3 F-T Cycles.

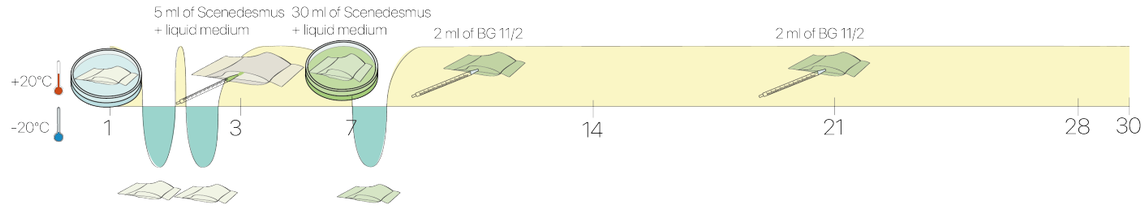

Figure 71: Timeline 2 - F-T Cycles Pre- and Post-Microalgae Addition

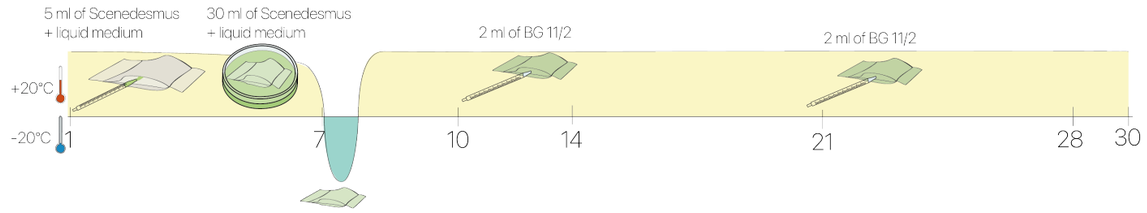

Figure 72: Timeline 3 - 1 F-T Cycle

3.6.5. Microscopic Observations

Timeline 1 - 3 F-T cycles: Throughout all three timelines, microscopic imaging was performed at key experimental stages to evaluate microalgae attachment efficiency, structural modifications in the textiles, and the degradation rate of the PVA component. These evaluations were conducted prior to the freeze-thaw cycles, immediately after their completion, and over the subsequent three-week period to monitor progressive changes.

Timeline 2 - F-T Cycles Pre- and Post-Microalgae Addition: Figure 74 illustrates that Timeline 2 - F-T Cycles Pre- and Post-Microalgae Addition showed significant recovery after three weeks in both subgroups—immersed and pipetted. However, microalgae were not fully attached to the hydrogel. This issue may be due to the sequence of treatments: the hydrogel first absorbed BG11, then underwent two freeze-thaw cycles, and only afterward were the microalgae introduced. This suggests that microalgae attachment occurs primarily during the initial soaking phase, when the textile first interacts with the medium. The freeze-thaw cycles may then serve to reinforce this immobilization, effectively sealing the microalgae within the hydrogel. Additionally, microscopic images revealed that microalgae subjected to identical conditions do not always respond uniformly, highlighting variability in their behavior within the textile structure.

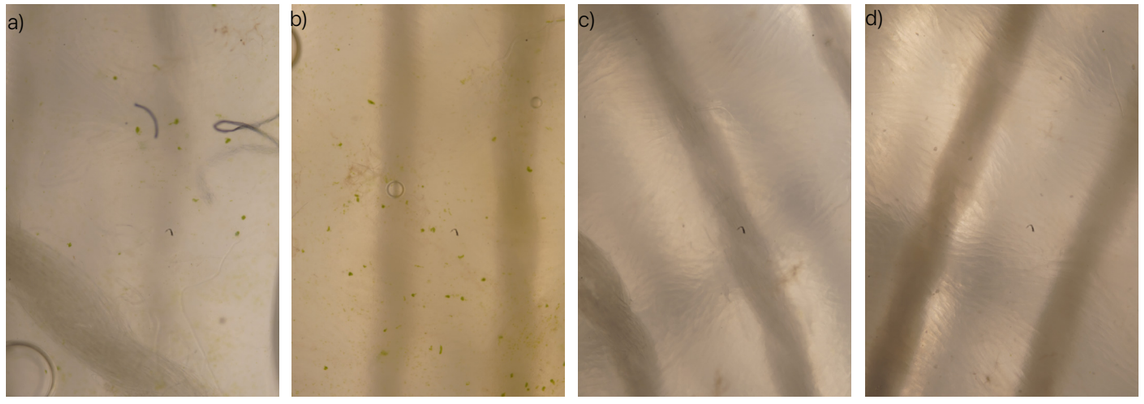

Figure 73: Timeline 1 - 3F-T cycles- *Scenedesmus* sp. a) Immersed sample. Microscopic image (50x); b) Immersed sample Copy. Microscopic image (50x); c) Pipetted sample. Microscopic image (50x); d) Pipetted sample Copy.Microscopic image (50x).

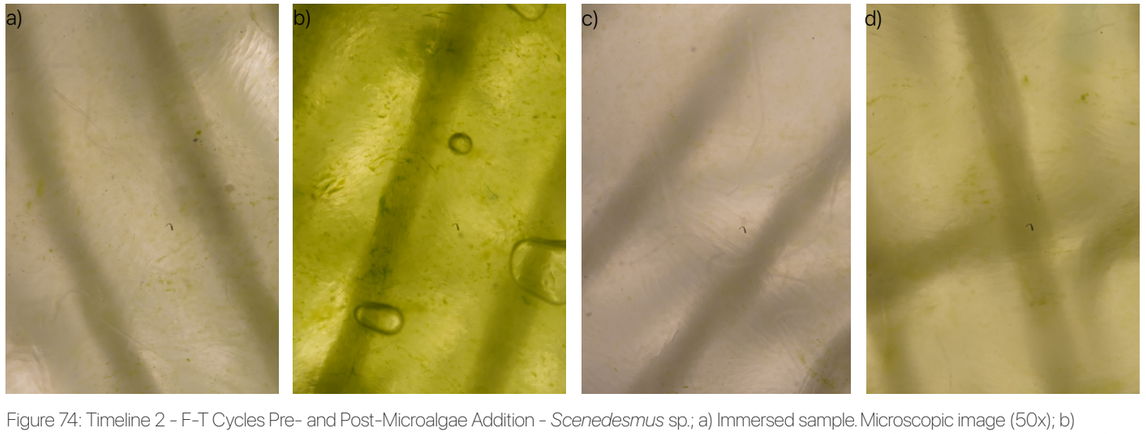

Figure 74: Timeline 2 - F-T Cycles Pre- and Post-Microalgae Addition - *Scenedesmus* sp.; a) Immersed sample. Microscopic image (50x); b) Immersed sample Copy. Microscopic image (50x); c) Pipetted sample. Microscopic image (50x); d) Pipetted sample Copy. Microscopic image (50x)

Timeline 3 - 1 F-T cycle : Finally, Figure 75 highlights the recovery of Timeline 3 - 1 F-T Cycle, albeit at a slower rate compared to Timeline 2 - F-T Cycles Pre- and Post-Microalgae Addition. However, Timeline 3 - 1 F-T Cycle successfully maintained adequate moisture levels without requiring additional BG11 supplementation, confirming its ability to sustain a well-hydrated environment. Moreover, microalgae appeared to be well attached to the hydrogel, indicating effective immobilization. Microscopic analysis showed that microalgae under identical conditions exhibit variable responses.

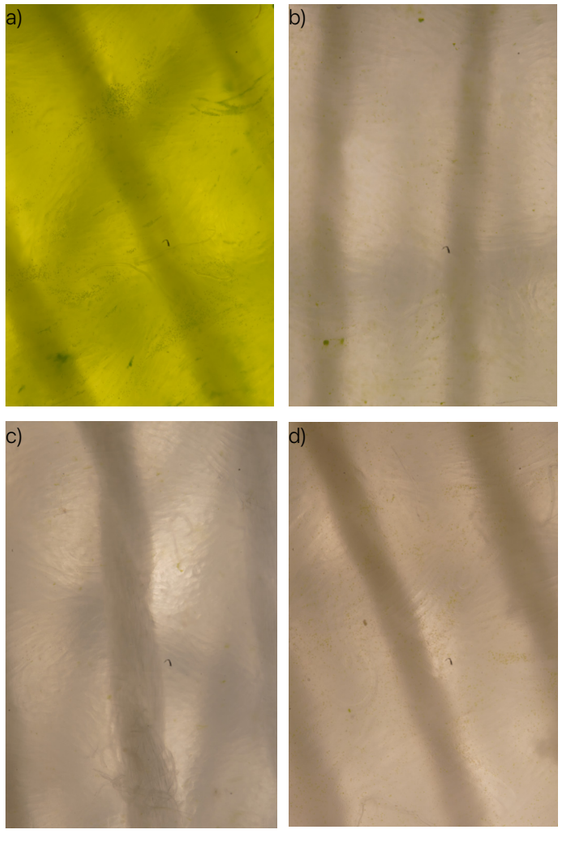

Figure 75: Timeline 3 - 1 F-T cycle - *Scenedesmus* sp. viability. a) Immersed sample. Microscopic image (50x); b) Immersed sample Copy. Microscopic image (50x); c) Pipetted sample. Microscopic image (50x); d) Pipetted sample Copy. Microscopic image (50x).

3.6.6. Photosynthesis tests

Photosynthetic activity tests were performed to assess the viability of the immobilized microalgae over time. Measurements were taken before and after the freeze-thaw cycles, followed by weekly assessments to track changes in photosynthetic performance.

The photosynthetic activity test was conducted inside the Laminar Air Flow (LAF) Cabinet, where the petri dishes were opened, and placed into a dark box. The MONITORING PAM device, connected to a laptop running the WinControl-3 software, was used to measure photosynthetic efficiency. By positioning the MONITORING PAM device, after being sterilized with Ethanol, over the living textiles and initiating the measurement via the software interface, a light emission was triggered, allowing for the quantification of photosynthetic activity. Recorded quantum yield values can range from 0 to 1, with values below 0.7 indicating poor photosynthetic performance, while readings between 0.7 and 1 were considered indicative of a healthy and active microalgal presence (Schuurmans et al., 2015).

3.6.7. Photosynthesis tests

The fourth photosynthesis test was conducted at the end of the experiment (after 28 days). Each sample was monitored on both sides in 5 different spots: Top Left, Top Center, Top Right, Bottom Left and Bottom Right.

After collecting all experimental data, the results were processed in several steps to ensure a comprehensive analysis. First, for each sample, the photosynthetic activity measurements from five different spots were averaged (Figure 76).

These data represent the photosynthetis of textiles samples in different part of the samples (Top left, Top center, Top right, Bottom Left, Bottom Right).

Unit= Fv/Fm

	Top Left	Top Center	Top Right	Bottom Left	Bottom Right	Average		
Timeline 1							Average o' Average of Timeline 1 pipetted	
Immersed	0.408	0.225	0.431	0.645	0.648	0.4714	0.4369	0.5275
Immersed Replicates	0.21	0.265	0.291	0.65	0.596	0.4024		
Pipetted	0.423	0.344	0.546	0.535	0.603	0.4902		
Pipetted Replicates	0.526	0.462	0.491	0.64	0.705	0.5648		
Standard Deviation	0.132	0.104445	0.10973	0.055151	0.050259	0.0668		
Timeline 2							Average o' Average of Timeline 2 pipetted	
Immersed	0.537	0.425	0.432	0.549	0.541	0.4968	0.5185	0.531
Immersed Replicates	0.566	0.493	0.471	0.594	0.577	0.5402		
Pipetted	0.453	0.498	0.479	0.558	0.593	0.5162		
Pipetted Replicates	0.407	0.594	0.424	0.731	0.573	0.5458		
Standard Deviation	0.0736	0.069496	0.02753	0.084273	0.021787	0.0226		
Timeline 3							Average o' Average of Timeline 3 pipetted	
Immersed	0.396	0.282	0.343	0.629	0.651	0.4602	0.5175	0.5943
Immersed Replicates	0.506	0.508	0.602	0.652	0.606	0.5748		
Pipetted	0.572	0.472	0.586	0.61	0.623	0.5726		
Pipetted Replicates	0.559	0.59	0.567	0.638	0.726	0.616		
Standard Deviation	0.0801	0.130379	0.12184	0.017595	0.053019	0.0668		
Scenedesmus in liquid medium	0.787	0.818	0.669			0.758		
							Average In Average Pipetted	
							0.491	0.550933333

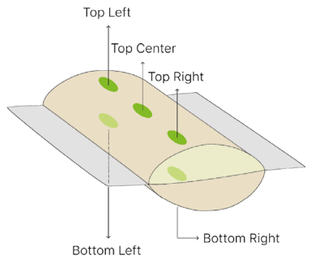

Figure 76: Overall final Photosynthesis test results.

Then, to account for duplicate samples, the results were grouped based on the method of microalgae introduction: for each timeline, the measurements from the immersed samples were averaged separately, as were those from the pipetted samples. This step ensured that a representative average was obtained and helped identify the most effective F-T process. Next, an overall average was calculated for all immersed samples and another for all pipetted samples, enabling a direct comparison between the two methods to determine which was more effective in introducing microalgae into the hydrogel. The measurements were first analyzed individually, then compared collectively, and ultimately were compared with *Scenedesmus* sp. in a liquid medium to evaluate the impact of textile embedding on microalgal viability and performance (Figure 77).

As illustrated in Figure 77, the samples from the 'Timeline 2 - F-T Cycles Pre- and Post-Microalgae Addition' experiment, followed by those from 'Timeline 3 - 1 F-T Cycle,' exhibit the highest photosynthetic activity.

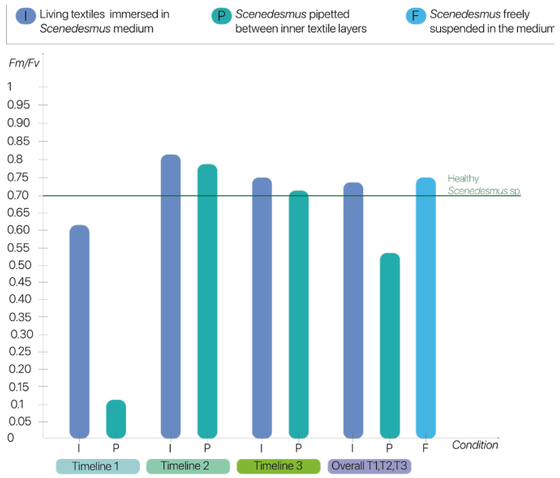

Figure 77: The graph illustrates the photosynthetic performance of immersed and pipetted samples across different timelines. Timeline 1 represents three consecutive Freeze-Thaw (F-T) cycles, Timeline 2 consists of three F-T cycles split into two before *Scenedesmus* sp. addition and one after, while Timeline 3 corresponds to a single F-T cycle. The Overall category represents the average photosynthetic activity of all immersed samples and all pipetted samples. Additionally, the green line indicates the threshold above which microalgae can be considered healthy. This comparative visualization highlights the impact of different F-T processes and sample preparation methods on microalgal photosynthetic activity.

3.6.8. Conclusion

After 28 days, *Scenedesmus* sp. demonstrated its ability to recover under three different conditions. As observed in both microscopic images and photosynthesis tests, samples from Timeline 1 - 3 F-T cycles - exhibited the poorest results. Instead of improving over the three-week period, the microalgae's condition deteriorated further. Timeline 2 - F-T Cycles Pre- and Post-Microalgae Addition, overall, achieved the best results across both samples, immersed and pipetted. However, microscopic images revealed that while *Scenedesmus* sp. was present, not all cells were firmly attached to the textile, with some still suspended in the surrounding medium. Despite this, Timeline 2 maintained excellent moisture retention, suggesting that the lack of full attachment may not necessarily indicate a negative outcome. Timeline 3 - 1 F-T cycle - also showed favorable results, albeit with a slower recovery rate compared to Timeline 2. However, in contrast to Timeline 2, the microalgae in Timeline 3 were well immobilized within the textile. Given that photosynthetic activity remained at an optimal level, could be taken into consideration that the microalgae were effectively encapsulated. Nevertheless, further studies are needed to confirm this hypothesis.

The best overall performance was observed in Timeline 3. Although it did not achieve the highest photosynthesis results, its structural and functional stability made it the most effective living textile configuration. Furthermore, determining whether the Immersed or Pipetted method is superior remains inconclusive, as fungal contamination risks could be influenced by prolonged surface moisture rather than the specific encapsulation method. Ultimately, the new textile structure features even greater warp spacing, enhancing both light penetration—thanks to the transparency of the gel-like PVA—and the durability of the PVA itself. Notably, after 30 days, the PVA remained intact.

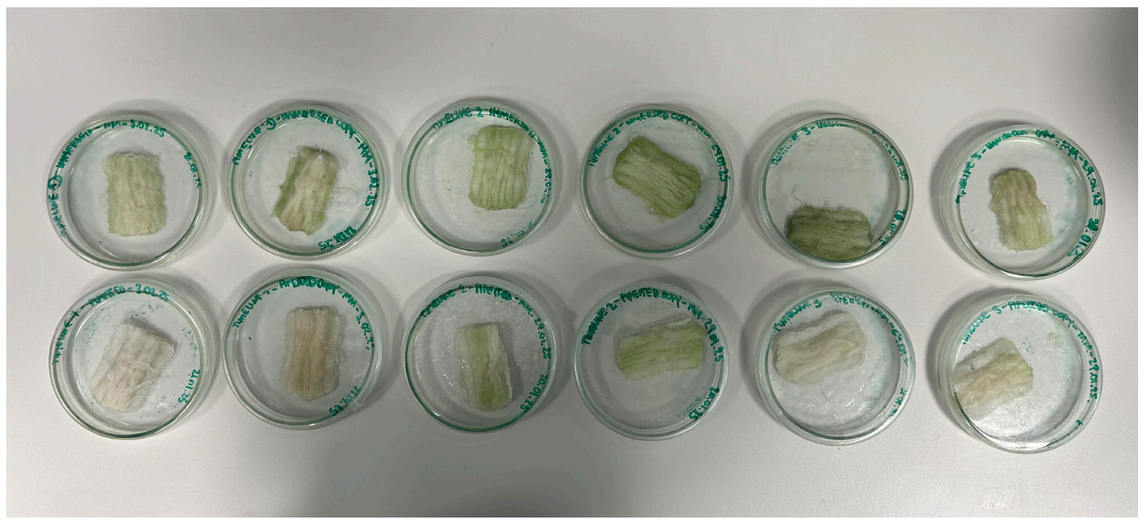

Figure 78: the 12 samples at the end of the experiment.

3.7. The Right Combination

Through six experimental sessions, this research systematically investigated the feasibility of integrating microalgae into a hydrogel-based textile using the Freeze-Thaw (F-T) method. Each experiment provided critical insights into the interactions between microalgae, hydrogels, and textile structures, refining the conditions necessary for stability, attachment, and viability (Figure 79).

The findings confirmed that the F-T process is an effective technique for microalgal immobilization and hydrogel formation and , with *Scenedesmus* sp. demonstrating greater adaptability than *Nostoc punctiformis* [*Freezing Living Textile*]. Textile structure and composition played a crucial role in both attachment and hydrogel performance [*Hydrogel Moisture Retention*], [*TheRight Combination*]. The study revealed that a triple-layer structure with well-spaced warp yarns enhanced light penetration by improving hydrogel transparency—addressing one of the key limitations in previous studies, where low photosynthetic activity was often linked to insufficient material transparency [*TheRight Combination*]. Additionally, the ability of hydrogels to retain moisture was identified as essential for the living textile self-sufficient survival [*Hydrogel Moisture Retention*].

A final discovery was that when PVA is not permanently immersed in a liquid medium and has sufficient spacing between the warp yarns to facilitate gel formation, its lifespan is significantly extended, remaining intact even after 30 days [*TheRight Combination*]. However, despite this improvement, PVA degradability remains a challenge that requires further investigation. Future research should focus on extending hydrogel longevity while ensuring optimal conditions for microalgal viability.

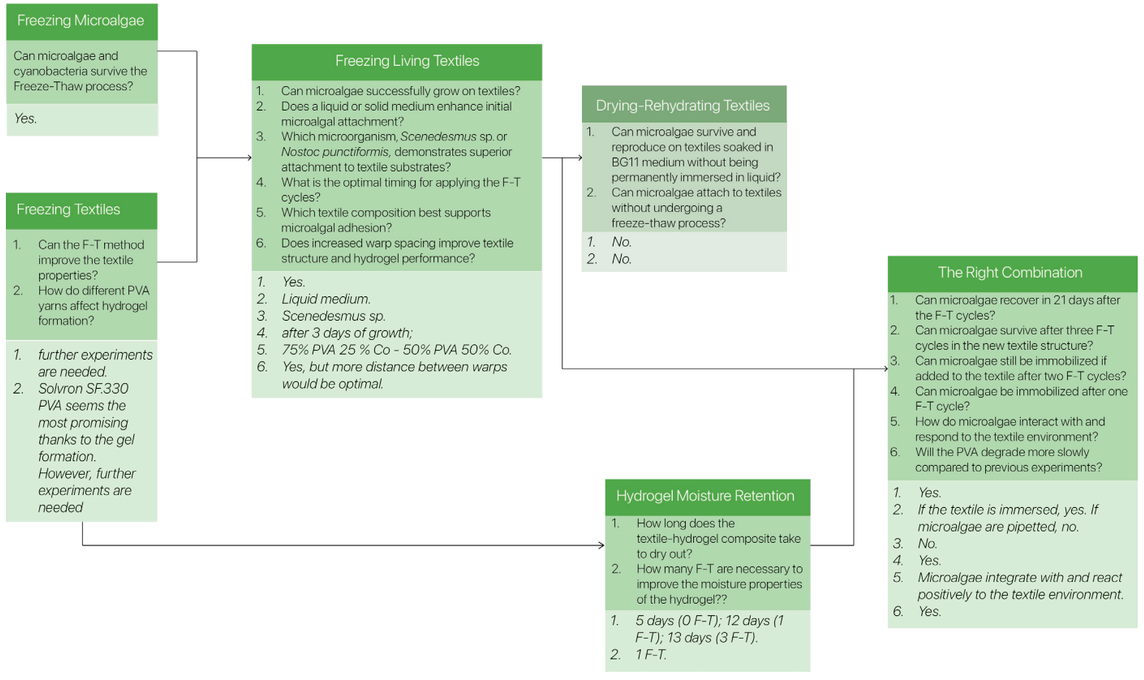

Figure 79: Experimental process scheme, their crucial questions and answers.

3.8. Recipe for Living Textiles

For the successful fabrication of the living textile, precise control over each step of the production process is essential.

3.8.1. Draft Design Procedure

The textile design process begins by creating a precise draft using AdaCAD software. Initially, a triple-layer textile structure is developed by applying the "Tabby" command three times, each repetition representing one distinct layer. The resulting structure consists of two protective outer layers composed of 90% PVA and 10% Cotton, enclosing an inner layer designated to host microalgae. A draft as been added so that each layer could be systematically assigned to a tabby pattern through specific layer identifiers, clearly distinguishing the arrangement and orientation of warp and weft yarns within each individual layer. Moreover, to balance stability and transparency, warp intersections and spacing are optimized, enhancing structural integrity and facilitating adequate light penetration essential for microalgae viability (Figure 80).

To bond the triple layer textile structure, a compound textile is created using an interlacing twill pattern. This involves sequentially applying the commands "Twill" (twice), "Shift," and "Interlace Wefts," resulting in a robust interconnected textile layer system (Figure 81d). The detailed positioning of the triple-layer structure and its compound within the final textile are defined through a precisely dimensioned visual map (2640×100 px) generated on Photoshop and uploaded into AdaCAD (Figure 82b and c). Finally, the complete textile design is exported as a bitmap file, enabling its direct transfer to a TC2 loom for fabrication.

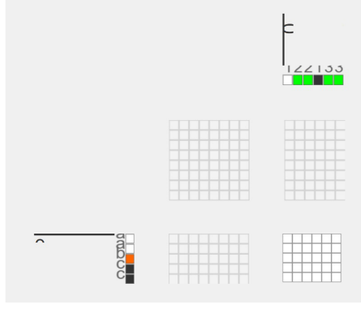

Figure 80: The weft yarns are alternated following a pattern of four PVA yarns followed by one Cotton yarn. White squares represent PVA weft yarns in the top layer, orange squares indicate Cotton yarns in the central layer, and black squares correspond to PVA yarns in the bottom layer.

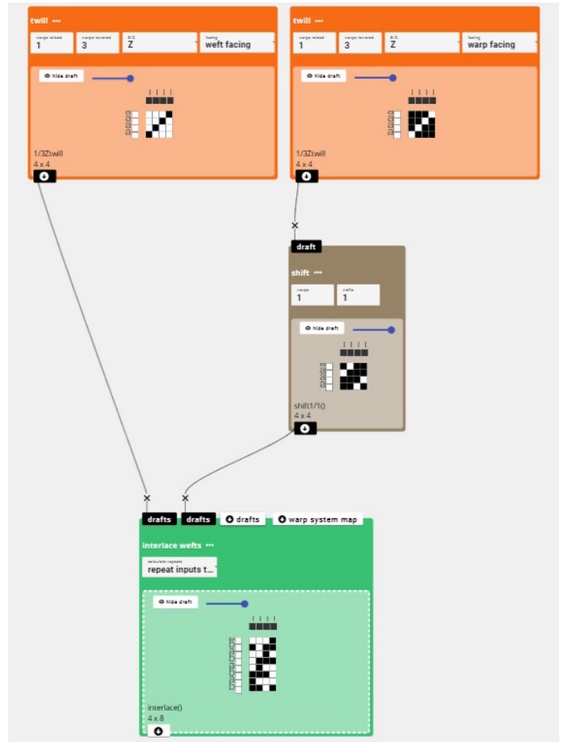

Figure 81: draft of a compound twill reverse twill.

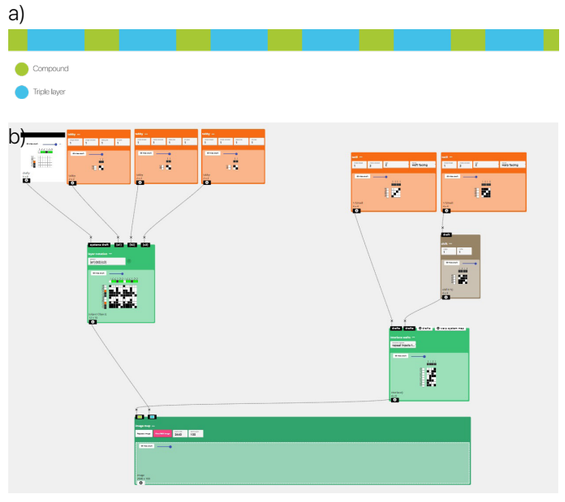

Figure 82: a) visual map (2640×100 px); b) final Image Map uploaded on ADACAD (unfortunately the software could not report the entire bitmap).

3.8.2. Weaving

3.8.2.1. Textile Materials

- Warp: Cotton yarn NE 38/2;
- Weft: Solvron SF.330 (Dissolvable 55c+ Yarn) 330x3 d tex - Count: 1/10 Nm;
- ADACAD software;
- Jacquard loom TC2;
- Boat shuttle;
- Bobbin;
- Scissors.

3.8.2.2. Textile Method

The textile sample is fabricated using the Jacquard loom TC2, requiring the BitMap file to be uploaded into the TC2 software. Once the design is loaded, the bobbin winder is set up, and PVA yarn is wound onto the bobbin from its cone. After the bobbin is fully loaded, it is placed into the boat shuttle. The same process is applied for the cotton yarns (Co) to prepare them for weaving. With the loom and shuttle set up, the weaving process begins. As the loom pedal is pressed, the cotton warp yarns alternate positions according to the draft uploaded in the TC2 weaving program, allowing the shuttle carrying the PVA yarn to pass through. This cyclical process continues until the textile reaches a length of 70 cm and a height of 5 cm. An additional 2 cm of textile is woven to separate the current sample from the next. Once weaving is complete, the textile is carefully removed from the loom and cut into 7x7 cm squares for further processing. With the textile sample fabricated, the next phase takes place in the BioLab, where the textile is transformed into a habitat for microalgae.

3.8.3. From Textile to Living Microalgal Textiles.

3.8.3.1. Experiment Materials

- 12 textiles;
- 12 plastic Petri dishes;
- 400 ml of BG 11 medium;
- 400 ml of *Scenedesmus* sp. and liquid medium;
- 16 glass Petri dishes;
- 4 Pipettes;
- Tweezers;
- Freezer;
- UV cube;
- Laminar Air Flow (LAF) Cabinet;
- Monitoring PAM tool;
- Microscope;
- Parafilm.

3.8.3.2. Method To Design Living Microalgal Textiles.

Upon arrival at the BioLab, proper laboratory protocols must be followed, including wearing a lab coat and thoroughly cleaning hands to maintain sterility. The first step involves sterilizing the textiles on both sides. To achieve this, the Laminar Air Flow (LAF) Cabinet must be turned on, and a UV light cube placed inside. The textiles are then positioned within the cube and exposed to UV light for 20 minutes per side to ensure effective sterilization. Following sterilization, each textile sample must receive 3 mL of *Scenedesmus* sp. and BG 11 liquid medium daily for four consecutive days through a pipette applied in between. The microalgae suspension myst be applied between the textile layers using a pipette. On the fourth day, all treated textiles are transferred to empty Petri dishes and kept under controlled conditions for three days before undergoing a single freeze-thaw (F-T) cycle - 23h freezing and 3h thawing under light condition at room temperature. The day after the F-T cycle, the textiles must be relocated to individual glass Petri dishes, sealed with parafilm, and maintained under controlled light conditions. To support microalgae recovery, 3 mL of BG11 medium must be added every three weeks, ensuring a sustained and stable environment for growth. Additionally, weekly monitoring is essential, involving microscopic imaging and photosynthetic analysis using the Monitoring PAM tool. Since microalgae are living organisms, their recovery and growth do not always follow a fixed protocol. Continuous assessment of their viability allows for adaptive adjustments, ensuring optimal conditions based on their specific needs.

Chapter 4
Exploration of Origami with hydrogels

This chapter explores the integration of origami-inspired folds in hydrogels through weaving techniques, examining how these structures influence the material's functionality and adaptability. As part of the two cyclical steps of the methodology—"Understanding the Materials" and "Manifesting (Organism-Centered) Materials Experience Patterns"—this chapter investigates the relationship between material behavior and structural design.

4.1. Prototype 1 - Origami with Co and PVA

As discussed in Chapter 3, origami is the traditional Japanese art of paper folding, transforming flat surfaces into intricate three-dimensional structures (Origami for Beginners: Easy Guide to Origami | Discount Art N Craft Warehouse, n.d.). In textile applications, one commonly used origami technique is tessellation, in which specific points on the textile are tied and knotted together to create geometric patterns and structured folds (Fabric Origami | Jiangmei Wu, n.d.-b). However, this approach is not suitable for the present study, as it relies on additional tools and interventions, whereas the goal here is to develop an origami structure without external machinery. To overcome this constraint, inspiration was drawn from Emilie Palle Holm's ORIORI, a project that employs a technique allowing a flat, rectangular woven textile to transform into a structured three-dimensional form (Emilie-palle-holm, n.d.). This is achieved by strategically embedding structural folding lines within the textile's warp and weft during its construction, allowing it to fold naturally into the desired shape (Emilie-palle-holm, n.d.).

Building on this concept, the study leveraged the unique properties of PVA, particularly its tendency to shrink and dissolve when exposed to moisture, to facilitate controlled folding. This strategy was influenced by Jane Scott's Responsive Knit project, which demonstrated how wool's natural ability to contract in response to water could be harnessed to create self-shaping textiles (Buso et al., 2022). Similarly, in this research, PVA's responsive behavior was strategically integrated into the woven structure, enabling the textile to undergo precise, self-induced transformations without the need for additional mechanical processes.

4.1.1. Textile Materials

- Warp: Cotton yarn NE 38/2;
- Weft: Solvron SF.330 (Dissolvable 55c+ Yarn) 330x3 d tex - Count: 1/10 Nm;
- ADACAD software;
- Jacquard loom TC2;
- Boat shuttle;
- Bobbin;
- Scissors.

4.1.2. Textile Method

As first thing, a prototype made with paper has been realized (Figure 83). After designing the lift plans for weaving using ADACAD software, the textile structure was developed based on the configurations used in *Hydrogel Moisture Retention* and *The Right Combination* experiments. The design retained the triple-layer construction, in which each layer was woven using a plain weave structure, while the edges featured a compound weave (twill and reverse twill) to ensure that the layers remained securely bonded. However, an additional structural modification was introduced to facilitate folding: a long float section—referred to as the "mountain/valley fold"—was incorporated (Figure 84). In this section, all the weft threads remained on the surface while all the warp threads stayed at the bottom. To create the intended folding effect, these long float sections were alternated, meaning that in one sequence, the PVA layer was positioned on top, while in the next, it was shifted to the bottom. This alternating pattern allowed the textile to adopt a structured fold, enabling controlled deformation and dynamic adaptability.
The textile samples were fabricated in the Material Lab using the Jacquard loom TC2. To prepare the materials, PVA yarn (Solvron SF.330) and cotton yarn were first wound onto separate bobbins using a bobbin winder. These bobbins were then placed into boat shuttles for the weaving process. On the Jacquard loom, cotton yarn was used as the warp, while the weft followed a structured sequence, alternating between four passes of PVA and one pass of cotton. This weaving pattern ensured that the PVA formed the external layers, while the cotton constituted the central layer, reinforcing the textile's structural integrity. The textile sample was woven to a length of 70 cm and a width of 5 cm.

4.1.3. Experiment Materials

- Woven textile;
- A stainless steel tray;
- water.

4.1.4. Method

As first thing, a prototype made with paper has been realized (Figure 83). Then, the textile was first immersed in a long water-filled container and left until it began to shrink (Figure 85).Once the shrinking process started, it was carefully transferred to a glass Petri dish for further observation..

Figure 83: Paper prototype of accordion folds.

Figure 84: Prototype 1 - Textile structure.

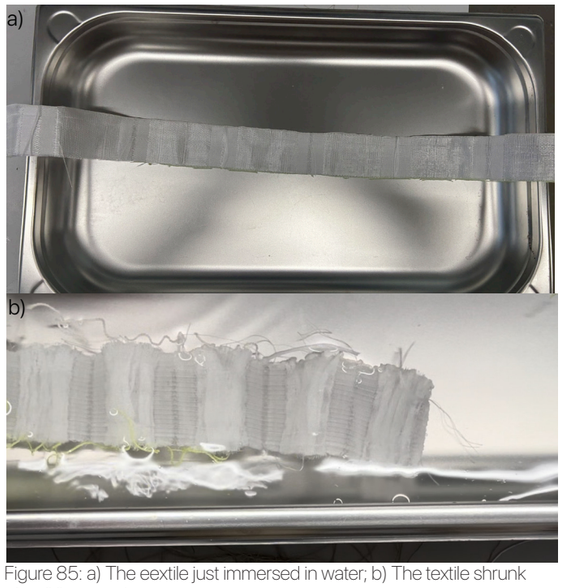

Figure 85: a) The eextile just immersed in water; b) The textile shrunk after 20 seconds.

4.1.5. Conclusion

At the end of the experiment, the textile was examined, revealing that while the folding mechanism functioned as intended, the overall weight of the textile made it difficult to maintain the folds in position as showed in Figure 86a and 86b. The excessive weight caused the structure to collapse, preventing the folds from holding their intended shape.

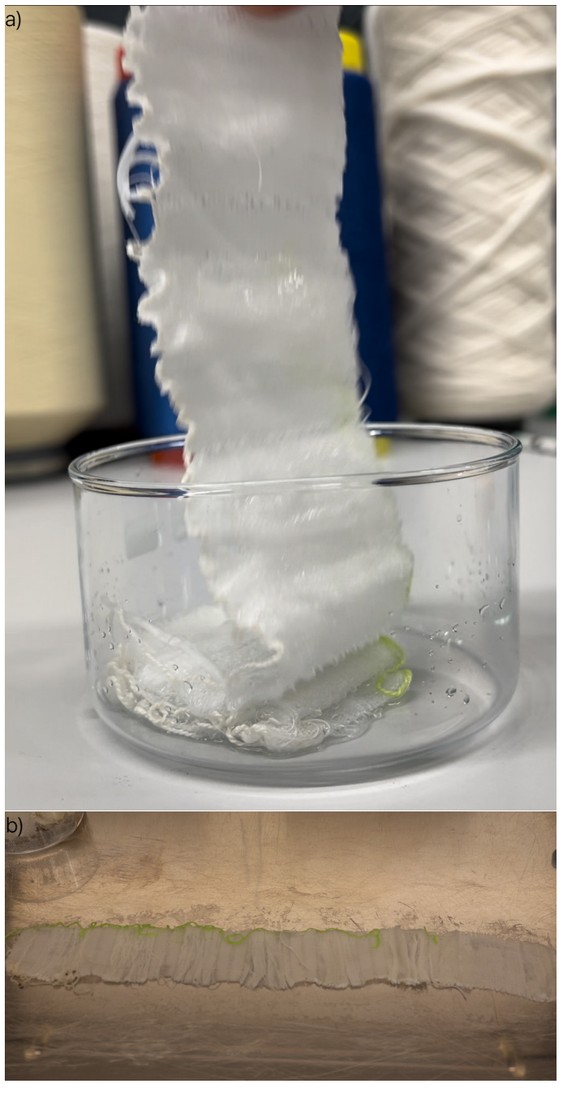

Figure 86: a) Textile weak folds; b) flat textile.

4.2. Prototype 2 and 3 - Origami with Hemp and PVA

After assessing the challenges encountered in Prototype 1, it became clear that forming origami structures with hydrogels presents unique complexities compared to conventional materials. To address this issue, an additional variable was introduced in the weaving process. While Prototype 1 followed a structured sequence of four passes of PVA followed by one pass of cotton, the new prototype replaced cotton with hemp paper yarn following the same structure. Hemp, a fast-growing bast fiber plant from the Cannabis family, is widely cultivated for its fibers and seeds (Barbash et al., 2022). It contains nanocellulose, a biodegradable material renowned for its exceptional mechanical strength, lightweight nature, and high chemical resistance (Barbash et al., 2022). Since both hemp and cotton are composed of cellulose, hemp could offer similar benefits to cotton in supporting microalgal attachment while providing superior mechanical stability. However, its effectiveness in supporting microalgal attachment remains unexplored. In this study, hemp was incorporated exclusively to reinforce the textile's folds, enhancing structural integrity and creating a more stable accordion-like form while preserving the hydrogel's biological functionality. Future research should investigate its interaction with microalgae to determine its full potential in living textile applications.

4.2.1. Textile Materials

- Warp prototype 2: Paper yarn;
- Warp prototype 3: Paper yarn - 100% Manila hemp; Solvron SF.330 (Dissolvable 55c+ Yarn) 330x3 d tex - Count: 1/10 Nm;
- ADACAD software;
- Jacquard loom TC2;
- Boat shuttle;
- Bobbin;
- Scissors.

4.2.2. Textile Method

During this experiment, two textile have been realized with two different type of Hemp - Paper yarn and Paper yarn - 100% Manila hemp - following the same weaving structure and technique utilized for Prototype 1 and experimental procedure remain consistent with Prototype 1 (Figure 87).

4.2.3. Experiment Materials

- Woven textile;
- A stainless steel tray;
- Water.

4.2.4. Method

The experimental procedure is the same used in paragraph 4.1.4.

Figure 87: Prototype 2 and 3 - Textile structure .

4.2.5. Conclusion

As observed in Figure 88, both Prototype 2 and Prototype 3 successfully maintain their mountain folds, while the valley folds struggle to hold their shape. This is likely due to the textile being placed on a surface rather than hanging freely. Although further investigation is needed to optimize the materials and structural composition, the textile demonstrates the ability to retain its shape, paving the way for the application of origami principles in hydrogel-based systems.

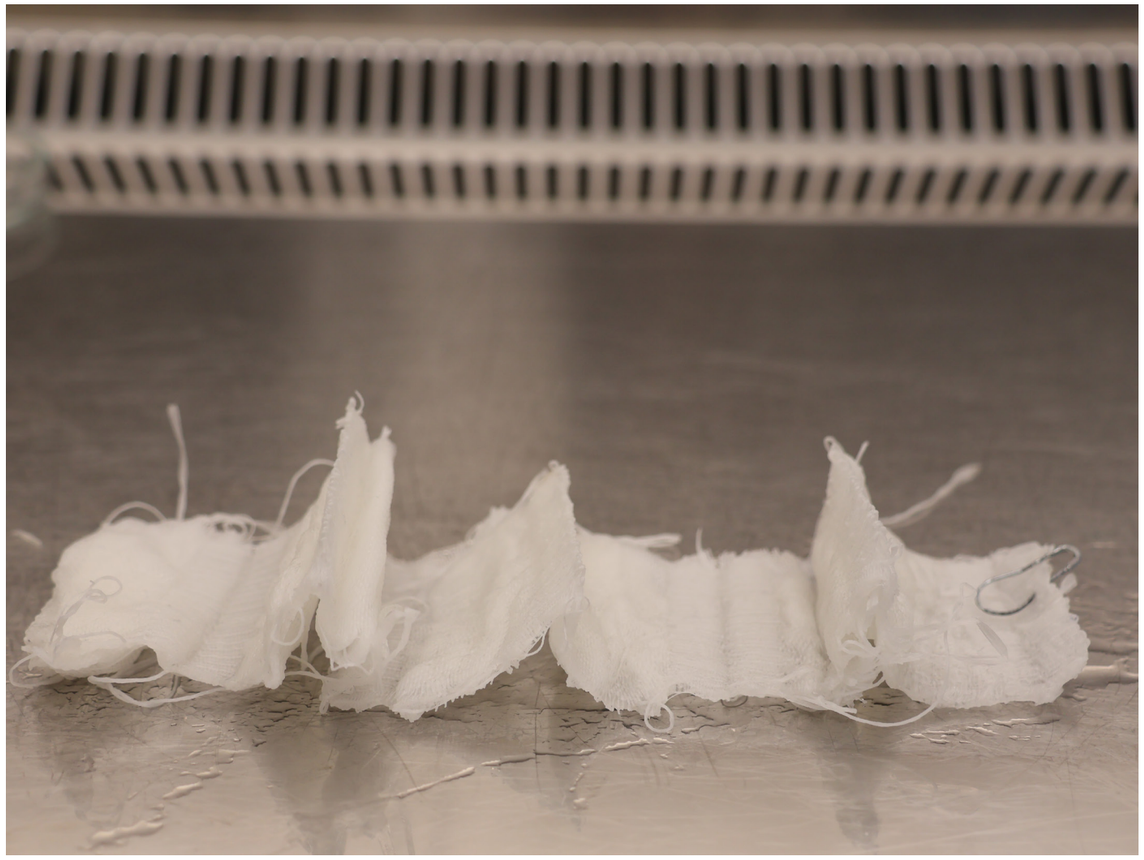

Figure 88: Prototype 2 made with Paper yarn

Figure 89: Prototype 3 made with Paper yarn - 100% Manila hemp.

Chapter 5
Creating Materials Experience Vision

This chapter delves into the third step of the methodology, where the vision is articulated, the concept is refined, and its potential application environments are analyzed. It defines the overarching framework that guides the development process, ensuring alignment between the textile's functionality and its intended real-world applications.

5.1. Vision

After six experimental iterations, the final living textile design was established, featuring a three-layer plain weave structure reinforced by a compound twill-reverse twill at the edges for cohesion. To enable origami folding, two long float sections, the "mountain fold" and "valley fold", were incorporated (Prototype 2 and 3). Once woven, the textile is immersed in liquid medium and subjected to a single Freeze-Thaw (F-T) cycle, a crucial step that enhances microalgal immobilization and hydrogel stability.

TThis living textile is more than a laboratory prototype—it represents a new generation of Engineering Living Materials that potentially can capture CO_2 and release oxygen, and redefines the relationship between architecture, design and biology. The living textile is designed for both indoor and outdoor applications, introducing an alternative to conventional cultivation systems already present on the market. A key strength of this textile lies in its ability to bridge the gap between two cultivation systems: open ponds and photobioreactors (PBRs), addressing their inherent limitations. Open ponds, though cost-effective and energy-free, suffer from excessive water consumption, contamination risks, and environmental instability (Encarnação et al., 2023; Abdur Razzak et al., 2024). Conversely, PBRs provide control and efficiency but demand high energy inputs and significant infrastructure costs (Encarnação et al., 2023). The living textile merges the strengths of both approaches while eliminating their limitations, offering a promising scalable, low-energy, and self-sustaining system that minimizes water use compared to open ponds without the high operational demands of PBRs.

Beyond its functional role, the living textile introduces a transformative approach to environmental integration. Its ability to regulate hydration through passive water retention ensures long-term viability without constant external inputs. Additionally, its structural flexibility enables dynamic adaptation, transforming it into a living interface between architecture and nature. By seamlessly merging biological performance with design, this textile introduces a new model in sustainable innovation, redefining the importance of material properties in influencing ecosystems.

5.2. Mechanism

To enable controlled movement and adaptability, the living textile will be integrated into a system that ensures stability and functionality while prioritizing sustainability. The structure is made from bamboo, a rapidly renewable resource that grows faster than any other plant (Weeden, 2025), reinforcing the project's commitment to environmentally responsible design.
At the top of the frame, a series of sliders - attached to a rail - guides the textile's upper and lower edge (Figure 90). This system allow the textile to move from left to right and viceversa, and prevents unwanted twisting or wrinkling. This controlled mobility not only preserves the textile's structural integrity but also enhances the biological performance of the microalgae housed within it. Since microalgae release oxygen during the day and CO_2 at night, regulating the textile's position in response to light cycles optimizes their efficiency. By fully extending during daylight, the system maximizes photosynthetic activity, while partially retracting at night supports metabolic recovery.

To further support biological stability, the system integrates a passive hydration mechanism. Embedded in the top section of the frame, a container holds BG11 medium, ensuring a consistent moisture supply. A humidity sensor within the textile continuously monitors hydration levels, detecting when the textile begins to dry out. When a critical threshold is reached, the sensor

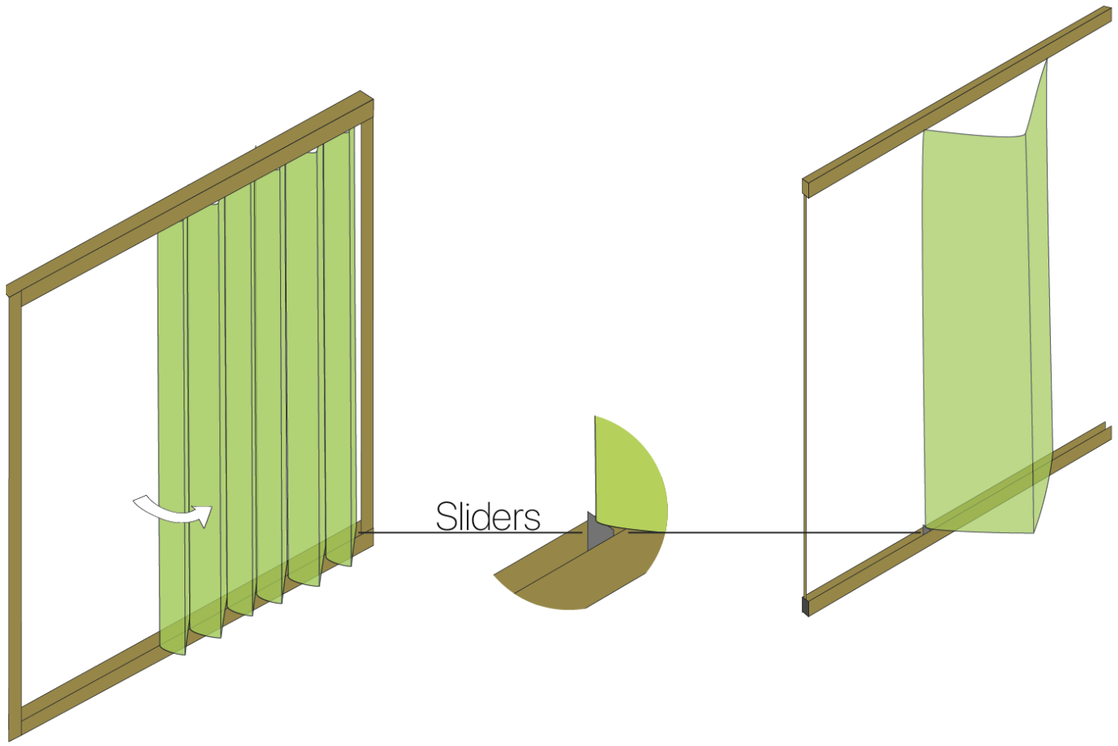

Figure 90: Living textile sliding system.

5.3 Conceptual Applications

5.3.1. Concept 1 - Adaptive Living Textile Shading System

This concept envisions the integration of the living textile into an adaptive shading system for buildings, offering both climatic protection and air purification (Figure 91). The textile is installed as a dynamic façade element, designed to regulate sunlight exposure, reduce indoor overheating, and simultaneously improve air quality by potentially capturing CO_2 and releasing oxygen.

The system operates using sliders, allowing the textile to expand, retract, or fold based on environmental conditions. In sunny conditions, the textile extends to provide shade, reducing solar heat gain and lowering indoor temperatures, thus improving thermal comfort and reducing the need for artificial cooling. During this time, when the textile is more exposed to high temperatures and prone to drying, a humidity sensor-controlled hydration system ensures that the embedded microalgae receive adequate moisture for continuous biological activity. In windy or rainy conditions, the textile can retract to prevent mechanical stress and excessive moisture exposure, increasing its durability (Figure 92).

Beyond its shading function, this system actively contributes to air purification. This makes it particularly beneficial in dense urban settings, where air quality and overheating are persistent challenges.

Figure 91: Shading system.

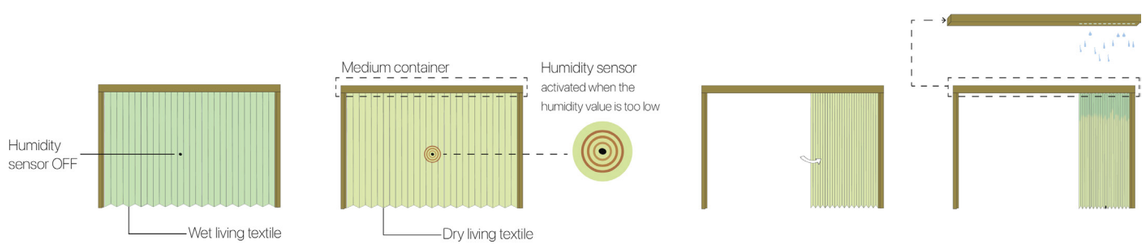

Figure 92: Storyboard of concept 1. Visual explanation of how the living textile react in drought conditions.

5.3.2. Concept 2 - Bio-Bus stop

This concept envisions a bus stop integrated with a living textile shading system, designed to provide climatic protection, improved air quality, and thermal comfort (Figure 93). With global warming causing extreme summer temperatures, waiting for public transport in direct sunlight can become unbearable, particularly for the elderly. This bio-integrated bus stop aims to regulate humidity, reducing heat stress while simultaneously enhancing air quality through microalgal photosynthesis.

The structure combines a fixed bamboo ceiling with dynamic living textile panels, each serving a distinct function. The bamboo roof shields passengers from rain and harsh winter conditions, ensuring year-round usability. Meanwhile, the living textile panels, suspended from sliders, provide adjustable shading, expanding to block excessive sunlight and heat during summer while retracting when not needed (Figure 94).

During hot and dry conditions, when the textile is most vulnerable to dehydration, an integrated humidity sensor-controlled hydration system ensures that the microalgae remain viable. When moisture levels drop, the sensor triggers a controlled release of BG11 medium from a container embedded in the frame (Figure 95).
The response of the textile to this hydration process differs based on its position within the structure. For the vertical panels, the textile remains fully extended even when dry, allowing the rehydration process to take place without affecting its shading function. The textile is rehydrated while at its maximum extension, ensuring continuous microalgal activity and air purification without disrupting the shading effect. In contrast, for the horizontal panels on the ceiling, the textile must temporarily close during rehydration to prevent water leakage. Once adequately hydrated, it reopens to restore its shading function while maintaining biological activity (Figure 96).

Through its ability to regulate shading, hydration, and air purification, the system helps public transport hubs become more resilient to extreme weather conditions while improving the overall well-being of users.

Figure 93: Bio-integrated bus stop.

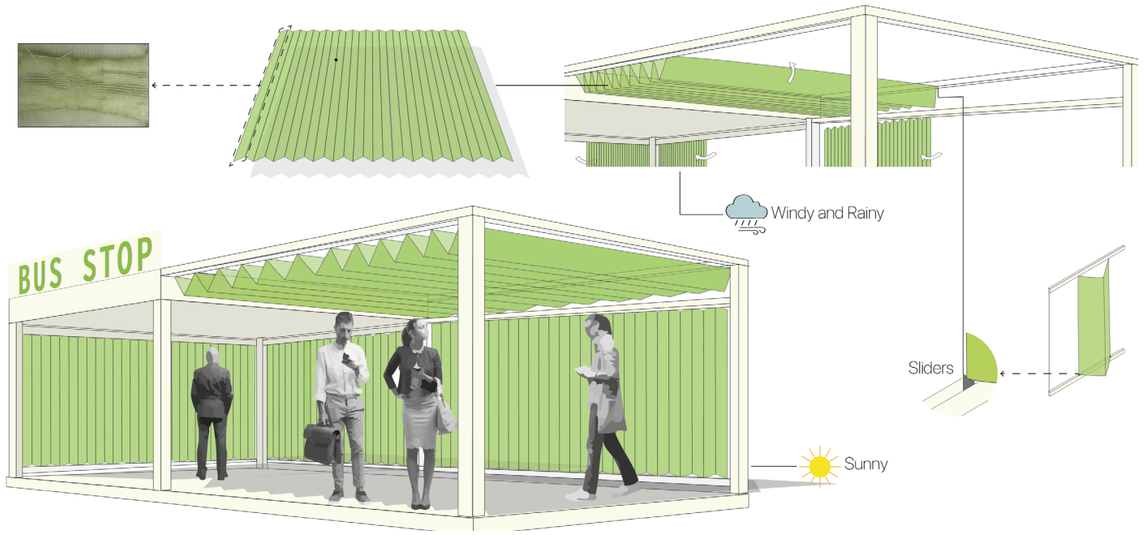

Figure 94: Visual explanation of how the living textile work in sunny and rainy conditions.

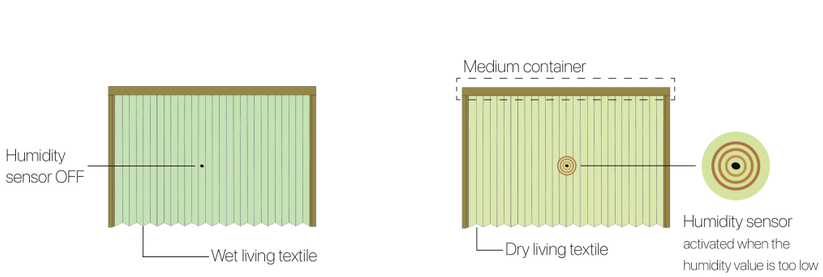

Figure 95: Mechanism of Rehydration in Vertical Living Textiles.

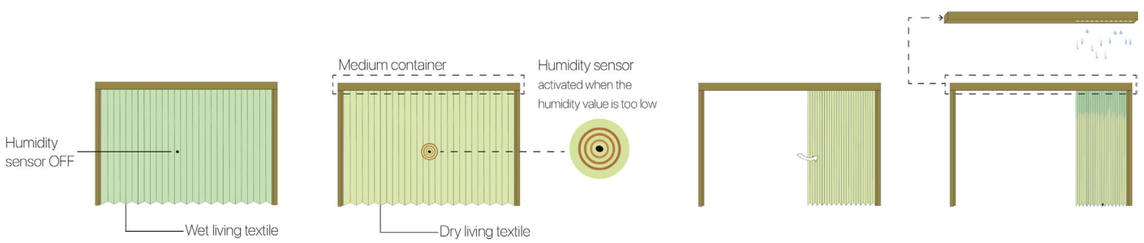

Figure 95: Mechanism of Rehydration in Horizontal Living Textiles.

5.3.3. Concept 3 - Living Climate Panels

This concept introduces living textile panels as modular dividers in open-space offices, providing a dynamic solution for workspace flexibility, air quality improvement, and humidity regulation (Figure 97). While open office layouts encourage interaction, they often lack adaptability for focused work. These panels create adjustable partitions that allow employees to reconfigure their environment, offering both privacy and collaboration spaces as needed.

The sliders enables effortless expansion, retraction, or repositioning of the panels, ensuring that workspaces can be modified throughout the day. Unlike rigid partitions, these dividers offer fluid adaptability, allowing teams to shape their workspace based on tasks and preferences.

Beyond their spatial function, the panels actively contribute to a healthier indoor environment. Office spaces, especially in winter, often suffer from excessively dry air due to heating systems, leading to discomfort. To address this, the living textile integrates a humidity sensor-controlled hydration system, which detects when moisture levels drop and releases small, controlled amounts of BG11 medium (Figure 98). This ensures that the textile maintains an optimal level of hydration, helping to regulate indoor humidity naturally.

Additionally, the CO_2-absorbing microalgae embedded within the textile enhance air quality by capturing CO_2 and releasing oxygen. This feature is particularly valuable in enclosed office spaces, where stagnant air can create a feeling of heaviness. By introducing a fresh and oxygen-rich atmosphere, the panels contribute to a more comfortable and invigorating workspace.
Additionally, the aesthetic appeal of these bio-integrated panels brings a natural, biophilic element into office spaces, promoting a sense of well-being. Unlike static walls, these adaptive dividers offer both flexibility and function, redefining how workspaces can dynamically support both collaboration and focus while integrating higher air quality.

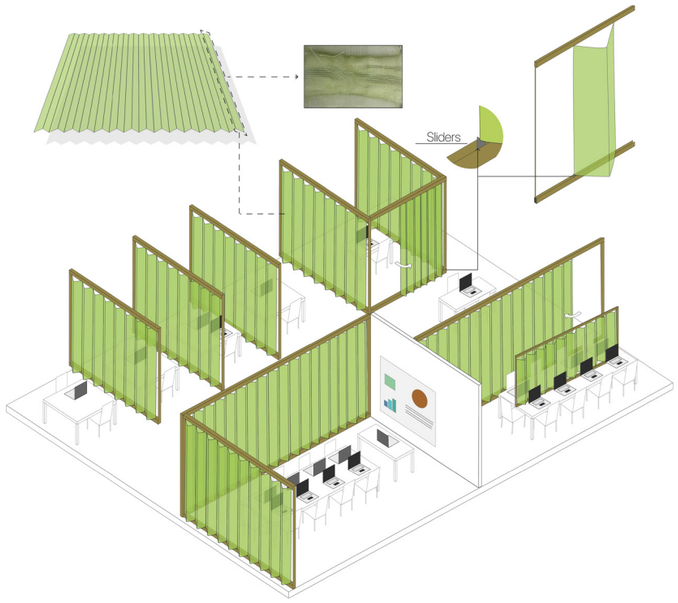

Figure 97: Living climate Panels.

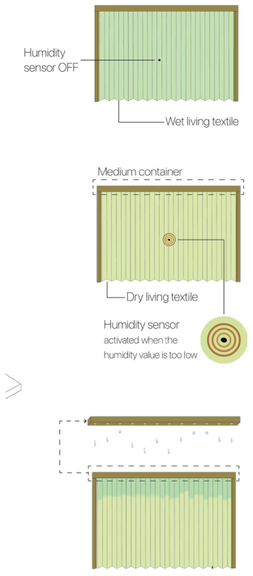

Figure 98: Rehydration system

5.4 Comparative Discussion of Concepts

Each of the three concepts presents a different approach to integrating the living textile into urban and architectural environments, offering both functional and environmental benefits. The adaptive shading system for buildings stands out as a highly scalable and impactful solution, addressing both urban overheating and air quality deterioration. The system has the potential to reduce energy consumption by providing effective solar shading, which minimizes heat gain and lowers artificial cooling demands. Additionally, the living textile's ability to regulate its own humidity helps maintain a stable microclimate around the panel, potentially contributing to improved environmental conditions within the building. However, while its environmental impact is significant, its feasibility for widespread implementation requires further refinement, particularly in terms of integration with existing building structures, long-term durability in harsh weather conditions. Structural modifications and urban planning constraints could also limit its adaptability. The bus stop concept provides a critical intervention in public spaces where extreme temperatures disproportionately affect the population. By incorporating both fixed and dynamic shading elements, it creates an environment that passively improves comfort and air quality. However, its exposure to high-traffic urban environments raises questions about durability, vandalism resistance, and long-term maintenance. The living climate panels for office spaces leverage the textile's ability to regulate air quality and humidity while providing functional workspace separation. This concept offers a high degree of flexibility and modularity, allowing employees to reconfigure their environment based on immediate needs, an increasingly valuable feature nowadays. Unlike the other two concepts, its installation poses fewer structural challenges, making it easier to implement in a variety of indoor settings, but its environmental impact is localized. However, Its effectiveness would be most substantial in employee daily life.

Chapter 6
Creating Material/ Product Concepts

This chapter delves into the final step of the methodology, where the final product is explored, demonstrating how the living textile can be utilized for microalgae cultivation while maintaining the textile under semi-controlled conditions. It examines the integration of the textile into functional systems, ensuring growth, stability, and usability for practical implementation.

6.1. Final iteration

The final design is based on Concept 3 – Living Climate Panels. This choice was driven by the fact that the other two concepts, Adaptive Living Textile Shading System and Bio-Bus Stop, are primarily designed for outdoor environments, where the textiles would be exposed to various external risks. By selecting Living Climate Panels, we ensure a more controlled setting for implementation, allowing for optimization and testing of the living textiles. Once further developments are made, the integration of these textiles into outdoor applications can be revisited to maximize their potential (Figure 99). The Living Climate Panels Concept has been further refined to accommodate the essential conditions required for the survival and optimal functionality of microalgae in an office environment. As previously discussed in Chapter 5, these panels are designed to be highly versatile, contributing not only to a more natural and aesthetically pleasing atmosphere—aligning with biophilic design principles—but also actively improving air quality through the photosynthetic activity of microalgae.

This chapter focuses on the latest technical improvements made to the Living Climate Panels, addressing key functional aspects such as the draining system, energy efficiency, and integration with office spaces to enhance both performance and usability.

Figure 99: Living Climate Panel integration into open-space offices.

6.1.1. Drayining System

A key challenge in the development of the Living Climate Panels has been the draining system, which must ensure that the nutrient medium is directed precisely onto the textile without unwanted leakage while also adapting to the opening and closing mechanism of the textile structure. To address this, a novel sliding system has been introduced, integrating a capillary function through a central hole. These sliders move along a rail ensuring that the liquid flow remains well-regulated. One end of each slider is connected to the medium container's outlet holes, while the other is seamlessly integrated into the triple-layer textile structure, allowing a consistent and controlled release of the BG-11 medium when necessary (Figure 100).

As explained in the Mechanism section, when the textile loses most of its retained moisture and begins to dry, a sensor detects the low humidity level and triggers the container to release the medium. The liquid descends in a controlled manner, forming small droplets instead of a continuous stream. This regulated flow is achieved through the precise size of the openings, which restrict the passage of liquid, allowing it to accumulate and be gradually released. The surface tension of the liquid, combined with the small diameter of the openings, prevents uncontrolled outpouring, ensuring a steady and measured release. This mechanism not only maintains the hydration of the living textile but also helps to enhance indoor humidity levels, contributing to a more comfortable office environment. Moreover, since the textile can be open and closed, based on the users necessity, it is not always said that the Capillar Sliders will perfectly end with the container's holes. To ensure precise alignment between the Capillary Sliders and the container's holes, the rail system has been designed with two stopping grooves positioned at the ends of the rail (Figure 101). These grooves define the maximum opening position of the textile, ensuring that when the textile reaches its fully extended state, the sliders naturally settle into the grooves. This mechanical guidance guarantees that the sliders are perfectly aligned with the holes of the container, allowing an accurate and controlled release of the medium onto the textile. By integrating the stopping grooves, the system passively corrects any potential misalignment, ensuring reliable performance without the need for additional adjustments.

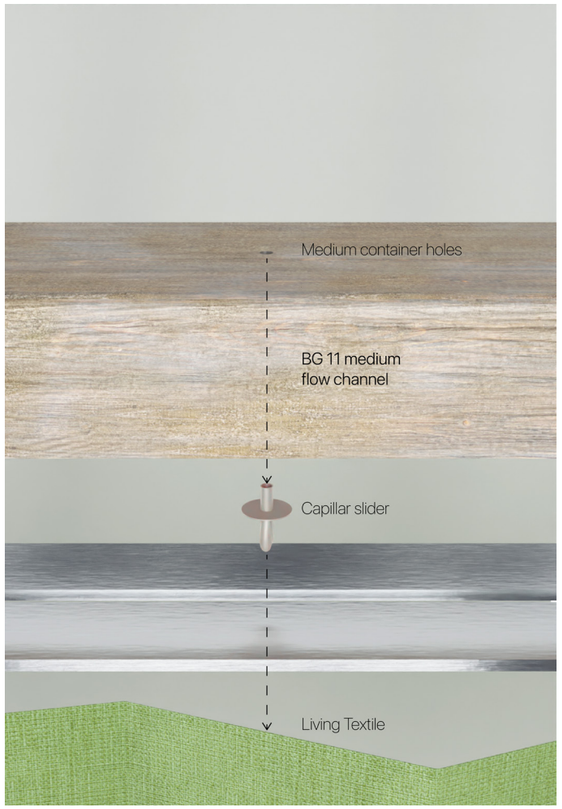

Figure 100: Flow channel where the BG 11 medium passes through to nurture and moisture the living textile.

Figure 101: Textile locking system.

6.1.2. Integration with Office Spaces

The Living Climate Panel is designed to offer maximum flexibility and adaptability, ensuring that workspaces can be easily adjusted to suit different needs. Equipped with a small wheel system, the panels can be effortlessly repositioned, allowing employees to modify their workspace configuration as required. These panels can be arranged to create distinct zones, whether for individual deep-focus work, collaborative group tasks, or formal meetings, enabling a dynamic and reconfigurable office environment (Figure 102).

One of the key advantages of this system is that it allows seamless movement within the office without the need to reposition the entire panel. Instead of shifting the structure itself, users can simply slide the textile open using a bamboo handle, creating an intuitive and user-friendly passageway. This design ensures uninterrupted spatial fluidity, preserving the intended division of space while allowing for natural transitions between different work areas. The combination of modularity, ease of use, and bio-integrated aesthetics makes the Living Climate Panels a versatile and functional addition to any indoor setting.

Figure 102: How the Living Textile structures the space.

Figure 103: The handle is attached to the living textile, ensuring no direct contact with the living system.

6.1.3. Energy Efficiency

As the textiles slide along the rails and the panels are repositioned based on user needs, small dynamos or kinetic energy harvesters can be implemented to capture the mechanical motion and transform it into a usable power source, preventing energy from being lost. The generated electricity can then be stored in small capacitors, which supply power to the sensors and drainage control system, ensuring automated operation without the need for an external power supply (Sleppy, 2021).

The feasibility of this energy recovery approach is supported by research on piezoelectric generators in automatic sliding doors, which demonstrated that motion-based energy harvesting can generate approximately 60.41 joules of energy, equating to 80.52 watts of power over a 120-minute daily usage period (Trans Tech Publications Ltd, Switzerland, n.d.). This study highlights the potential of harnessing mechanical motion as an efficient and sustainable solution for powering low-energy devices, aligning with the self-sustaining design of the Living Climate Panels.

6.1.4. Conclusion

The Living Climate Panels have been carefully designed to address both functional and environmental challenges, offering a versatile and sustainable solution for indoor spaces. While not necessarily the final product, this system provides a controlled environment that ensures microalgae survival without the instability of open systems or the high energy demands of fully enclosed technologies. By regulating humidity, nutrient distribution, and textile hydration, it maintains optimal conditions without requiring a resource-intensive infrastructure.

A key innovation is the drainage system, featuring capillary sliders and stopping grooves to ensure precise nutrient delivery while preventing waste. Additionally, the integration of a kinetic energy harvesting system eliminates dependence on external power sources, making it a self-sustaining, low-maintenance solution. The ability to customize spatial configurations through mobile panels further enhances its flexibility as a bio-integrated architectural concept. Rather than being a fixed final design, this system represents an adaptive and scalable approach that can be further optimized and refined. Future developments will focus on improving efficiency, scalability, and long-term performance, while also exploring how similar controlled and low-energy approaches can be applied in broader contexts beyond the office environment. This implementation serves as a step forward in demonstrating how living textiles can be sustained in a controlled and energy-efficient manner, providing a stable alternative to open systems while avoiding the high energy demands of fully enclosed technologies.

Chapter 7
Challenges, Opportunities, and Future Directions in Living Textile Developments

This chapter examines the challenges, opportunities, and future directions in living textile development. It addresses key limitations, such as material durability and contamination risks, while highlighting potential applications in sustainability and bioremediation. Finally, it explores strategies for improving material performance and scalability for real-world use.

7.1. Experimental Nature and Present Limitations

While the living textile presents a promising vision for bio-integrated architecture, it requires further research and refinement before it can be utilized on a larger scale. Several critical factors must be considered to support its lifespan and its functionality, particularly in relation to material durability and contamination risks.
One important critical aspect requiring further investigation is related to the encpasulation of microalgae: where they effectively encapsulated within the hydrogel or merely adhered to its surface? This distinction is crucial, as insufficient encapsulation leaves microalgae vulnerable to external environmental stresses, notably fungal contamination. It is important, however, to recognize that fungal contamination may occur in either scenario, particularly if moisture persists not only within the hydrogel but also on its external surface. Indeed, water activity is widely recognized as the primary factor driving fungal growth (Hallak et al., 2023), highlighting the importance of controlling surface moisture. Preliminary observations suggest that the textile structure itself may offer partial protection against contamination, yet additional research is necessary to confirm whether the current hydrogel formulation effectively encapsulates microalgae and resists fungal proliferation over extended periods. Future studies should also consider adjustments to the hydrogel composition aimed at improving durability and antifungal properties while maintaining its biological functionality.

Additionally, a key limitation remains the hydrogel's durability. *Freezing Living Textiles* experiment demonstrated that PVA degradation occurs rapidly, raising concerns about its longevity in real-world conditions. However, insights from *The Right Combination* experiment suggest that hydrogel stability improves significantly when the spacing between warps increase and when the PVA is not permanently immersed in liquid medium. In these conditions, the hydrogel maintains its structural integrity for over four weeks, with the potential to last even longer. While these adjustments offer a promising path forward, further testing is necessary.

Lastly, even if in *The Right Combination* experiment has been proved that increasing the distance between the warps and not immersing permanently the living textile in liquid medium, the lifespan of PVA improve, still the possibility that PVA will not last more that some months is under the corner. Therefore, careful consideration must be given not only to the further improvement of the hydrogel, but also to the end-of-life strategy for this material. While the hydrogel's biodegradable nature could be an advantage, its degradation timeline must be carefully managed to prevent environmental pollution. A dismissal program will be necessary to ensure that the textile can be safely deconstructed and repurposed once it reaches the end of its functional life. Paragraph 7.2. will introduce this aspect in detail, proposing a strategy that mitigates waste and maximizes resource recovery.

Addressing these challenges through ongoing material optimization and lifecycle planning will be essential in transitioning the living textile from an experimental concept to a scalable architectural solution.

7.2. Future Directions

Even though significant advancements have been made in this project, there are still many areas for improvement. A key priority is to demonstrate that hemp—referenced in Section 4.2—offers the same beneficial effects on *Scenedesmus* sp. as cotton. To validate this, it is essential to replicate the experiment using the new yarn. Then, it is necessary to make sure that the encapsulation is successful, which must be addressed before considering large-scale implementation. The first step in refining the system would be to replicate the experiment under controlled conditions to validate the results and assess its long-term stability. Once a stable system is achieved, the textile should be tested in semi-controlled indoor environments before transitioning to outdoor conditions, ensuring that its performance is systematically evaluated against external environmental factors.

If the encapsulation still remains an issue, modifications to the woven structure may be necessary to create a more protective environment for microalgae. One potential improvement is designing a fully enclosed textile system, where all textile edges are reinforced with a compound twill-reverse twill structure to limit external exposure (Figure 104). Additionally, in the triple-layer structure, a tabby weave (100% Co) for the central layer could be combined with twill-woven outer layers (90% PVA, 10% Co). This configuration would facilitate the pipetting of microalgae while offering greater protection against contaminants. Following these modifications, further indoor testing would be required before evaluating the material's performance in outdoor settings.

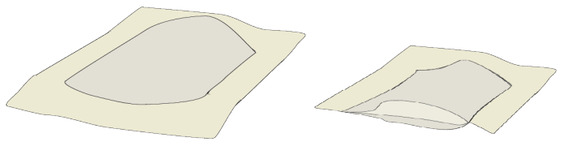

Figure 104: Fully enclosed textile system, where all textile edges are reinforced with a compound. On the right its section.

Another critical aspect is the susceptibility of the hydrogel itself to fungal contamination. As already mentioned in the paragraph above, constant exposure to moisture may promote microbial growth, potentially limiting its long-term viability. If this proves to be a recurring challenge, an alternative solution could involve membrane-based technologies to regulate gas exchange while acting as a protective barrier. Gas separation membranes have been widely studied for their ability to selectively control gas permeation (Chen et al., 2021). In particular, functional polymeric membranes are known for their customizable gas transport properties and energy-efficient separation capabilities (Animesh Jana et al., 2024). These membranes have already been successfully implemented in CO_2 separation applications, demonstrating both their scalability and practicality (Animesh Jana et al., 2024). Integrating a selective gas-permeable membrane into the living textile system could provide encapsulation and an effective balance between CO_2 uptake and O_2 release, while simultaneously reducing the risk of contamination. By incorporating this technology, the system would become more resilient and sustainable, offering a viable alternative to traditional cultivation methods.

Once the living textile demonstrates resistance to fungal contamination, the next stage of development should focus on adapting the system for urban environments. The objective is not only to optimize the cultivation system for cities but also to enhance air quality and provide shaded areas, particularly in regions where temperatures exceed 50°C. A promising inspiration for this application is Curtyard, a foldable umbrella structure developed by SL Rasch GmbH Special and Lightweight Structures (Courtyard | SL Rasch, n.d.). Implementing foldable umbrellas incorporating living textiles would introduce an innovative approach to urban sustainability, contributing to citizen well-being while mitigating the effects of extreme heat (Figure 105). If this concept proves feasible, further exploration of origami with diagonal folding techniques (for example, origami herringbone tessellation) would be necessary to ensure that the umbrellas open and close in the most functional way (Figure 106). These folding mechanisms would allow for optimal spatial efficiency while maintaining the textile's biological integrity, paving the way for a dynamic and adaptive bio-integrated shading system for urban spaces.

Another way to integrate living textiles into urban environments is through permanent installations, similar to KnitNervi, a pavilion-scale demonstrator designed by Mariana Popescu. This project showcased a flexible formwork system for constructing ribbed concrete shells (Mpopescu & Mpopescu, 2023). But what if this concept evolved beyond a demonstrator? Imagine a new kind of pavilion, made entirely from living textile. These dynamic structures could be placed near bus stops, in parks, or city squares, transforming urban spaces into self-sustaining, air-purifying environments (Figure 107). By merging architecture and biology, these installations could redefine how cities interact with nature, offering shade, improving air quality, and fostering new ways for people to engage with their surroundings.

Figure 105: Conceptual visualization of living textile-integrated foldable umbrellas for urban environments. The original umbrella structure, designed by SL Rasch GmbH Special and Lightweight Structures, has been digitally modified to illustrate the potential integration of living textiles in shading systems. By replacing conventional materials with bioactive textiles, these structures could enhance air quality and provide climate-responsive shading solutions in regions experiencing extreme heat. Original structure by SL Rasch GmbH (Courtyard | SL Rasch, n.d.). Image digitally modified for conceptual representation.

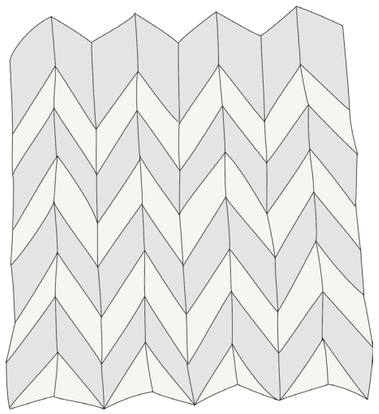

Figure 106: Origami herringbone tessellation

Figure 107: Conceptual visualization of a living textile pavilion. The original pavilion, designed by Mariana Popescu, was adapted in this image to illustrate how living textiles could replace conventional materials, integrating biological functionality into architectural structures. The original pavilion structure remains unchanged, but the surfaces have been modified to represent a bio-integrated textile system. Original pavilion design by Mariana Popescu (Mpopescu & Mpopescu, 2023). Image digitally modified for conceptual purposes.

To ensure that living textiles remain circular and continue serving new functions beyond their initial use, further research on adaptive material design is needed. This concept aligns with Multimorphic Textile-Forms, which promote textiles capable of evolving through design, production, and use, thereby extending their lifecycle and minimizing waste (McQuillan & Karana, 2023).

A key aspect of this strategy is allowing the natural degradation of PVA, which occurs rapidly, facilitating the separation of microalgal biomass from the cotton fibers without compromising the remaining textile structure. Once separated, the *Scenedesmus* sp. biomass can be preserved through indirect solar drying, a low-energy method that maintains its functionality while reducing energy consumption (Schmid et al., 2022). Once dried, the biomass offers several key repurposing pathways. First, it can be converted into biodiesel, utilizing its neutral lipids for renewable energy production (Narasimman Kalaiselvan et al., 2024). Second, the tried biomass of *Scenedesmus* sp. can also be used for bioplastic production, as it has been shown to synthesize polyhydroxyalkanoates (PHA) at 29% w/w under phosphorus-limiting conditions (Arul, 2024; Adetunji & Erasmus, 2024). Another option is also using dried biomass of *Scenedesmus* sp. for wastewater treatment, as it has been shown to effectively break down textile dyes, removing up to 97% of certain dyes at specific concentrations (Yirgu et al., 2020; Selvan et al., 2022). This makes it a promising option for cleaning dye-contaminated water. Meanwhile, the remaining cotton fibers, as a natural material, should be mechanically recycled to prevent textile waste and reduce dependence on virgin fiber production (Russell, 2023). This process involves cutting, shredding, and carding the fibers for reuse in new yarns, non-woven materials, industrial rags, carpets, or insulation panels, thereby limiting landfill accumulation (Abrishami et al., 2024). If the fibers become too degraded for textile applications, they can still be compressed into soundproofing and insulation materials for industrial and construction use (Abrishami et al., 2024). This aligns with the growing need to rethink textile recycling strategies, ensuring that cotton fibers can be efficiently reintegrated into circular material cycles rather than being discarded. By addressing fungal contamination, structural resilience, urban applications, and circularity, future research can unlock new possibilities for living textiles, ensuring they become a scalable, adaptable, and truly sustainable material for the built environment.

7.3. Conclusion

This research has demonstrated the feasibility of integrating microalgae into 3D woven textiles through a hydrogel-based immobilization system, utilizing the freeze-thaw (F-T) process. The findings highlight the potential of this approach to support microalgal viability, potentially enabling CO_2 capture and O_2 release, while maintaining a structurally stable living textile. By merging textile engineering with biological systems, this study lays the foundation for future advancements in bio-integrated materials, opening new possibilities for sustainable design and environmental applications.
Several key discoveries emerged from this research. One of the most significant findings was that hydrogel stability and microalgal attachment were greatly enhanced when PVA was not permanently immersed in liquid medium and the distance between the warp was increased, allowing for an extended lifespan of the living textile. Additionally, the study provided new insights into microalgae recovery following freezing at subzero temperatures, revealing that three weeks were required for full restoration of photosynthetic activity. Furthermore, the research underscored the critical role of textile structure in microalgal attachment and viability. Fiber composition, porosity, and weave pattern were shown to significantly influence microalgae stability, reinforcing the importance of material selection and textile architecture in developing bio-integrated systems. These findings contribute to a deeper understanding of how living textiles can be designed making them a promising tool for sustainable urban applications, air quality improvement, and climate-responsive design.While this study marks a significant step forward, it also highlights areas for further exploration, particularly in enhancing material resilience, optimizing CO_2 capture efficiency, and large-scale implementation strategies. The successful integration of living textiles into real-world applications will require continued interdisciplinary research, bridging textile engineering, microbiology, and sustainable design.

Ultimately, this research serves as a proof of concept, demonstrating that microalgae-based living textiles are not just a theoretical innovation but a tangible step toward bio-responsive materials. As we move toward more sustainable material solutions, these textiles could play a crucial role in reshaping how we interact with our built environment, fostering a future where design and biology seamlessly coexist to support environmental well-being.

7.4. Self-Reflection

When I decided to apply to this faculty, I felt somewhat disoriented. My primary goal was to improve my English and immerse myself in a country where sustainability is deeply embedded in everyday life. My ambition to work on sustainable products never hesitated. Indeed, even during my application process, when asked to propose a possible Master's thesis topic, I developed the idea of designing a wearable gadget capable of capturing CO_2—despite having no clear understanding of how to turn such a complex vision into reality. Two years later, that initial ambition materialized into something tangible: my thesis on a living textile capable of capturing CO_2 and releasing oxygen. This opportunity arose from my participation in the course Fundamentals of Biodesign, where I had the chance to meet my current thesis chair. The journey, however, has been anything but easy. Working on a research-intensive thesis like this has presented numerous challenges, pushing me to develop essential skills such as time management, determination, patience, consistency, charisma, and precision. At times, it was difficult, but each challenge strengthened my ability to adapt and persist. Some skills came more naturally than others, but I never lost sight of my goal. Thanks to the guidance and support of my chair and mentor, I was able to navigate these 20 weeks of research. Now, as I conclude this journey, I can confidently say that I have successfully developed a functional living textile prototype, demonstrating its potential applicability in sustainable material innovation.

8. Bibliography

Salolainen, M. (2022). Interwoven: Exploring Materials and Structures. (Aalto University publication series ART + DESIGN + ARCHITECTURE; Vol. 2022, No. 1). Aalto ARTS Books.

Shenton, J. (2014). Woven Textile Design. Laurence King Publishing.

9. References

Abbass, K., Qasim, M. Z., Song, H., Murshed, M., Mahmood, H., & Younis, I. (2022). A review of the global climate change impacts, adaptation, and sustainable mitigation measures. Environmental Science and Pollution Research, 29(28), 42539–42559. https://doi.org/10.1007/s11356-022-19718-6

Abdul Hai Alami, Shamma Alasad, Mennatalah Ali, Maitha Alshamsi, (2021). Investigating algae for CO2 capture and accumulation and simultaneous production of biomass for biodiesel production. Science of The Total Environment, Volume 759, 143529, ISSN 0048-9697. https://doi.org/10.1016/j.scitotenv.2020.143529.

Abid, N., Ceci, F., & Ikram, M. (2021). Green growth and sustainable development: dynamic linkage between technological innovation, ISO 14001, and environmental challenges. Environmental Science and Pollution Research, 29(17), 25428–25447. https://doi.org/10.1007/s11356-021-17518-y

Abrishami S, Shirali A, Sharples N, Kartal GE, Macintyre L, Doustdar O. Textile Recycling and Recovery: An Eco-friendly Perspective on Textile and Garment Industries Challenges. Textile Research Journal. 2024;94(23-24):2815-2834. doi:10.1177/00405175241247806

Adetunji, A., & Erasmus, M. (2024). Green Synthesis of Bioplastics from Microalgae: A State-of-the-Art Review. Polymers, 16(10), 1322. https://doi.org/10.3390/polym16101322

agar. (2025). In Merriam-Webster Dictionary. https://www.merriam-webster.com/dictionary/agar

Aisyah, H. A., Paridah, M. T., Sapuan, S. M., Ilyas, R. A., Khalina, A., Nurazzi, N. M., Lee, S. H., & Lee, C. H. (2021). A Comprehensive Review on Advanced Sustainable Woven Natural Fibre Polymer Composites. Polymers, 13(3), 471. https://doi.org/10.3390/polym13030471

Ambika, Pradeep Pratap Singh, A. (2021). 11 - Natural polymer-based hydrogels for adsorption applications. In Natural Polymers-Based Green Adsorbents for Water Treatment (pp. 267-306). https://doi.org/10.1016/B978-0-12-820541-9.00008-9.

An, B., Wang, Y., Huang, Y., Wang, X., Liu, Y., Xun, D., Church, G. M., Dai, Z., Yi, X., Tang, T., & Zhong, C. (2022). Engineered living materials for sustainability. Chemical Reviews, 123(5), 2349–2419. https://doi.org/10.1021/acs.chemrev.2c00512

Anderson TR, Hawkins E, Jones PD (2016). CO2, the greenhouse effect and global warming: from the pioneering work of Arrhenius and Callendar to today's Earth System Models. Endeavour 40(3):178–187. https://doi.org/10.1016/j.endeavour.2016.07.002

Anila Satish, Sheela Sobana Rani, Saranya B, (2017). Fabric Texture Analysis and Weave Pattern Recognition by Intelligent Processing. https://www.researchgate.net/publication/319328133_Fabric_Texture_Analysis_and_Weave_Pattern_Recognition_by_Intelligent_Processing.

Animesh Jana, Akshay Modi,(2024). Recent progress on functional polymeric membranes for CO2 separation from flue gases: A review, Carbon Capture Science & Technology, Volume 11, 100204, ISSN 2772-6568. https://doi.org/10.1016/j.ccst.2024.100204.

Antoni Mateu Vera-Vives, Tim Michelberger, Tomas Morosinotto, Giorgio Perin, (2024). Assessment of photosynthetic activity in dense microalgae cultures using oxygen production. Plant Physiology and Biochemistry, Volume 208, 108510, ISSN 0981-9428. https://doi.org/10.1016/j.plaphy.2024.108510.

Aqdas Noreen, Khalid Mahmood Zia, Mohammad Zuber, Shazia Tabasum, Ameer Fawad Zahoor, (2016). Bio-based polyurethane: An efficient and environment friendly coating systems: A review. Progress in Organic Coatings, Volume 91, Pages 25-32, ISSN 0300-9440. https://doi.org/10.1016/j.porgcoat.2015.11.018.

Arul, S. (2024). Microalgae Scenedesmus SP. SAR1 as a potential source for bioplastic production. www.academia.edu. https://www.academia.edu/126187478/Microalgae_Scenedesmus_Sp_SAR1_as_a_Potential_Source_for_Bioplastic_Production

Ayoub El Idrissi, Badr-eddine Channab, Younes Essamlali, Mohamed Zahouily, Y. (2024). Superabsorbent hydrogels based on natural polysaccharides: Classification, synthesis, physicochemical properties, and agronomic efficacy under abiotic stress conditions: A review. International Journal of Biological Macromolecules. Volume 258, Part 2. https://doi.org/10.1016/j.ijbiomac.2023.128909.

B. Jagannathan, J.H. Golbeck, (2009). Photosynthesis: Microbial. Editor(s): Moselio Schaechter. Encyclopedia of Microbiology (Third Edition). Academic Press. Pages 325-341. ISBN 9780123739445. https://doi.org/10.1016/B978-012373944-5.00352-7.

Balasubramanian, S., Yu, K., Meyer, A. S., Karana, E., & Aubin-Tam, M. (2021). Bioprinting of regenerative photosynthetic living materials. Advanced Functional Materials, 31(31). https://doi.org/10.1002/adfm.202011162

Begum, M. S., & Milašius, R. (2022). Factors of weave estimation and the Effect of weave structure on fabric Properties: a review. Fibers, 10(9), 74. https://doi.org/10.3390/fib10090074

Bernal-Chávez, S. A., Romero-Montero, A., Hernández-Parra, H., Peña-Corona, S. I., Del Prado-Audelo, M. L., Alcalá-Alcalá, S., Cortés, H., Kiyekbayeva, L., Sharifi-Rad, J., & Leyva-Gómez, G. (2023). Enhancing chemical and physical stability of pharmaceuticals using freeze-thaw method: challenges and opportunities for process optimization through quality by design approach. Journal of Biological Engineering, 17(1). https://doi.org/10.1186/s13036-023-00353-9

Bulathsinghala, R. L. (2022). Investigation on material variants and fabrication methods for microstrip textile antennas: A review based on conventional and novel concepts of weaving, knitting and embroidery. Cogent Engineering, 9(1). https://doi.org/10.1080/23311916.2022.2025681

Buso, A., McQuillan, H., Jansen, K., & Karana, E. (n.d.). The unfolding of textileness in animated textiles: An exploration of woven textile-forms. DRS Digital Library. https://dl.designresearchsociety.org/drs-conference-papers/drs2022/researchpapers/208/

Byung Sun Yu, Ha Eun Yang, Ranjna Sirohi, Sang Jun Sim, (2022). Novel effective bioprocess for optimal CO2 fixation via microalgae-based biomineralization under semi-continuous culture. Bioresource Technology, Volume 364, 128063, ISSN 0960-8524, https://doi.org/10.1016/j.biortech.2022.128063.

Chen, X., Fan, Y., Wu, L. et al. Ultra-selective molecular-sieving gas separation membranes enabled by multi-covalent-crosslinking of microporous polymer blends. Nat Commun 12, 6140 (2021). https://doi.org/10.1038/s41467-021-26379-5

C.Y. Tong, C.J.C. Derek, (2023). Bio-coatings as immobilized microalgae cultivation enhancement: A review, Science of The Total Environment, Volume 887, ISSN 0048-9697. https://doi.org/10.1016/j.scitotenv.2023.163857.

Courtyard | SL Rasch. (n.d.). https://www.sl-rasch.com/en/projects/courtyard/

David F. Williams, (2019). Chapter 36 - Hydrogels in Regenerative Medicine, Editor(s): Anthony Atala, Robert Lanza, Antonios G. Mikos, Robert Nerem, Principles of Regenerative Medicine (Third Edition), Academic Press, Pages 627-650, ISBN 9780128098806, https://doi.org/10.1016/B978-0-12-809880-6.00036-9.

Davidson, E. A. (2024, December 16). Carbohydrate | Definition, Classification, & Examples. Encyclopedia Britannica. https://www.britannica.com/science/carbohydrate

Davidson, & A, E. (2025, February 15). Carbohydrate | Definition, Classification, & Examples. Encyclopedia Britannica. https://www.britannica.com/science/carbohydrate

Devendorf, L., De Koninck, S., & Sandry, E. (2022b). An Introduction to Weave Structure for HCI: a how-to and reflection on modes of exchange. Designing Interactive Systems Conference. https://doi.org/10.1145/3532106.3534567

drape. (2025). https://dictionary.cambridge.org/dictionary/english/drape

Education, U. C. F. S. (n.d.). Biogeochemical Cycles | Center for Science Education. UCAR. https://scied.ucar.edu/learning-zone/earth-system/biogeochemical-cycles

emilie-palle-holm. (n.d.). ARTS THREAD. https://www.artsthread.com/profile/emilie-palle-holm

Emmi Pouta, Jussi Ville Mikkonen, and Antti Salovaara. 2024. Opportunities with Multi-Layer Weave Structures in Woven E-Textile Design. ACM Trans. Comput.-Hum. Interact. 31, 5, Article 62 (October 2024), 38 pages. https://doi.org/10.1145/3689039

Encarnação, T., Ramos, P., Mohammed, D., McDonald, J., Lizzul, M., Nicolau, N., Da Graça Campos, M., & Sobral, A. J. F. N. (2023). Bioremediation using microalgae and cyanobacteria and biomass valorisation. In Environmental challenges and solutions (pp. 5–28). https://doi.org/10.1007/978-3-031-17226-7_2

Engineering, T. (n.d.-b). TC2 Loom. Tronrud Engineering. https://www.tronrud.no/en/industrialized-products/products/tc2-loom

EuropaWire PR Editor. (2023, July 19). Brilliant Planet Partners with Schneider Electric and Platinum Electrical Engineering to Scale Algae-Based Carbon Capture Process. EuropaWire. https://news.europawire.eu/brilliant-planet-partners-with-schneider-electric-and-platinum-electrical-engineering-to-scale-algae-based-carbon-capture-process/eu-press-release/2023/07/19/15/02/44/1970/?utm_source=rss&utm_ medium=rss&utm_campaign=brilliant-planet-partners-with-schneider-electric-and-platinum-electrical-engineering-to-scale-algae-based-carbon-capture-process

Fagorite, V. I., Onyekuru, S. O., Opara, A. I., & Oguzie, E. E. (2022). The major techniques, advantages, and pitfalls of various methods used in geological carbon sequestration. International Journal of Environmental Science and Technology, 20(4), 4585–4614. https://doi.org/10.1007/s13762-022-04351-0

Gigova L, Marinova G. 2016. Significance of microalgae areas and soils. Genet Plant Physiol 6: 85-100. https://www.researchgate.net/publication/306960016_Significance_of_microalgae_-_grounds_and_areas

Gries, T., Bettermann, I., Blaurock, C., Bündgens, A., Dittel, G., Emonts, C., Gesché, V., Glimpel, N., Kolloch, M., Grigat, N., Löcken, H., Löwen, A., Jacobsen, J., Kimm, M., Kelbel, H., Kröger, H., Kuo, K., Peiner, C., Sackmann, J., & Schwab, M. (2022b). Aachen Technology Overview of 3D textile materials and recent innovation and applications. Applied Composite Materials, 29(1), 43–64. https://doi.org/10.1007/s10443-022-10011-w

Hallak, M. A., Verdier, T., Bertron, A., Roques, C., & Bailly, J. (2023). Fungal contamination of building materials and the aerosolization of particles and toxins in indoor air and their associated risks to health: a review. Toxins, 15(3), 175. https://doi.org/10.3390/toxins15030175

Holly McQuillan and Elvin Karana. 2023. Conformal, Seamless, Sustainable: Multimorphic Textile-forms as a Material-Driven Design Approach for HCI. In Proceedings of the 2023 CHI Conference on Human Factors in Computing Systems (CHI '23). Association for Computing Machinery, New York, NY, USA, Article 727, 1–19. https://doi.org/10.1145/3544548.3581156

hydrodynamics. (n.d.). In Merriam-Webster Dictionary. https://www.merriam-webster.com/dictionary/hydrodynamics

Huan Fang, Jihui Wang, Lin Li, Longquan Xu, Yuxuan Wu, Yi Wang, Xu Fei, Jing Tian, Yao Li, (2019). A novel high-strength poly(ionic liquid)/PVA hydrogel dressing
for antibacterial applications. Chemical Engineering Journal, Volume 365, Pages 153-164, ISSN 1385-8947. https://doi.org/10.1016/j.cej.2019.02.030.

Hugo Barbosa, Marc Barthelemy, Gourab Ghoshal, Charlotte R. James, Maxime Lenormand, Thomas Louail, Ronaldo Menezes, José J. Ramasco, Filippo Simini, Marcello Tomasini, (2018). Human mobility: Models and applications, Physics Reports, Volume 734, Pages 1-74, ISSN 0370-1573, https://doi.org/10.1016/j.physrep.2018.01.001.

Ignacio Moreno-Garrido, (2008). Microalgae immobilization: Current techniques and uses, Bioresource Technology, Volume 99, Issue 10, 2008, Pages 3949-3964, ISSN 0960-8524, https://doi.org/10.1016/j.biortech.2007.05.040.

Industries, T. T. (2023, August 29). New research in 3D woven fabrics reveals the potential for higher performance textiles - Tex tech industries. Tex Tech Industries. https://textechindustries.com/blog/new-research-3d-woven-fabrics-reveals-potential-higher-performance-textiles/

In-Na, P., Lee, J., & Caldwell, G. (2021). Living textile biocomposites deliver enhanced carbon dioxide capture. Journal of Industrial Textiles, 51(4_suppl), 5683S-5707S. https://doi.org/10.1177/15280837211025725

In-Na, P., Sharp, E. B., Caldwell, G. S., Unthank, M. G., Perry, J. J., & Lee, J. G. M. (2022). Engineered living photosynthetic biocomposites for intensified biological carbon capture. Scientific Reports, 12(1). https://doi.org/10.1038/s41598-022-21686-3

Islam MR, Karim FE, Khan AN. Statistical analysis of Cotton-Jute blended ratio for producing good quality blended yarn. Heliyon. 2024 Jan 19;10(2):e25027. doi: 10.1016/j.heliyon.2024.e25027. PMID: 38312702; PMCID: PMC10835373.

Kaparapu, J. (2017). Micro algal Immobilization Techniques. In J. Algal Biomass Utln. (Vol. 8, Issue 1, pp. 64–70). https://storage.unitedwebnetwork.com/files/521/37e92165730327cd9d2b1493130db139.pdf

Karana, E., Barati, B., Rognoli, V., & Zeeuw Van Der Laan, A., (2015). Material driven design (MDD): A method to design for material experiences. International Journal of Design, 9 (2), 35-54.

Kesari, S. (2019, September 24). Parallel prototyping. https://ixd.prattsi.org/2019/09/parallel-prototyping/#:~:text=Parallel%20Prototyping%20is%20a%20method,to%20more%20effective%20design%20result.

Kirchman, David L.(2018). 92Microbial primary production and phototrophy. Processes in Microbial Ecology. 10.1093/oso/9780198789406.003.0006. Oxford University Press. https://doi.org/10.1093/oso/9780198789406.003.0006

Koc, U., Eren, R., & Aykut, Y. (2020). Yarn-reinforced hydrogel composite produced from woven fabrics by simultaneous dissolution and cross-linking. Polymers and Polymer Composites, 29(2), 117–126. https://doi.org/10.1177/0967391120903648

Lasser, R. (2013, March 21). Engineering Method – Electrical and Computer Engineering design Handbook. https://sites.tufts.edu/eeseniordesignhandbook/2013/engineering-method/#:~:text=The%20engineering%20method%20(also%20known,problem%20definition%20to%20desired%20result.

Laura Devendorf and Chad Di Lauro. 2019. Adapting Double Weaving and Yarn Plying Techniques for Smart Textiles Applications. In Proceedings of the Thirteenth International Conference on Tangible, Embedded, and Embodied Interaction (TEI '19). Association for Computing Machinery, New York, NY, USA, 77–85. https://doi.org/10.1145/3294109.3295625

Li, Y., Wu, X., Liu, Y., & Taidi, B. (2024). Immobilized microalgae: principles, processes and its applications in wastewater treatment. World Journal of Microbiology and Biotechnology, 40(5). https://doi.org/10.1007/s11274-024-03930-2

Lin, J., Jiao, G., & Kermanshahi-Pour, A. (2022). Algal Polysaccharides-Based Hydrogels: Extraction, synthesis, Characterization, and Applications. Marine Drugs, 20(5), 306. https://doi.org/10.3390/md20050306

Masojídek J, Torzillo G, Koblížek M. 2013. Photosynthesis in microalgae. In: Richmond A, Hu Q eds. Handbook of microalgal culture: applied phycology and biotechnology. John Wiley & Sons, p.21-36, https://doi.org/10.1002/9781118567166.ch2.

McGowan, T. (2016). Capitalism and desire. In Columbia University Press eBooks. https://doi.org/10.7312/mcgo17872

McQuillan, H. (2020). Zero Waste Systems Thinking : Multimorphic Textile-Forms. DIVA. https://www.diva-portal.org/smash/record.jsf?pid=diva2%3A1478307&dswid=4102

McQuillan, H., & Karana, E. (2023). Conformal, Seamless, Sustainable: Multimorphic Textile-forms as a Material-Driven Design Approach for HCI. ACM DL DIGITAL LIBRARY, 1–19. https://doi.org/10.1145/3544548.3581156

medium. (2025). In Merriam-Webster Dictionary. https://www.merriam-webster.com/dictionary/medium

Meina Han, Chaofan Zhang, Shih-Hsin Ho, (2023). Immobilized microalgal system: An achievable idea for upgrading current microalgal wastewater treatment, Environmental Science and Ecotechnology, Volume 14, ISSN 2666-4984. https://doi.org/10.1016/j.ese.2022.100227.

Monique Ellen Torres da Silva, Kely de Paula Correa, Marcio Arêdes Martins, Sérgio Luis Pinto da Matta, Hércia Stampini Duarte Martino, Jane Sélia dos Reis Coimbra, (2020). Food safety, hypolipidemic and hypoglycemic activities, and in vivo protein quality of microalga Scenedesmus obliquus in Wistar rats, Journal of Functional Foods, Volume 65, 103711, ISSN 1756-4646. https://doi.org/10.1016/j.jff.2019.103711.

N. Shahrubudin, T.C. Lee, R. Ramlan, (2019). An Overview on 3D Printing Technology: Technological, Materials, and Applications, Procedia Manufacturing, Volume 35, 286-1296, https://doi.org/10.1016/j.promfg.2019.06.089.

Narasimman Kalaiselvan, Mysoon M. Al-Ansari, Thangavel Mathimani,(2024). Biodiesel production from the Scenedesmus sp. and utilization of pigment from de-oiled biomass as sensitizer in the dye-sensitized solar cell (DSSC) for performance enhancement. Environmental Research, Volume 251, Part 2, 118726, ISSN 0013-9351,https://doi.org/10.1016/j.envres.2024.118726.

Nguyen, P. Q., Courchesne, N. D., Duraj-Thatte, A., Praveschotinunt, P., & Joshi, N. S. (2018). Engineered Living Materials: Prospects and challenges for using biological systems to direct the assembly of smart materials. Advanced Materials, 30(19). https://doi.org/10.1002/adma.201704847

Oh, J., Ammu, S., Vriend, V. D., Kieffer, R., Kleiner, F. H., Balasubramanian, S., Karana, E., Masania, K., & Aubin-Tam, M. (2023). Growth, distribution, and photosynthesis of chlamydomonas reinhardtii in 3D hydrogels. Advanced Materials, 36(2). https://doi.org/10.1002/adma.202305505

Oldenburg, C. M. (2019). Geologic Carbon Sequestration: sustainability and environmental risk. In Springer eBooks (pp. 219–234). https://doi.org/10.1007/978-1-4939-8787-0_200

Origami for Beginners: Easy Guide to Origami | Discount Art n Craft Warehouse - Discount Art n Craft Warehouse | Buy Art Supplies Online. (n.d.). https://discountartncraftwarehouse.com.au/blog-2138/origami-folding-techniques-to-master#:~:text=Origami%20comes%20from%20the%20Japanese,the%20simple%20act%20of%20folding.

Pauliuk, S., Heeren, N., Berrill, P., Fishman, T., Nistad, A., Tu, Q., Wolfram, P., & Hertwich, E. G. (2021). Global scenarios of resource and emission savings from material efficiency in residential buildings and cars. Nature Communications, 12(1). https://doi.org/10.1038/s41467-021-25300-4

Perera, Y. S., Muwanwella, R. M. H. W., Fernando, P. R., Fernando, S. K., & Jayawardana, T. S. S. (2021). Evolution of 3D weaving and 3D woven fabric structures. Fashion and Textiles, 8(1). https://doi.org/10.1186/s40691-020-00240-7

Photobioreactor. (2011, April 14). Chlorelle. https://chlorelle.wordpress.com/2011/04/14/the-different-kinds-of-chlorellas-production/allemagne-016/

Pichaya In-na, Abbas A. Umar, Adam D. Wallace, Michael C. Flickinger, Gary S. Caldwell, Jonathan G.M. Lee, (2020). Loofah-based microalgae and cyanobacteria biocomposites for intensifying carbon dioxide capture. Journal of CO2 Utilization, Volume 42, 101348, ISSN 2212-9820. https://doi.org/10.1016/j.jcou.2020.101348.

R. Gayathri, Shahid Mahboob, Marimuthu Govindarajan, Khalid A. Al-Ghanim, Zubair Ahmed, Norah Al-Mulhm, Masa Vodovnik, Shankar Vijayalakshmi, (2021). A review on biological carbon sequestration: A sustainable solution for a cleaner air environment, less pollution and lower health risks. Journal of King Saud University - Science, Volume 33, Issue 2, 1018-3647, https://doi.org/10.1016/j.jksus.2020.101282.

Rodrigo-Navarro, A., Sankaran, S., Dalby, M. J., Del Campo, A., & Salmeron-Sanchez, M. (2021). Engineered living biomaterials. Nature Reviews Materials, 6(12), 1175–1190. https://doi.org/10.1038/s41578-021-00350-8

Russell, S. (2023, November 28). The impact of cotton recycling on the future of sustainability. Environment Co. https://environment.co/cotton-recycling/

Sarkar, P. (2019, November 19). What is Crimp% in Fabric and How to Measure Warp and Weft Crimp%. Online Clothing Study. https://www.onlineclothingstudy.com/2014/06/what-is-crimp-in-fabric-and-how-to.html#google_vignette

Schmid, B., Navalho, S., Schulze, P. S. C., Van De Walle, S., Van Royen, G., Schüler, L. M., Maia, I. B., Bastos, C. R. V., Baune, M.-C., Januschewski, E., Coelho, A., Pereira, H., Varela, J., Navalho, J., & Cavaco Rodrigues, A. M. (2022). Drying Microalgae Using an Industrial Solar Dryer: A Biomass Quality Assessment. Foods, 11(13), 1873. https://doi.org/10.3390/foods11131873

Schuurmans, R. M., Van Alphen, P., Schuurmans, J. M., Matthijs, H. C. P., & Hellingwerf, K. J. (2015). Comparison of the photosynthetic yield of cyanobacteria and green algae: Different methods give different answers. PLoS ONE, 10(9), e0139061. https://doi.org/10.1371/journal.pone.0139061

Scott, J. (2018). Responsive Knit: the evolution of a programmable material system Design as a catalyst for change - DRS International Conference 2018, Limerick, Ireland. https://doi.org/10.21606/drs.2018.566

Selvan, B. K., Pandiyan, R., Vaishnavi, M., Das, S., & Thirunavoukkarasu, M. (2022). Ameliorative biodegradation of hazardous textile industrial wastewater dyes by potential microalgal sp. Biomass Conversion and Biorefinery, 13(15), 13481–13492. https://doi.org/10.1007/s13399-022-02725-5

Shaikh Abdur Razzak, Khairul Bahar, K.M. Oajedul Islam, Abdul Khaleel Haniffa, Mohammed Omar Faruque, S.M. Zakir Hossain, Mohammad M. Hossain, (2024). Microalgae cultivation in photobioreactors: sustainable solutions for a greener future. Green Chemical Engineering, Volume 5, Pages 418-439, ISSN 2666-9528. https://doi.org/10.1016/j.gce.2023.10.004.

Sijia Wu, Hongxun Huo, Yixiao Shi, Feiran Zhang, Tingting Gu, Zhen Li, (2023). Chapter Three - Extraction and application of extracellular polymeric substances from fungi. Editor(s): Geoffrey Michael Gadd, Sima Sariaslani. Advances in Applied Microbiology. Academic Press. Volume 125. Pages 79-106. ISSN 0065-2164. ISBN 9780443192760. https://doi.org/10.1016/bs.aambs.2023.08.001.

Sleppy, J. (2021, April 22). Energy harvesting, storage, and management — Capacitech Energy. Capacitech Energy. https://www.capacitechenergy.com/blog/energy-harvesting-storage-and-management

Soumaya Grira, Hadil Abu Khalifeh, Mohammad Alkhedher, Mohamad Ramadan, (2023). 3D printing algae-based materials: Pathway towards 4D bioprinting. Bioprinting, Volume 33, ISSN 2405-8866. https://doi.org/10.1016/j.bprint.2023.e00291.

Sources of greenhouse gas emissions | US EPA. (2025, January 16). US EPA. https://www.epa.gov/ghgemissions/sources-greenhouse-gas-emissions

Structure and form | School of Materials Science and Engineering - UNSW Sydney. (n.d.). UNSW Sites. https://www.unsw.edu.au/science/our-schools/materials/engage-with-us/high-school-students-and-teachers/online-tutorials/polymers/structure-and-form#:~:text=Polymers%20are%20a%20range%20of,to%20form%20complex%20compositional%20arrangements.

Subburaj Suganya, Madhava Anil Kumar, Soumya Haldar, (2021). Chapter 27 - Effect of bacterial attachment on permeable membranes aided by extracellular polymeric substances. Microbial and Natural Macromolecules. Academic Press, Pages 733-749, ISBN 9780128200841. https://doi.org/10.1016/B978-0-12-820084-1.00028-4.

Supriya Pandey, Ishvarya Narayanan, Ramesh Vinayagam, Raja Selvaraj, Thivaharan Varadavenkatesan, Arivalagan Pugazhendhi, (2023). A review on the effect of blue green 11 medium and its constituents on microalgal growth and lipid production, Journal of Environmental Chemical Engineering, Volume 11, Issue 3. 109984, ISSN 2213-3437,https://doi.org/10.1016/j.jece.2023.109984.

Tajarudin, H. A., & Ng, C. W. C. (2022). Introduction to biocoating. In SpringerBriefs in applied sciences and technology (pp. 1–8). https://doi.org/10.1007/978-981-19-6035-2_1

The challenge of reducing industrial pollution. (n.d.). European Environment Agency. https://www.eea.europa.eu/signals-archived/signals-2020/articles/ the-challenge-of-reducing-industrial-pollution

The Editors of Encyclopaedia Britannica. (2009, January 30). BitMap | Definition & Facts. Encyclopedia Britannica. https://www.britannica.com/technology/bitmap

The Editors of Encyclopaedia Britannica. (2023, April 11). Hydroxyl group | Definition, Structure, & Facts. Encyclopedia Britannica. https://www.britannica.com/science/hydroxyl-group

The Editors of Encyclopaedia Britannica. (2025a, January 3). Van der Waals forces | Intermolecular Interactions & Applications. Encyclopedia Britannica. https://www.britannica.com/science/van-der-Waals-forces

The Editors of Encyclopaedia Britannica. (2025, January 18). Adenosine triphosphate (ATP) | Definition, Structure, Function, & Facts. Encyclopedia Britannica. https://www.britannica.com/science/adenosine-triphosphate

The Editors of Encyclopaedia Britannica. (2025a, January 11). Biofilm | Microorganisms, bacteria, Microbial Communities. Encyclopedia Britannica. https://www.britannica.com/science/biofilm

Trans Tech Publications Ltd, Switzerland. (n.d.). Harvesting electrical energy from automatic sliding doors use - IIUM Repository (IRep). http://irep.iium.edu.my/100273/

Valdivia-Rivera, S.; Ayora-Talavera, T.; Lizardi-Jiménez, M.A.; García-Cruz, U.; Cuevas-Bernardino, J.C.; Pacheco, N. Encapsulation of microorganisms for bioremediation: Techniques and carriers. Rev.Environ.Sci.Biotechnol. 2021, 20, 815–838. https://www.researchgate.net/publication/352101296_Encapsulation_of_microorganisms_for_bioremediation_Techniques_and_carriers

Vasilieva, S., Lobakova, E., & Solovchenko, A. (2020). Biotechnological applications of immobilized microalgae. In Environmental chemistry for a sustainable world (pp. 193–220). https://doi.org/10.1007/978-3-030-48973-1_7

Vieira, M. V., Pastrana, L. M., & Fuciños, P. (2020). Microalgae encapsulation systems for food, pharmaceutical and cosmetics applications. Marine Drugs, 18(12), 644. https://doi.org/10.3390/md18120644

Vladan Koncar, (2019). 2 - Composites and hybrid structures. In The Textile Institute Book Series, Smart Textiles for In Situ Monitoring of Composites. Woodhead Publishing, Pages 153-215, ISBN 9780081023082. https://doi.org/10.1016/B978-0-08-102308-2.00002-4.

Vrenna, M., Peruccio, P. P., Liu, X., Zhong, F., & Sun, Y. (2021). Microalgae as Future Superfoods: Fostering Adoption through Practice-Based Design Research. Sustainability, 13(5), 2848. https://doi.org/10.3390/su13052848

Waresindo, W. X., Luthfianti, H. R., Priyanto, A., Hapidin, D. A., Edikresnha, D., Aimon, A. H., Suciati, T., & Khairurrijal, K. (2023). Freeze–thaw hydrogel fabrication method: basic principles, synthesis parameters, properties, and biomedical applications. Materials Research Express, 10(2), 024003. https://doi.org/10.1088/2053-1591/acb98e

Weeden, M. (2025, January 14). 8 Amazing bamboo Facts. One Tree Planted. https://onetreeplanted.org/blogs/stories/bamboo#:~:text=According%20to%20Guinness%20World%20Records,just%20grow%20before%20your%20eyes!

Weisan Hua, Yishun Sha, Xuelai Zhang, Hongfen Cao, (2023). Research progress of carbon capture and storage (CCS) technology based on the shipping industry. Ocean Engineering, Volume 281, 0029-8018. https://doi.org/10.1016/j.oceaneng.2023.114929.

What is NADPH in photosynthesis? - full form, functioning. (2020, March 3). Toppr-guides. https://www.toppr.com/guides/biology/cell-the-unit-of-life/what-is-nadph-in-photosynthesis/#:~:text=The%20full%20form%20of%20NADPH,the%20first%20level%20of%20photosynthesis.

“What Is the Triple Planetary Crisis?” Unfccc.int, 13 Apr. 2022, unfccc.int/news/what-is-the-triple-planetary-crisis.

When the material grows: A case study on designing (with) mycelium-based materials. Available from: https://www.researchgate.net/publication/323749568_When_the_material_grows_A_case_study_on_designing_with_mycelium-based_materials.

Wei Xiong, Yiyan Peng, Weimin Ma, Xurong Xu, Yueqi Zhao, Jinhui Wu, Ruikang Tang, National Science Review, Volume 10, Issue 10, October 2023, nwad200, https://doi.org/10.1093/nsr/nwad200

What is NADPH in photosynthesis? - full form, functioning. (2020, March 3). Toppr-guides. https://www.toppr.com/guides/biology/cell-the-unit-of-life/what-is-nadph-in-photosynthesis/#:~:text=Nicotinamide%20Adenine%20Dinucleotide%20Phosphate%20Hydrogen%20(NADPH)&text=NADPH%20is%20a%20product%20of,of%20the%20process%20of%20photosynthesis.

Wikipedia contributors. (2024, December 10). Laminar flow cabinet. Wikipedia. https://en.wikipedia.org/wiki/Laminar_flow_cabinet#:~:text=A%20laminar%20flow%20cabinet%20or,or%20any%20particle%2Dsensitive%20materials.

Wikipedia contributors. (2025b, January 16). Shuttle (weaving). Wikipedia. https://en.wikipedia.org/wiki/Shuttle_(weaving)#:~:text=A%20shuttle%20is%20a%20tool,to%20weave%20in%20the%20weft.

Yajun Liu, Canyi Huang, Hong Xia, Qing-Qing Ni, (2021). Research on development of 3D woven textile-reinforced composites and their flexural behavior. Materials & Design, Volume 212, ISSN 0264-1275. https://doi.org/10.1016/j.matdes.2021.110267.

Yirgu, Z., Leta, S., Hussen, A., & Khan, M. M. (2020). Nutrient removal and carbohydrate production potential of indigenous Scenedesmus sp. grown in anaerobically digested brewery wastewater. ENVIRONMENTAL SYSTEMS RESEARCH, 9(1). https://doi.org/10.1186/s40068-020-00201-5

Zhao, S., Guo, C., Kumarasena, A., Omenetto, F. G., & Kaplan, D. L. (2019). 3D printing of functional microalgal silk structures for environmental applications. ACS Biomaterials Science & Engineering, 5(9), 4808–4816. https://doi.org/10.1021/acsbiomaterials.9b00554

Appendix

APPENDIX A - Carbon Caputre

Carbon Capture and Sequestration

An approach to removing CO_2 from the atmosphere is geological carbon capture and sequestration (GCS). This process involves pumping high-purity CO_2 into sealed geological formations underground, where it is stored in rock pore spaces. Impermeable rock layers act as a barrier, containing the CO_2 permanently (Hua et al., 2023).

However, geological carbon sequestration has several limitations. A primary limitation is the challenge of effective CO_2 injection (Oldenburg, 2019). Some underground formations may have adequate capacity, but low permeability or natural barriers can restrict CO_2 from spreading uniformly, potentially increasing injection costs (Oldenburg, 2019). Another limitation is the need for geological storage sites to be located near CO_2 sources to control transport expenses; otherwise, the high costs could undermine the economic viability of CCS (Carbon Capture and Storage). Additionally, the potential for groundwater contamination represents another limitation, as CO_2 leakage into surrounding water resources could harm local ecosystems, and compromise water quality (Oldenburg, 2019).

APPENDIX B - Weaving Structures.

In the context of textile composites, textile properties are shaped by the weaving technique, which typically falls into three primary categories: plain, twill, and satin weaves—each offering distinct mechanical characteristics suited for specific applications (Aisyah et al., 2021).

Plain Weave, also known as tabby, structure is entirely composed of interlacements, where each warp fiber alternately passes over and under each weft fiber (Devendorf et al., 2022; Aisyah et al., 2021). This configuration results in a symmetrical and stable textile with reasonable porosity and exceptional strength due to the close binding of warp and weft fibers (Shenton, 2014). Plain weave textiles are commonly employed in applications requiring durability and stability (Aisyah et al., 2021).

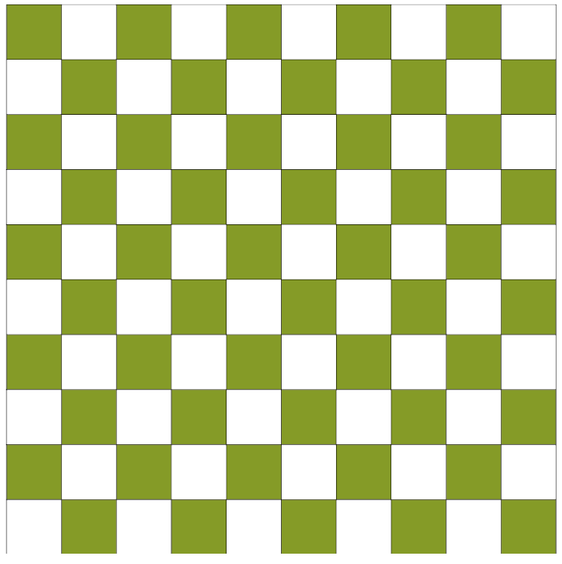

Figure C1: Plane wave.

Twill weave draft is characterized by a diagonal pattern (Shenton, 2014). In this structure, one or more warp threads alternately cross over and under two or more weft threads (Shenton, 2014). This structure results in stronger and thicker textiles (Devendorf et al., 2022). Compared to plain weave, twill textiles have reduced crimping, enhanced flexibility, and improved drape, making them softer and ideal for applications requiring both stability and comfort (Aisyah et al., 2021; Shenton, 2014).

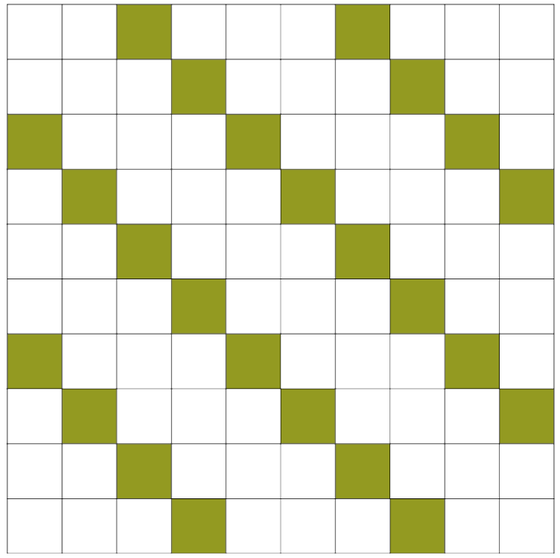

Figure C2: Twill.

Satin weave structures maximize the spacing between interlacements, creating thicker textiles with tightly stacked yarns and smooth, flat surfaces (Devendorf et al., 2022). These textiles exhibit excellent drapability, low crimp, and are well-suited for curved surfaces due to their mechanical properties (Aisyah et al., 2021). However, their low structural stability and asymmetry should be taken into account (Aisyah et al., 2021).

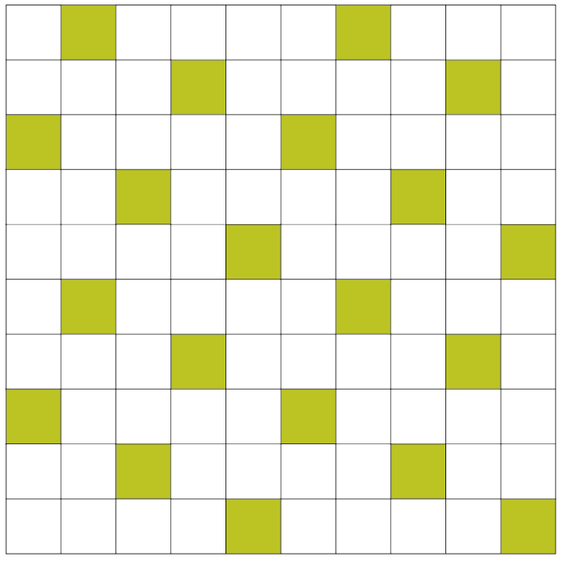

Figure C3: Satin

Beyond these fundamental weaves, additional structures are derived through modifications. Basket Weave is an enlarged variation of plain weave, where warp and weft fibers interlace every nth row and column, creating a visually distinct texture (Devendorf et al., 2022). Invert Weave structure exchanges all weft floats with warp floats and vice versa, effectively reversing the pattern on the back face of the textile (Devendorf et al., 2022). Interlace Weave combines rows from two different structures, producing a hybrid design (Devendorf et al., 2022).

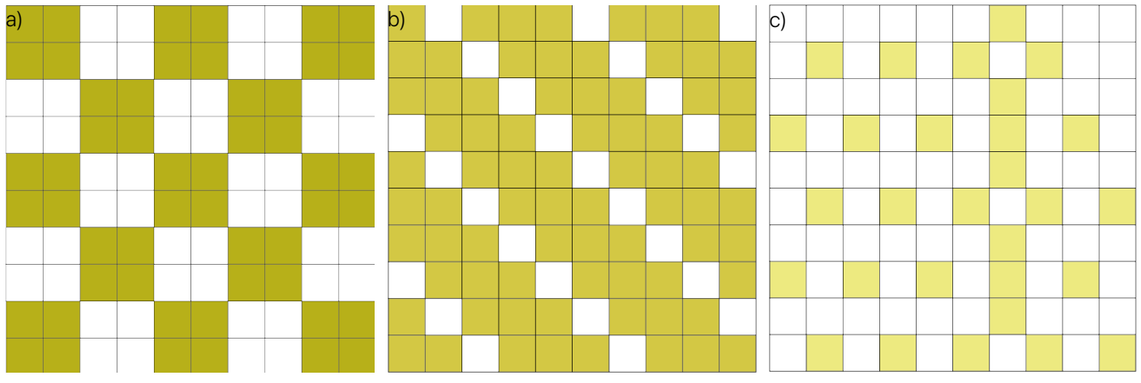

Figure C4: a) Basket Wave; b) Invert Wave; c) Interlace Wave.

APPENDIX C - Photosynthesis tests.

Photosynthetic activity tests were performed to assess the viability of the immobilized microalgae over time. Measurements were taken before and after the freeze-thaw cycles, followed by weekly assessments to track changes in photosynthetic performance. The photosynthetic activity tests were conducted by placing the petri dishes containing the living textiles inside a dark box. The MONITORING PAM device, connected to a laptop running the WinControl-3 software, was used to measure photosynthetic efficiency. By positioning the MONITORING PAM over each petri dish and initiating the measurement via the software interface, a light emission was triggered, allowing for the quantification of Recorded quantum yield values can range from 0 to 1, with values below 0.7 indicating poor photosynthetic performance, while readings between 0.7 and 1 were considered indicative of a healthy and active microalgal presence (Schuurmans et al., 2015).

Figure D1: Stage asssembled to measure the samples photosynthetic activity.

C.1. - Photosynthesis tests Results

A PAM was used to measure the first Photosynthesis Test before freezing the twelve samples. Each sample was monitored on both sides in 5 different spots: Top Left, Top Center, Top Right, Bottom Left and Bottom Right.

1st Photosynthesis test.

The first photosynthetic activity test was conducted before subjecting the twelve textile samples to the freeze-thaw process. It was conducted to evaluate the photosynthetic performance of both immersed and pipetted samples from each timeline.

After collecting all experimental data, the results were processed in several steps to ensure a comprehensive analysis. First, for each sample, the photosynthetic activity measurements from five different spots were averaged (Figure D2). Then, to account for duplicate samples, the results were grouped based on the method of microalgae introduction: for each timeline, the measurements from the immersed samples were averaged separately, as were those from the pipetted samples. This step ensured that a representative average was obtained and helped identify the most effective F-T process. Next, an overall average was calculated for all immersed samples and another for all pipetted samples, enabling a direct comparison between the two methods to determine which was more effective in introducing microalgae into the hydrogel. The measurements were first analyzed individually, then compared collectively, and ultimately were compared with *Scenedesmus* sp. in a liquid medium to evaluate the impact of textile embedding on microalgal viability and performance (Figure D3).

These data represent the photosynthetis of textiles samples in different part of the samples (Top left, Top center, Top right, Bottom Left, Bottom Right).

Unit= Fv/Fm

	Top Left	Top Center	Top Right	Bottom Left	Bottom Right	Average		
Timeline 1							Average σ Average of Timeline 1 pipetted	
Immersed	0.408	0.225	0.431	0.645	0.648	0.4714	0.4369	0.5275
Immersed Replicates	0.21	0.265	0.291	0.65	0.596	0.4024		
Pipetted	0.423	0.344	0.546	0.535	0.603	0.4902		
Pipetted Replicates	0.526	0.462	0.491	0.64	0.705	0.5648		
Standard Deviation	0.132	0.104445	0.10973	0.055151	0.050259	0.0668		
Timeline 2							Average σ Average of Timeline 2 pipetted	
Immersed	0.537	0.425	0.432	0.549	0.541	0.4968	0.5185	0.531
Immersed Replicates	0.566	0.493	0.471	0.594	0.577	0.5402		
Pipetted	0.453	0.498	0.479	0.558	0.593	0.5162		
Pipetted Replicates	0.407	0.594	0.424	0.731	0.573	0.5458		
Standard Deviation	0.0736	0.069496	0.02753	0.084273	0.021787	0.0226		
Timeline 3							Average σ Average of Timeline 3 pipetted	
Immersed	0.396	0.282	0.343	0.629	0.651	0.4602	0.5175	0.5943
Immersed Replicates	0.506	0.508	0.602	0.652	0.606	0.5748		
Pipetted	0.572	0.472	0.586	0.61	0.623	0.5726		
Pipetted Replicates	0.559	0.59	0.567	0.638	0.726	0.616		
Standard Deviation	0.0801	0.130379	0.12184	0.017595	0.053019	0.0668		
Scenedesmus in liquid medium	0.787	0.818	0.669			0.758		
							Average In Average Pipetted	
							0.491	0.550933333

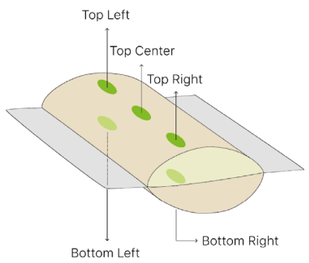

Figure D2: Overall first Photosynthesis test results.

As illustrated in Figure D3, the pipetted samples demonstrated the highest photosynthetic activity, yielding the best overall results. A possible explanation for this phenomenon is that in the immersed condition, microalgae have unrestricted access to both the medium and the textile, allowing them to exist in both environments without a selective preference. Conversely, in the pipetted condition, microalgae are directly placed between the textile layers, limiting their ability to disperse into the surrounding medium. This condition may promote stronger microalgal adherence to the textile structure, resulting in higher localized photosynthetic activity. However, the quantum yield of the samples remains too low to indicate that the microalgae are in a healthy condition.

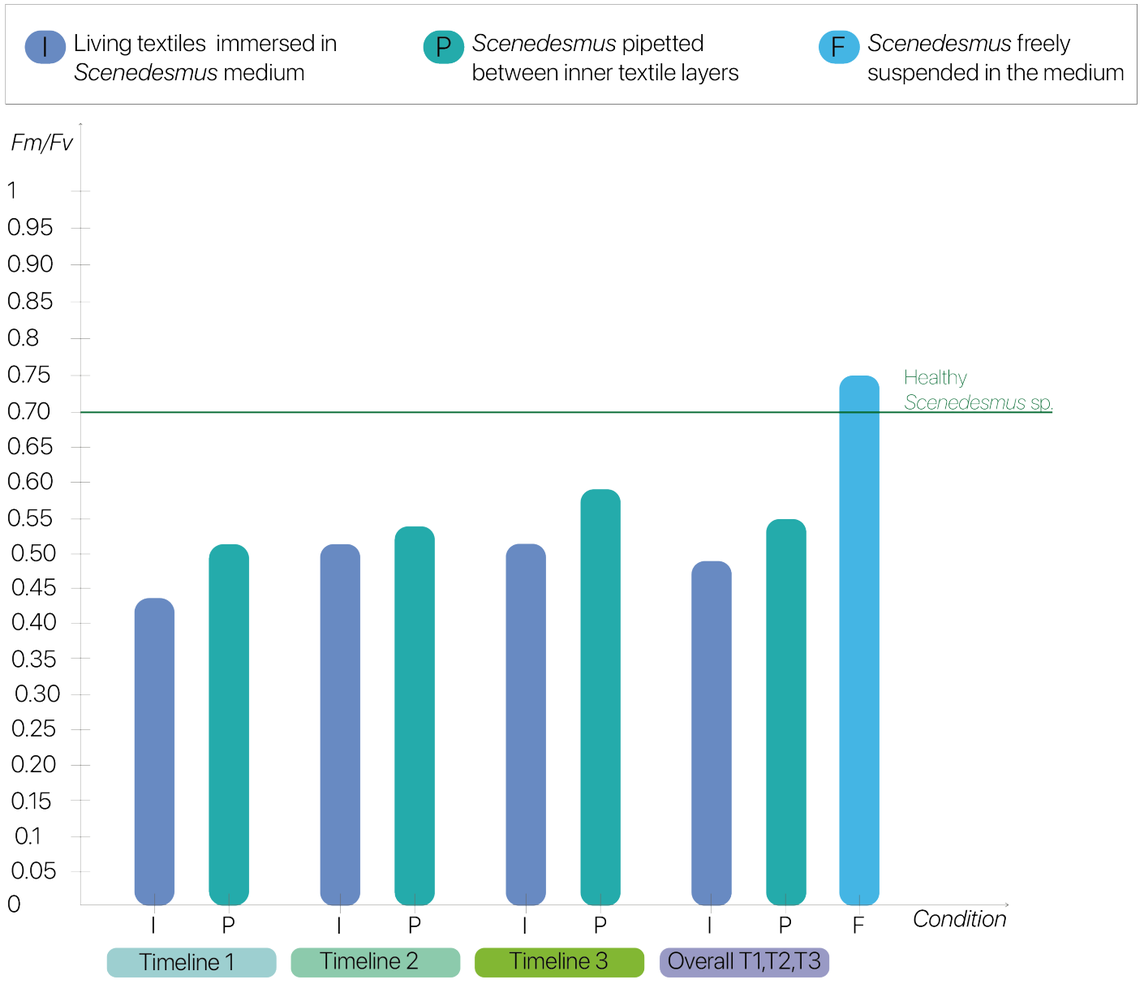

Figure D3: Photosynthetic performance of immersed and pipetted samples across different timelines. Timeline 1 corresponds to three Freeze-Thaw (F-T) cycles, Timeline 2 to three F-T cycles split into two before *Scenedesmus* sp. addition and one after, and Timeline 3 to a single F-T cycle. The graph provides a comparative visualization of photosynthetic activity across these conditions and the sample preparations.

Scenedesmus sp. suspended freely in the liquid medium exhibited the highest photosynthetic activity. However, it is important to consider that the measured photosynthetic activity of the immersed and pipetted samples may have been affected by technical limitations in the measurement process. Specifically, the initial measurements for the Top Left, Top Center, and Top Right positions may not be entirely reliable, as the textiles were positioned at the bottom of the petri dish due to gravitational settling, while the measurement device was placed at the top (Figure D4). This discrepancy in positioning likely introduced an inconsistency in the recorded values. To improve the accuracy of future assessments, the methodology will be refined by flipping the petri dishes prior to measurement, ensuring that all measurement spots are evaluated from a consistent and standardized distance.

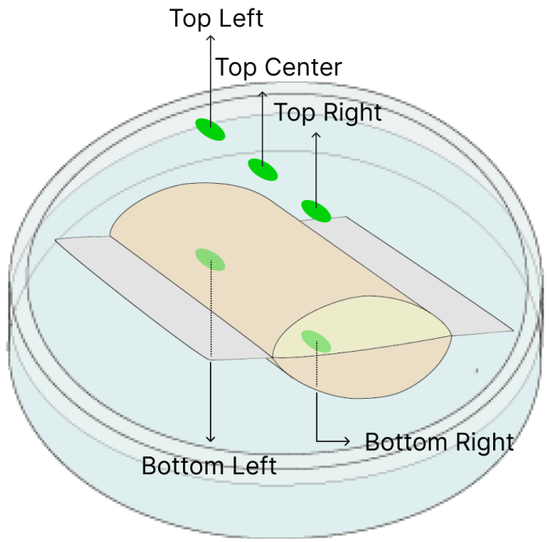

Figure D4: Initial photosynthetic measurement method.

2nd Photosynthesis test.

The second photosynthesis test was conducted seven days after the first, following the completion of all Freeze-Thaw cycles. Each sample was analyzed on both sides to ensure a comprehensive evaluation. Measurements were first taken at the Bottom Left and Bottom Right positions, after which the petri dish was flipped to assess the Top Left, Top Center, and Top Right positions, providing a reliable assessment of the textile's photosynthetic activity (Figure D5).

Due to the negative results, further in-depth analysis was not feasible. However, the findings indicated that the *Scenedesmus* sp. in Timeline 1 - 3 F-T cycles, where the textile was immersed and subjected to three Freeze-Thaw cycles, exhibited the most favorable response. This outcome was unexpected, as these microalgae had endured freezing temperatures for a longer period compared to those in Timeline 2 - F-T Cycles Pre- and Post-Microalgae Addition - and Timeline 3 - 1 F-T cycle. Nonetheless, as anticipated, the microalgae remained in a weakened state and required additional time to fully recover, as already verified in Freezing Living Textiles.

3rd Photosynthesis test.

The third photosynthesis test was conducted seven days after the second. However, due to insufficient results, adjustments were made to improve data accuracy. This time, the experiment was conducted inside the Laminar Air Flow (LAF) Cabinet, where the petri dishes were opened, and the MONITORING PAM device was first sterilized and then placed in direct contact with the living textile. This modification aimed to enhance measurement precision by ensuring a more direct and accurate assessment of the textile's photosynthetic activity. As in the 1st photosynthesis test, the third analysis examined the photosynthetic performance of both immersed and pipetted samples across different timelines. Individual measurements were first analyzed separately, followed by an overall comparison of the immersed and pipetted samples. Finally, the results were contrasted with the photosynthetic activity of *Scenedesmus* sp. in a liquid medium to evaluate the impact of textile embedding.

These data represent the photosynthetis of textiles samples in different part of the samples (Top left, Top center, Top right, Bottom Left, Bottom Right).

Unit= Fv/Fm

	Top Left	Top Center	Top Right	Bottom Left	Bottom Right	Average		
Timeline 1							Average of Timeline 1 immersed	Average of Timeline 1 pipetted
Immersed	0	/	0.12	0.147	0.019	0.0715	0.12225	#DIV/0!
Immersed Replicates	0.073	0.175	0.181	0.044	0.392	0.173		
Pipetted	/	/	/	/	/	#DIV/0!		
Pipetted Copy	/	/	/	/	/	#DIV/0!		
Standard Deviation	0.0516	#DIV/0!	0.04313	0.072832	0.263751	#DIV/0!		
Timeline 2							Average of Timeline 2 immersed	Average of Timeline 2 pipetted
Immersed	/	/	/	/	/	#DIV/0!	#DIV/0!	#DIV/0!
Immersed Replicates	/	/	0.683	/	0.737	0.71		
Pipetted	/	/	/	/	/	#DIV/0!		
Pipetted Replicates	/	/	/	/	/	#DIV/0!		
Standard Deviation	#DIV/0!	#DIV/0!	#DIV/0!	#DIV/0!	#DIV/0!	#DIV/0!		
Timeline 3							Average of Timeline 3 immersed	Average of Timeline 3 pipetted
Immersed	/	/	/	/	/	#DIV/0!	#DIV/0!	#DIV/0!
Immersed Replicates	/	/	0.424	0.221	0.288	0.311		
Pipetted	/	/	/	/	/	#DIV/0!		
Pipetted Replicates	/	/	/	/	/	#DIV/0!		
Standard Deviation	#DIV/0!	#DIV/0!	#DIV/0!	#DIV/0!	#DIV/0!	#DIV/0!		
Scenedesmus in liquid medium	0.787	0.818	0.669			0.758		
							Average Immersed	Average Pipetted
							#DIV/0!	#DIV/0!

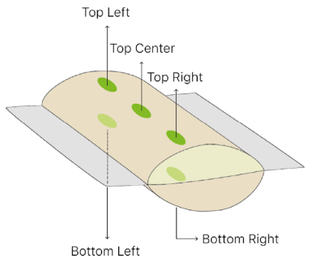

Figure D5: Overall second Photosynthesis test results

These data represent the photosynthetis of textiles samples in different part of the samples (Top left, Top center, Top right, Bottom Left, Bottom Right).

Unit= Fv/Fm

	Top Left	Top Center	Top Right	Bottom Left	Bottom Right	Average		
Timeline 1							Average of Timeline 1 immersed	Average of Timeline 1 pipetted
Immersed	0.425	0.623	0.583	0.444	0.47	0.509	0.5348	0.0943
Immersed Replicates	0.534	0.521	0.402	0.658	0.688	0.5606		
Pipetted	0	0	0	0.433	0.51	0.1886		
Pipetted Replicates	0	0	0	0	0	0		
Standard Deviation	0.2804	0.332859	0.29379	0.2760029	0.29370507	0.26656		
Timeline 2							Average of Timeline 2 immersed	Average of Timeline 2 pipetted
Immersed	0.782	0.481	0.553	0.611	0.53	0.5914	0.6577	0.593225
Immersed Replicates	0.716	0.743	0.654	0.598	0.909	0.724		
Pipetted	0.78	/	0.69	0.644	0.811	0.73125		
Pipetted Replicates	0.478	0.423	0.454	0.44	0.481	0.4552		
Standard Deviation	0.144	0.170493	0.10637	0.0909189	0.20950159	0.13045		
Timeline 3							Average of Timeline 3 immersed	Average of Timeline 3 pipetted
Immersed	0.733	0.619	0.807	0.884	0.835	0.7756	0.7155	0.6224
Immersed Replicates	0.603	0.516	0.811	0.706	0.641	0.6554		
Pipetted	0.465	0.321	0.61	0.711	0.574	0.5362		
Pipetted Replicates	0.781	0.794	0.54	0.888	0.54	0.7086		
Standard Deviation	0.1419	0.197711	0.1381	0.102513	0.13185472	0.10125		
Scenedesmus in liquid medium	0.787	0.818	0.669			0.758		
							Average Immersed	Average Pipetted
							0.636	0.436641667

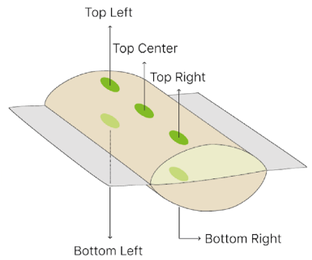

Figure D6: Overall third Photosynthesis test results.

As illustrated in Figure D7, the results showed that *Scenedesmus* sp. in Timeline 1, where the textile had been immersed and subjected to three Freeze-Thaw cycles, exhibited the weakest performance, a predictable outcome given the extended exposure to freezing conditions. In contrast, both Timeline 2, where the textile underwent two Freeze-Thaw cycles before the addition of *Scenedesmus* sp. and BG11 medium followed by a final Freeze-Thaw cycle, and Timeline 3, where the living textile experienced only a single Freeze-Thaw cycle, demonstrated promising results. However, even after two weeks, the pipetted samples showed a slower recovery compared to the immersed ones. Finally, only the immersed samples from Timeline 3 (single F-T cycle) exhibited satisfactory photosynthetic activity.

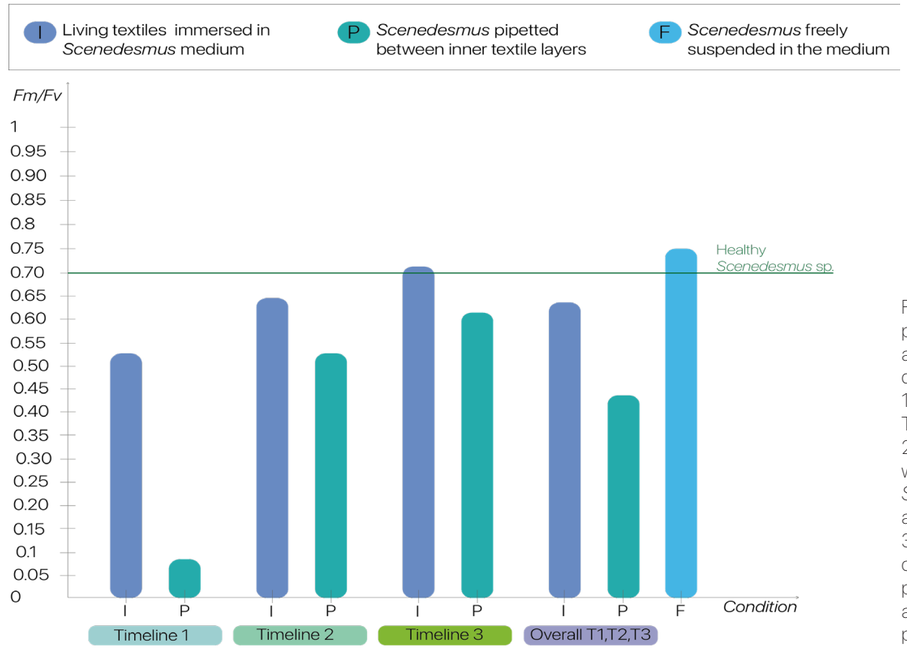

Figure D7: Photosynthetic performance of immersed and pipetted samples across different timelines. Timeline 1 represents three Freeze-Thaw (F-T) cycles, Timeline 2 involves a split F-T process with two cycles before *Scenedesmus* sp. addition and one after, while Timeline 3 corresponds to a single F-T cycle. The graph compares photosynthetic activity across these conditions and preparation methods.

4th Photosynthesis test.

The photosynthetic activity test was conducted inside the Laminar Air Flow (LAF) Cabinet, where the petri dishes were opened, and placed into a dark box. The MONITORING PAM device, connected to a laptop running the WinControl-3 software, was used to measure photosynthetic efficiency. By positioning the MONITORING PAM device, after being sterilized with Ethanol, over the living textiles and initiating the measurement via the software interface, a light emission was triggered, allowing for the quantification of photosynthetic activity. Recorded quantum yield values can range from 0 to 1, with values below 0.7 indicating poor photosynthetic performance, while readings between 0.7 and 1 were considered indicative of a healthy and active microalgal presence (Schuurmans et al., 2015).

The fourth photosynthesis test was conducted at the end of the experiment (after 28 days). Each sample was monitored on both sides in 5 different spots: Top Left, Top Center, Top Right, Bottom Left and Bottom Right.

After collecting all experimental data, the results were processed in several steps to ensure a comprehensive analysis. First, for each sample, the photosynthetic activity measurements from five different spots were averaged (Figure D8). Then, to account for duplicate samples, the results were grouped based on the method of microalgae introduction: for each timeline, the measurements from the immersed samples were averaged separately, as were those from the pipetted samples. This step ensured that a representative average was obtained and helped identify the most effective F-T process. Next, an overall average was calculated for all immersed samples and another for all pipetted samples, enabling a direct comparison between the two methods to determine which was more effective in introducing microalgae into the hydrogel. The measurements were first analyzed individually, then compared collectively, and ultimately were compared with *Scenedesmus* sp. in a liquid medium to evaluate the impact of textile embedding on microalgal viability and performance (Figure D9).

These data represent the photosynthetis of textiles samples in different part of the samples (Top left, Top center, Top right, Bottom Left, Bottom Right).

Unit= Fv/Fm

	Top Left	Top Center	Top Right	Bottom Left	Bottom Right	Average		
Timeline 1							Average of Timeline 1 immersed	Average of Timeline 1 pipetted
Immersed	0.491	0.444	0.603	0.612	0.806	0.5912	0.6288	0.1316
Immersed Replicates	0.657	0.612	0.734	0.704	0.625	0.6664		
Pipetted	0	0	0	0.714	0.602	0.2632		
Pipetted Replicates	0	0	0	0	0	0		
Standard Deviation	0.3383	0.312461	0.3896	0.341434	0.3509	0.30804		
Timeline 2							Average of Timeline 2 immersed	Average of Timeline 2 pipetted
Immersed	0.881	0.773	0.726	0.838	0.85	0.8136	0.8172	0.777
Immersed Replicates	0.718	0.851	0.888	0.82	0.827	0.8208		
Pipetted	0.789	0.721	0.733	0.893	0.868	0.8008		
Pipetted Replicates	0.705	0.888	0.674	0.7	0.799	0.7532		
Standard Deviation	0.0808	0.075372	0.0923	0.081328	0.029833	0.03041		
Timeline 3							Average of Timeline 3 immersed	Average of Timeline 3 pipetted
Immersed	0.707	0.73	0.81	0.742	0.88	0.7738	0.7548	0.7038
Immersed Replicates	0.703	0.522	0.845	0.731	0.878	0.7358		
Pipetted	0.702	0.61	0.602	0.773	0.63	0.6634		
Pipetted Replicates	0.755	0.891	0.662	0.58	0.833	0.7442		
Standard Deviation	0.0256	0.159805	0.1164	0.086188	0.118831	0.04686		
Scenedesmus in liquid medium	0.787	0.818	0.669			0.758		
							Average Immersed	Average Pipetted
							0.7336	0.537466667

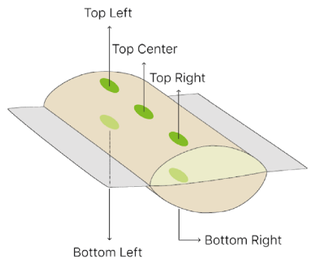

Figure D8: Overall final Photosynthesis test results.

As illustrated in Figure D9, samples submitted to Timeline 2 experiments, and then to follow Timeline 3, seem to be the ones with higher photosynthetic activity.

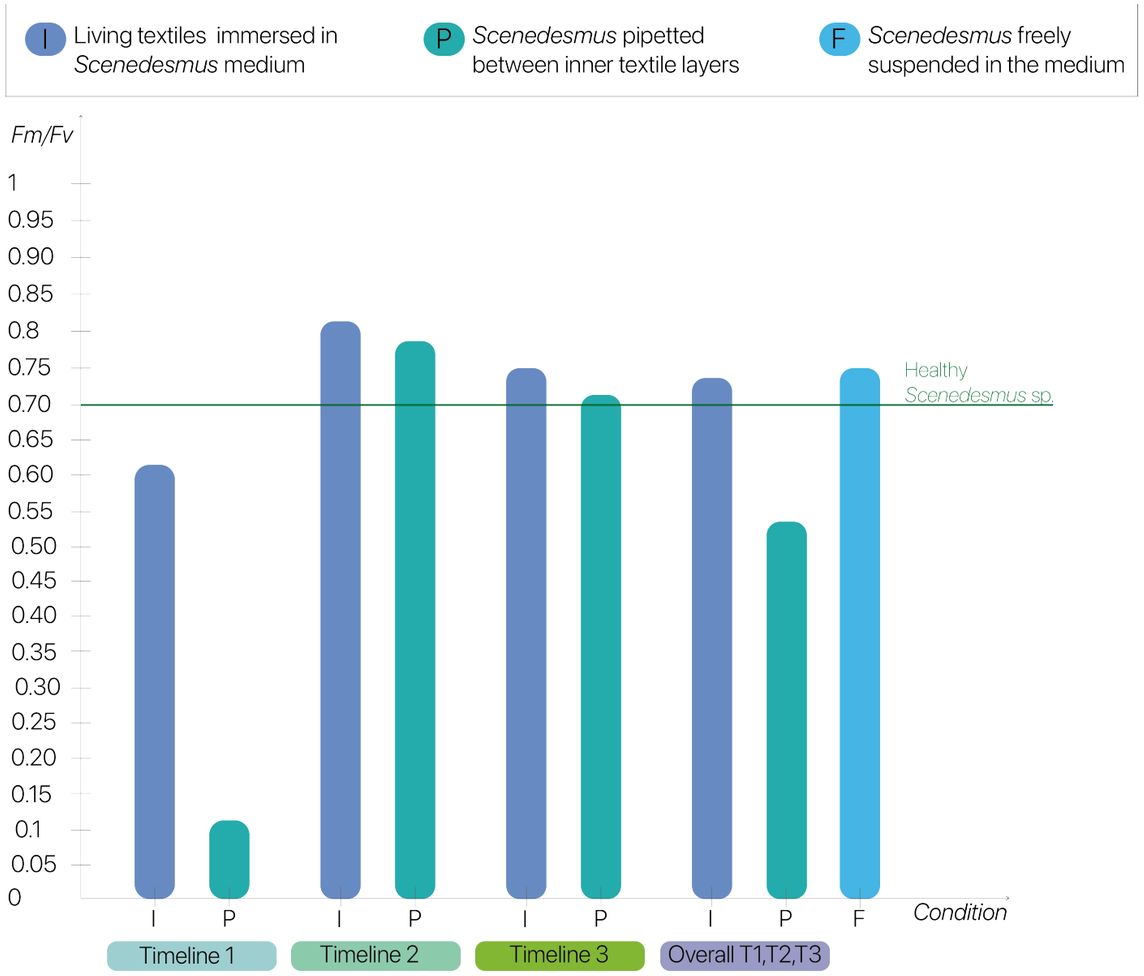

Figure D9: The graph illustrates the photosynthetic performance of immersed and pipetted samples across different timelines. Timeline 1 represents three consecutive Freeze-Thaw (F-T) cycles, Timeline 2 consists of three F-T cycles split into two before *Scenedesmus* sp. addition and one after, while Timeline 3 corresponds to a single F-T cycle. The Overall category represents the average photosynthetic activity of all immersed samples and all pipetted samples. Additionally, the green line indicates the threshold above which microalgae can be considered healthy. This comparative visualization highlights the impact of different F-T processes and sample preparation methods on microalgal photosynthetic activity.

APPENDIX D - Detailed Explanation of Draft Design Procedure

The first objective is to develop the microstructure of the textile. To begin, the software AdaCAD must be downloaded and installed. Within AdaCAD, the textile draft is designed, starting with the creation of a triple-layer structure. To achieve this, the user must navigate to the "*Operation*" tab and input the command "*Tabby*" three times, as shown in Figure D1 and Figure D2. Each tabby corresponds to one of the three layers in the textile. Once this is set, the "*Layer Notation*" command must be applied to define the multilayer structure (Figure D3). Since AdaCAD's default setting supports two layers, an additional adjustment is required to incorporate the third layer. By modifying the notation and adding *(c1)* alongside the existing *(a1)(b1)* configuration—where letters represent the weft yarns and numbers indicate the warp yarns—the structure is extended. Each tabby is then assigned to its respective layer: the first tabby corresponds to *(a1)*, the second to *(b2)*, and the third to *(c3)*, as illustrated in Figure D4.

Finalizing the triple-layer structure requires defining the warp intersections and spacing, which play a crucial role in balancing structural integrity and light permeability. To accomplish this, an additional draft must be created. to regulate the intersection of warp and weft yarns. This step ensures optimal spacing between warp yarns, directly influencing the textile's functionality. By selecting "*Add Draft*" (Figure D5), the warp spacing is adjusted to enhance light penetration while maintaining stability.

The final design consists of two protective outer layers made of 90% PVA and 10% Cotton, enclosing an inner layer that serves as the habitat for the microalgae. Since adequate light exposure is essential for microalgal survival, increasing the warp spacing allows the PVA to gelatinize and become transparent, facilitating light penetration. The weft yarns are alternated following a pattern of four PVA yarns followed by one Cotton yarn, forming the structure depicted in Figure D6. In the draft visualization, white squares represent PVA weft yarns in the top layer, orange squares indicate Cotton yarns in the central layer, and black squares correspond to PVA yarns in the bottom layer. Once the draft is complete, it is attached to the layer notation box to fully integrate it into the textile design (Figure D7)

After creating the triple-layer structure, the next step involves designing the compound that will be placed at the edges of each layer to ensure strong bonding. This process requires returning to the "*Operations*" tab in AdaCAD, where the structure is refined by defining the interlacing pattern. To achieve this, the commands "Twill" (entered twice), followed by "*Shift*", and then "*Interlace Wefts*" must be applied, as illustrated in Figure DA1. To properly configure the twill pattern, it is necessary to adjust the diagonal direction. Therefore, switch from "*S*" to "*Z*" as shown in Figure DA2. Additionally, one of the two twill layers must have its facing changed from "*Weft-facing*" to "*Warp-facing*" (Figure DA3), ensuring a balanced interaction between warp and weft yarns. Once these modifications are in place, the "Twill Warp-Facing" layer is linked to "*Shift*", while both "*Shift*" and "*Twill Weft-Facing*" are connected to "Interlace wefts", as illustrated in Figure DA4. This final adjustment secures the layers together, reinforcing the textile's structural integrity.

After completing the triple-layer structure and the compound, the next step is to integrate them into a cohesive textile design. This process begins by returning to the "*Operation*" tab in AdaCAD and selecting "*Image Map*" (Figure DB1). An image must then be created in Photoshop with dimensions of 2640x100 px, visually defining the areas where the triple layer and the compound will be positioned within the textile, as illustrated in Figure DB2. Once the image is ready, it is uploaded into the Image Map function in AdaCAD. At this stage, the triple-layer structure is assigned to the light blue rectangle, while the compound is mapped onto the green rectangle, ensuring proper placement within the textile, as shown in Figure DB3. This step finalizes the integration of both components, establishing the structural and functional layout of the design.

Once the draft is completed, it must be saved for further processing. In the "*Image Map box*", three dots can be found, which need to be clicked to access the "*Download BitMap*" option. After downloading the bitmap file, it should be transferred to a pen drive to facilitate its upload onto the TC2 loom.

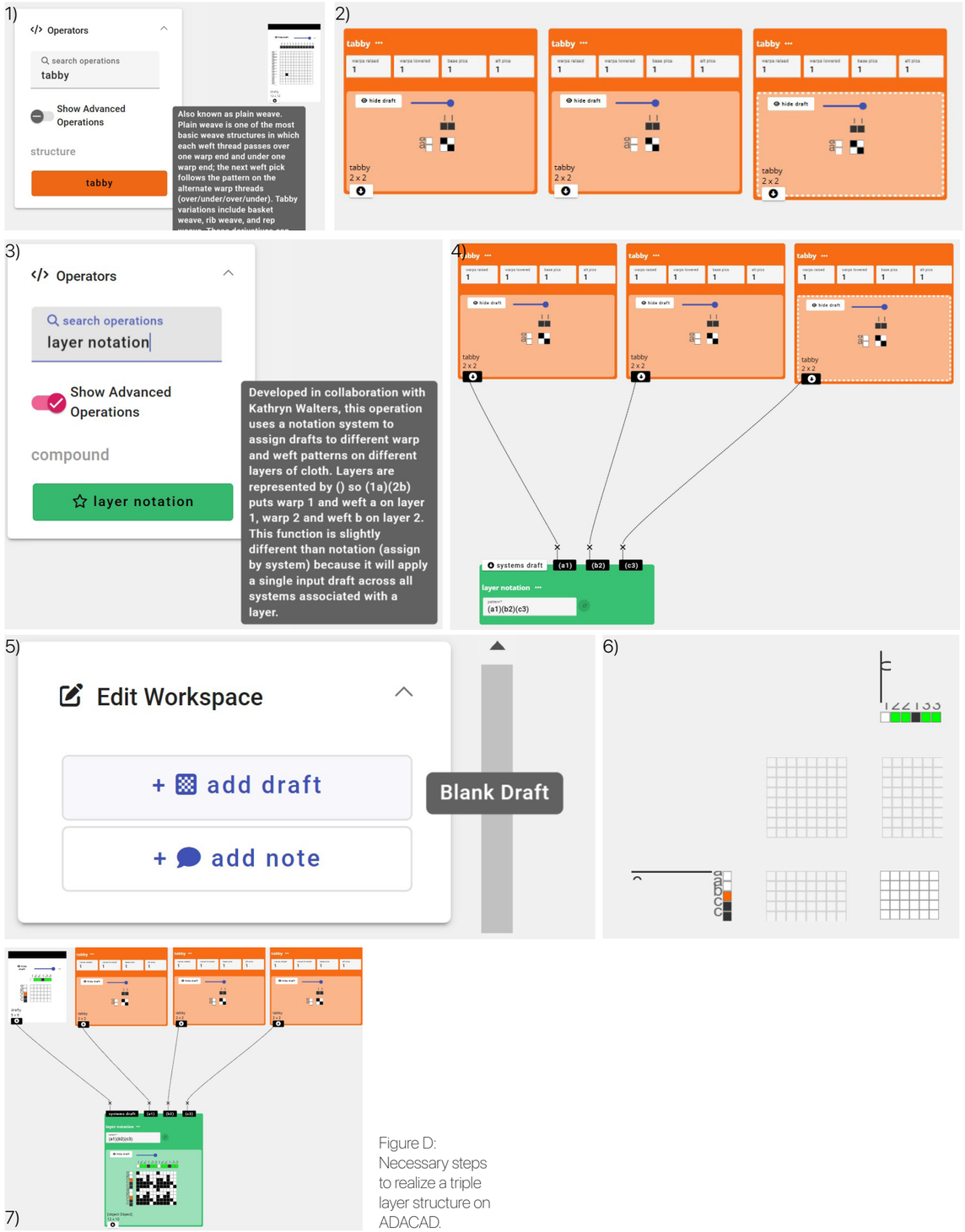

Figure D: Necessary steps to realize a triple layer structure on ADACAD.

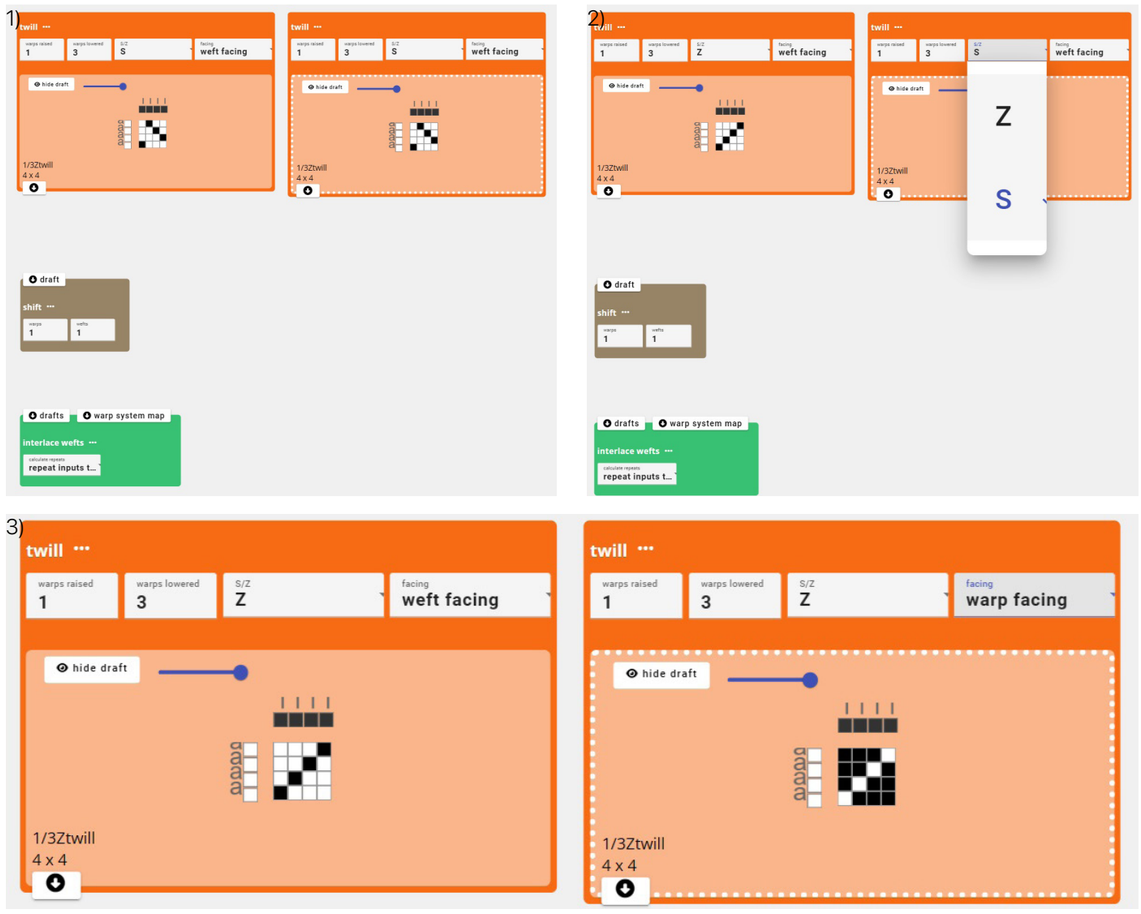

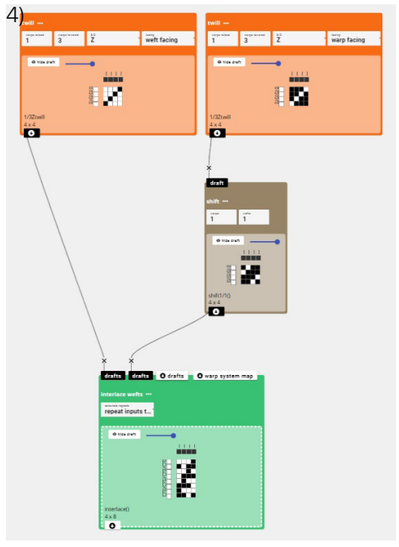

Figure DA: Necessary steps to realize a twill reverse twill compound on ADACAD.

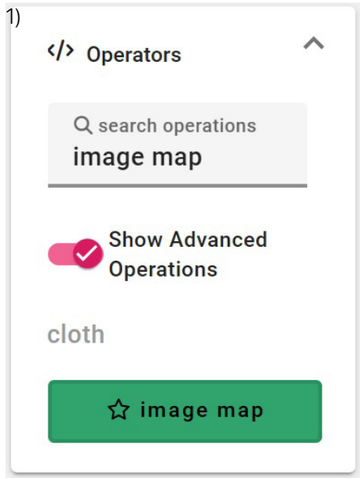

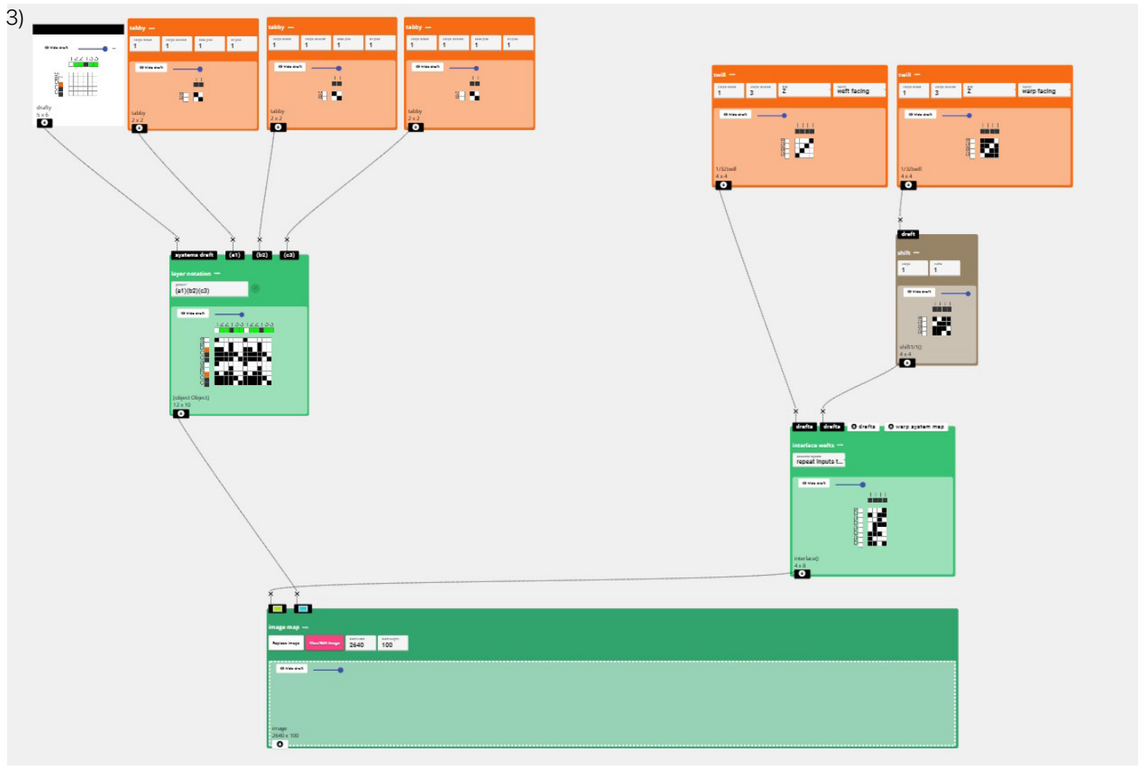

Figure DB: Necessary steps to realize the Image Map on ADACAD.

APPENDIX E - Graduation Project Brief

DESIGN FOR our future

TUDe

Personal Project Brief – IDE Master Graduation Project

Name student Martina Mancini **Student number**

PROJECT TITLE, INTRODUCTION, PROBLEM DEFINITION and ASSIGNMENT
Complete all fields, keep information clear, specific and concise

Project title Living Textiles: Exploring Microalgae Growth on 3D Woven Structures in Design

Please state the title of your graduation project (above). Keep the title compact and simple. Do not use abbreviations. The remainder of this document allows you to define and clarify your graduation project.

Introduction

Describe the context of your project here; What is the domain in which your project takes place? Who are the main stakeholders and what interests are at stake? Describe the opportunities (and limitations) in this domain to better serve the stakeholder interests. (max 250 words)

In recent decades, the textile industry has depended heavily on non-renewable raw materials, creating a harmful production cycle, causing substantial environmental harm, and contributing to rising CO_2 emissions. Although natural carbon sinks have absorbed nearly 50% of global emissions from 2011 to 2020 (NOAA, 2024), and industries have begun implementing mechanical recycling processes (Moorhouse, 2023), these efforts alone are insufficient to counteract the growing environmental impact. This has heightened the urgency for sustainable solutions that can reduce the industry's ecological footprint.

In response, researchers are turning to innovative alternatives, such as Engineered Living Materials (ELMs) containing photosynthetic microorganisms, that are embedded in self-healing matrices or artificial scaffolds, that can potentially contribute to improve air quality, e.g., through CO_2 capture. The development of these materials enables the growth of photosynthetic organisms in non-arable environments, allowing them to thrive without competing with food crops or relying on arable land (An et al., 2022; Arashiro et al., 2022; Introduction to the Cyanobacteria, n.d.).

By integrating microorganisms like microalgae into textiles, researchers aim to develop living materials capable of addressing the environmental impact (Scott, 2022). These living textiles utilize the photosynthetic abilities of microalgae to reduce CO_2 levels and generate energy (Tripathi et al., 2023). However, sustaining the viability of microalgae on ELMs remains a significant technical challenge. Additionally, while preliminary experiments have demonstrated promising results (In-Na et al., 2022), no study has systematically employed a design methodology to investigate the integration of microalgae into textiles or evaluate how such an approach could shape the research trajectory.

Addressing these limitations could unlock the full potential of living textiles, enabling their use in climate adaptation, urban sustainability, and ecological remediation. Consequently, applying a structured design method could offer a pathway to overcome these barriers and unlock the way for transformative innovations in living textile development.

→ *space available for images / figures on next page*

introduction (continued): space for images

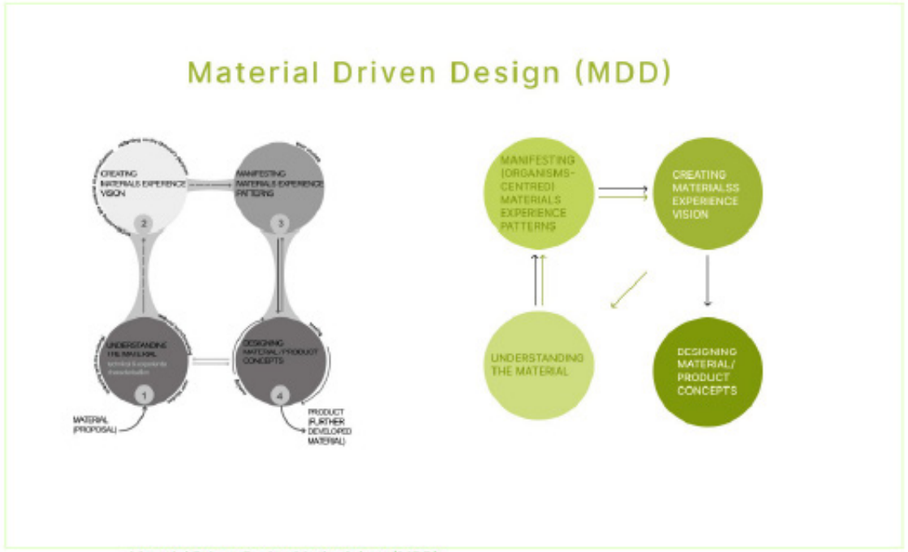

image / figure 1 Material Driven Design Methodology (MDD)

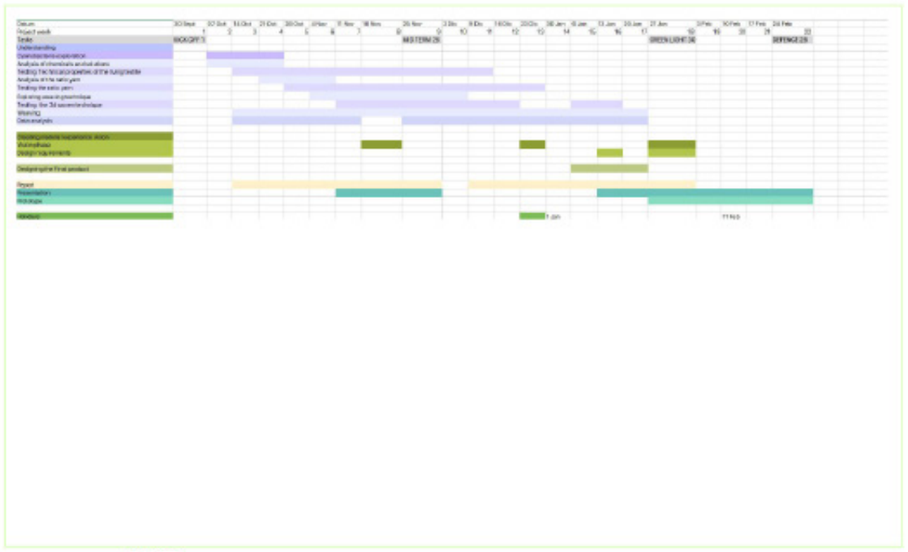

image / figure 2 GANTT

DESIGN FOR our future

TUDelft

Personal Project Brief – IDE Master Graduation Project

Problem Definition

What problem do you want to solve in the context described in the introduction, and within the available time frame of 100 working days? (= Master Graduation Project of 30 EC). What opportunities do you see to create added value for the described stakeholders? Substantiate your choice.
(max 200 words)

As previously reported, studies found that ELMs leverage the photosynthetic abilities of microalgae to reduce the overall environmental impact, demonstrating promising results. However, existing textile structures are not designed to accommodate microalgae, the used techniques are not completely sustainable, and these findings vary in reliability. Consequently, the challenge is to design a 3D woven textile capable of hosting microalgae and promoting their growth.

Achieving this goal requires answering two key questions:
Can we design a 3D woven textile that supports microalgae survival?
What opportunities can be seized to create added value for the stakeholders described?

Assignment

This is the most important part of the project brief because it will give a clear direction of what you are heading for. Formulate an assignment to yourself regarding what you expect to deliver as result at the end of your project. (1 sentence) As you graduate as an industrial design engineer, your assignment will start with a verb (Design/Investigate/Validate/Create), and you may use the green text format:

Designing a 3D-woven textile able to maintain the livingness of microalgae.

Then explain your project approach to carrying out your graduation project and what research and design methods you plan to use to generate your design solution (max 150 words)

This research follows a modified Material Driven Design (MDD) methodology to develop a living textile. The original MDD framework consists of four phases: Understanding the Materials, Creating Materials Experience Vision, Manifesting Materials Experience Patterns, and Creating Material/Product Concepts. However, in this project, the phases have been adapted to the following sequence: Understanding the Materials, Manifesting (Organism-Centred) Materials Experience Patterns, Creating Materials Experience Vision, and finally, Creating Material/Product Concepts. The Understanding the Materials phase will focus on analyzing and testing various materials to ensure they meet the biological requirements of microalgae. The Parallel Prototyping Method will be employed to enhance this phase's efficiency. This approach involves conducting multiple experiments simultaneously, enabling the exploration of different material configurations in a shorter timeframe. The Manifesting (Organism-Centred) Materials Experience Patterns phase, where microalgae are considered the primary "users" of the textile, will evaluate how well the textile environment supports their growth, activity, and survival. Next, the Creating Materials Experience Vision phase will involve reflecting on these results to outline the next steps needed and to envision potential outcomes of this research. These three phases will be iteratively applied throughout the project. The final phase, Creating Material/Product Concepts, will synthesize the most successful solutions into the final design.

Project planning and key moments

*To make visible how you plan to spend your time, you must make a planning for the full project. You are advised to use a Gantt chart format to show the different phases of your project, deliverables you have in mind, meetings and in-between deadlines. Keep in mind that all activities should fit within the given run time of 100 working days. Your planning should include a **kick-off meeting**, **mid-term evaluation meeting**, **green light meeting** and **graduation ceremony**. Please indicate periods of part-time activities and/or periods of not spending time on your graduation project, if any (for instance because of holidays or parallel course activities).*

Make sure to attach the full plan to this project brief.
The four key moment dates must be filled in below

Kick off meeting	1 Oct 2024
Mid-term evaluation	26 Nov 2024
Green light meeting	30 Jan 2025
Graduation ceremony	28 Feb 2025

In exceptional cases (part of) the Graduation Project may need to be scheduled part-time. Indicate here if such applies to your project

Part of project scheduled part-time	
For how many project weeks	
Number of project days per week	

Comments:

Motivation and personal ambitions

Explain why you wish to start this project, what competencies you want to prove or develop (e.g. competencies acquired in your MSc programme, electives, extra-curricular activities or other).

Optionally, describe whether you have some personal learning ambitions which you explicitly want to address in this project, on top of the learning objectives of the Graduation Project itself. You might think of e.g. acquiring in depth knowledge on a specific subject, broadening your competencies or experimenting with a specific tool or methodology. Personal learning ambitions are limited to a maximum number of five.
(200 words max)

Climate change is a pressing global challenge driven by various sources, including the pollution caused by textile production and incineration. Focusing my thesis on developing living textiles offers the opportunity to address this critical issue while advancing a scientific field that aligns with my research and development career aspirations. My interest in sustainability, as emphasized in my motivational letter to TU Delft, underlines my dedication to creating innovative solutions for carbon capture and contributing to a more sustainable future. In pursuing this project, I aim to gain in-depth knowledge of weaving techniques. Mastering them will enable me to innovate and expand design possibilities in future projects. Furthermore, I am willing to delve into Engineering Living Materials (ELMs), which have emerged as promising carbon capture and wastewater treatment solutions. Additionally, this project offers an opportunity to strengthen my management skills by integrating knowledge from diverse disciplines and improving my ability to identify and mitigate potential risks throughout the research process. My commitment to addressing this relevant challenge inspires me to put my best effort into this project.